


# Studsvik Arbetsrapport - Technical Note

Projektidentifikation – Project identification		Datum – Date	Rapport nr – Report No.
SKI B39/83-G.2.1/812/82		84-06-04	SD-84/43, NR-84/423
Titel och författare – Title and author			
<p>PRELIMINARY DATA COMPARISON REPORT FOR ISP17</p> <p>An international containment standard problem based on the Marviken full scale experiment Blowdown No 18</p> <p>Jan-Erik Marklund</p>			
Distribution			
NR	E Hellstrand (2)	SNPI (5)	
NRS	R Blomquist	NEA (10)	
	K Johansson	ISP17 Participants (6)	
	R Persson	File (7)	
	O Sandervåg		
NRX	J Collén		
<input type="checkbox"/>	Begränsad distribution – Restricted distribution	<input type="checkbox"/>	Rapporten skall ej förhandsviseras – Internal note
Godkänd av – Approved by		Kontonr – Internal note	Antal ex – No. of copies
		PN5395A	35
<p>ABSTRACT</p> <p>In the November 1982 CSNI meeting it was decided that the test BD18 from the second series of Marviken full scale containment experiments would serve as a basis for an open international standard problem, ISP17, with STUDSVIK, Sweden as host organization.</p> <p>The purpose of ISP17 is to get insight in best-estimate modelling capacities of present containment computer codes, primarily concerning</p> <ul style="list-style-type: none"> <li>- Vent clearing transients</li> <li>- Medium-time pressure suppression characteristics.</li> </ul> <p>The present report contains brief information on the basis for the standard problem and a preliminary comparison and assessment of the six submitted results.</p> <p>The vent clearing transients are quite well modelled by most submittals, while the pressure level development to a large extent depends on the assumptions made for air transfer to the wetwell.</p> <p>The work has been financially supported by the Swedish Nuclear Power Inspectorate (SNPI).</p>			

I.209042/I.209043 (Ej repr) 83-11

## LIST OF CONTENTS

	<u>Page</u>
1. BACKGROUND AND SUMMARY	2
2. EXPERIMENTAL BASIS AND CHOICE OF TEST	6
2.1 Brief description of the test facility	6
2.2 Test program for the Marviken II tests	7
2.3 Instrumentation and data acquisition systems	8
2.4 Data accuracy	10
2.5 Choice of test for ISP17	12
3. BRIEF PRESENTATION OF THE SELECTED STANDARD PROBLEM	14
3.1 Basic data for Marviken Blow-down 18	14
3.2 Requested computations	18
4. SUBMITTED RESULTS	20
4.1 Computer codes used	20
4.2 Basic input data used	32
4.3 Main differences between codes and data as related to ISP17	33
5. COMPARISON OF CALCULATED RESULTS AND EXPERIMENTAL DATA	36
5.1 Short-time behaviour	36
5.2 Long-time behaviour	45
5.3 Concluding remarks	59
6. COMMENTS BY PARTICIPANTS	60
7. PARAMETER STUDIES	61
8. REFERENCES	62

## APPENDICES

- A. LIST OF TABLES
- B. LIST OF FIGURES
- C. LIST OF DIAGRAMS

## 1. BACKGROUND AND SUMMARY

Four international containment standard problems have already been carried out under the supervision of CSNI/NEA working groups.

- Two open (blind/open) standard problems (1, 2) based on experiments performed by Battelle Frankfurt at a 1:64 (volume scale) model of the BIBLIS-A reactor.
- An open standard problem (3) based on an experiment in a small-scale ( $\sim 2 \text{ m}^3$ ) two-compartment model at the Australian Lucas Heights Laboratories.
- A blind standard problem (4) based on the full-scale HDR experiments, carried out during 82/83.

All of these experimental facilities simulate dry containments.

In the February 1982 meeting (5) with the Containment Working Group of CSNI, interest was expressed for a standard problem based on some experiment in a BWR-type containment, i.e. with a pressure suppression pool.

A proposal (6) made by Sweden for an open standard problem based on some test of the altogether 25 Marviken full scale containment experiments (7, 8) was approved as a potential candidate for ISP17 by the CSNI Principal Working Group meeting in October 1982.

After consultations with potential participants, the test No 18 was chosen for the standard problem, and this was approved by the CSNI full meeting in November 1982.

Specifications (9) for ISP17 were distributed in June 1983 and a workshop (10) discussing these specifications and other questions related to the standard problem was held at Marviken on August 18, 1983.

The deadline for submittals was originally set to December 31, 1983 but was later moved 2 months ahead to February 29, 1984.

Submittals were obtained from four participants, ECN (Energy research Centre, Netherlands), University of Pisa (Italy), VTT (Technical Research Centre, Finland) and STUDSVIK (Sweden). Italy and Sweden contributed with two different submittals, so there were altogether six submitted results as well as some parameter studies from Italy, Finland and Sweden.

The codes used for the submittals were ARIANNA-1 (Italy), CONTEMPT-LT/26 (Italy), CONTEMPT-LT/28 (Finland), COPTA-7 (Sweden) and ZOCO-V (Netherlands).

ARIANNA-1 is the only dry containment code participating and as such could quite naturally produce sensible results only for the time up to the vent clearing, which occurred around 1.4 s after blow-down start. Still this run was valuable, since due to the many drywell nodes (17 compared to 4 and 1 for the other codes) it could give more information on pressure differences and flow paths etc than the other codes.

All the other codes contain wetwell models and could therefore produce results for the whole blow-down period. Two of these codes (COPTA and ZOCO) allow subdivision of the drywell into a fairly large (around 10) number of subcompartments, while the two CONTEMPT versions do not have that possibility.

The evaluation of the results was split into two different time-frames, short-time cases covering the first 4.4 s (0 - 1.4 s for the ARIANNA-1 run) and long-time cases covering the period 0 - 200 s (0 - 75 s for the ZOCO-V run).

The short-time cases were further separated into two groups, group A containing cases with subdivided drywell and group B with one-node drywell modelling. This separation was made mainly to ensure readable comparison diagrams.

For the short-time cases the most important parameters are the differential pressures, the vent clearing transient and the pool swell phenomenon.

The differential pressure between drywell and wetwell as well as the vent clearing transient are quite well modelled by most of the codes.

The differential pressures in the drywell are also fairly well modelled by those codes allowing this (ARIANNA-1, COPTA-7 and ZOCO-V).

Only two of the codes, COPTA-7 and ZOCO-V, contain special pool swell models, that allow a fairly correct modelling of the pool swell phenomenon.

In the long-time cases, the parameter of largest interest is the pressure build-up. This is influenced by the mass transfer to the wetwell and by heat soakage of the pool and into solid structures, such as the concrete confinements and the great number of metal structures in the containment.

The pressure levels after roughly 50 s are to a large extent controlled by the total mass of air transferred from the drywell to the wetwell through the vent pipes. Different approaches were used by the codes to model the air transfer. Most codes were using knowledge of the measured air flow rates. Only one of the submittals (ZOCO-V) tried to avoid this by using a 4-compartment subdivision of the drywell throughout the transient.

As a whole the success in the modelling was satisfactory, and useful experiences were obtained.

Minor deficiencies in code behaviour were discovered by some of the participants during the runs and corrected code versions were created.

The present report contains first a brief summary of the test conditions for the Marviken tests. Then there are given summary data for the selected test BD18. Finally the main part is devoted to descriptions of the codes used and comparisons of the submitted results as well as related parameter studies. In appendices are given comments received from the participants after the presentation of draft comparison report.

## 2. EXPERIMENTAL BASIS AND CHOICE OF TEST

The first series of 16 full scale containment response tests (7) was carried out at Marviken, Sweden, in 1973 - 74.

A second series of nine tests (8) was carried out in 1976.

The measurement system had been significantly augmented as compared with that of the previous test series and allowed oscillations to be studied for frequencies up to 100 Hz.

These experiments were carried out as a multinational project, as in the first series of tests. The organizations represented were from Denmark, the Federal Republic of Germany, Finland, France, Japan, the Netherlands, Norway, Sweden and the United States.

In the remaining part of this chapter will be given a brief description of the common test conditions for the second series of Marviken experiments, as well as a motivation for the choice of blowdown 18 as the basis for ISP17.

### 2.1 Brief description of the test facility

The Marviken station (see Figure B.1) was originally built to operate as a boiling heavy-water direct-cycle reactor with natural circulation. The station had been completed up to acceptance testing, including pre-operational light water tests.

The main parts of the facility are the pressure vessel and the containment (see Figure B.2). Discharge flow from the pressure vessel was fed into the containment through a discharge pipe.

The containment consists of a drywell part, connected with the wetwell through a vent system.

## 2.2 Test program for the Marviken II tests

In the second series of tests a total of 9 blowdowns were performed starting with Blowdown 17 in order to indicate the continuity with the first series of 16 blowdown test. A presentation of the main test parameters in the second series is given in Table A.1.

In all tests the pressure vessel was filled with 280 - 290 tons of water which were heated and pressurized to approximately 6 MPa.

In Blowdown 17 the water was heated to a nearly homogeneous saturation temperature of 260°C while in all the subsequent blowdowns a temperature stratification was established with about 25°C subcooling in the lower region and with saturation temperature in the upper region. The reason for establishing temperature stratification was to prolong the period of subcooled single-phase liquid flow into the containment and facilitate the measurements of the discharge flow rate in the early phase of the blowdowns.

### 2.2.1 Containment conditions

The changes that were made in the containment between the tests were largely confined to the vent system and the wetwell as shown in Table A.1.

The first change, made after Blowdown 17, was the blocking of twenty-nine vent pipes which reduced the total vent pipe flow area from around 4 m<sup>2</sup> to around 2 m<sup>2</sup>. Before Blowdown 25, the last blowdown



run, a special arrangement was made, referred to as the single cell, in which another vent pipe was chosen to be open on the secondary side of the partition wall.

The purpose of the single cell, consisting of a vent pipe encircled by a pipe of larger diameter (900 mm) was to permit comparisons of the pressure oscillations and pressure spikes for an isolated vent pipe in a bounded single cell with those in a multi-vent region.

The pool partition wall was installed between Blowdowns 20 and 21 and divided the wetwell pool into two regions, the primary region with 27 open vent pipes and the secondary region with the single vent pipe.

Before Blowdown 24 two of the four blowdown channels were blocked in order to establish the so-called detuning of the vent system.

Variations in the depth of the wetwell pool and thereby in the pool mass and vent submergence were made in Blowdowns 20 and 25.

The containment tightness was investigated by means of air pressurization before the series of tests was begun.

### 2.3 Instrumentation and data acquisition systems

---

A list of the data channels that comprise the measurement system for the blowdown tests is given in Table A.2. This list is not completely valid for all tests as modifications were made between the tests.

A lay-out of the measurement system is shown in Figure B.3. The sensing elements were in most cases located at the measurement positions in the pressure vessel or in the containment (cf Figures B.4, B.5 and B.6). For some channels, mainly those measuring pressure, the sensing elements were located outside the containment with a connecting arrangement to the measurement position.

### 2.3.1 Types of sensing elements and other equipment

-----

#### Pressure and differential pressure

Strain gauges were used to measure pressure and differential pressure in the vessel.

#### Temperature

All temperatures were measured with thermocouples of chromel-alumel type. They were shielded with inconel, insulated with magnesium oxide and had an insulated measuring junction. Three different dimensions, 0.5 mm, 1 mm and 2 mm in diameter, were used so as to meet the different time-constant requirements.

#### Mass flow

The items of measurement related to mass flow rate were those of the pitot-static tubes, the radioactive tracer method and the infrared light attenuation technique.

The pitot-static tubes, installed in the main discharge pipe, were merely aimed at measuring the discharge flow rate in periods of subcooled liquid flow.

The radioactive tracer method and the infrared light attenuation technique were adopted to measure vent flow related parameters in one of the four blowdown channels.

#### Liquid level and phase boundary

The level probes installed in the vent pipes and in the wetwell were of the spark plug type.

Measurements of the liquid level were also performed with differential pressure channels.

#### Impact load

The impact targets above the wetwell water pool exposed, in Blowdowns 17 - 20, flat and quadratic surfaces of stain-less steel which were welded on to horizontal rods that were fastened to vent pipes. In the subsequent tests cylindrical targets were also used.

The sensing elements were strain gauges and accelerometers. The triaxial piezoresistive accelerometers failed to work due to water leakage.

#### 2.4 Data accuracy

The error limits of the data channels are determined in the form of maximum errors and probable errors. The maximum error calculation applied to the whole channel gives with high confidence the limits of the systematic errors. The probable error is defined as one standard deviation and is a measure of the spread of data from identical channels measuring the same quantity. Provided the systematic errors are negligible the probability that the data lie within the probable error limits is generally 68 per cent.

The errors thus evaluated are presented in Table A.3.

The error limits of the calculated data, referred to as non-measured quantities, are more difficult to deduce since in addition to considerations of the accuracy of the basic data an assessment of the calculational technique is required.

#### 2.4.1 Discharge flow rate

The discharge flow rate is for most of the blow-down periods determined from the DP-over-vessel data with error limits of about  $\pm 7$  per cent. For the more rapid transients the errors are larger but are not likely to exceed  $\pm 20$  per cent.

#### 2.4.2 Specific enthalpy

The uncertainty of the specific enthalpy of the discharge flow is estimated at  $\begin{matrix} +30 \\ -10 \end{matrix}$  kJ/kg which is equivalent to  $\begin{matrix} +3 \\ -1 \end{matrix}$  per cent.

#### 2.4.3 Flow rate of air into the wetwell

During periods of relatively stabilized air flow rate the error is estimated at 5 - 6 per cent but larger errors exist for short periods.

#### 2.4.4 Steam flow rate into the wetwell

Error limits of 10 - 15 per cent are estimated for relatively stable flow rates while in periods of strong flow variations the error limits may be as large as 30 - 40 per cent.

#### 2.4.5 Water flow rate into the wetwell

No reasonable accuracy can be claimed for the flow rate of water into the wetwell pool.

#### 2.4.6 Gas velocity in downcomers

The error limits of the velocity measured with the radiotracer method are  $\pm 5$  per cent.

#### 2.4.7 The infrared absorption method

The evaluation of maximum error limits of the infrared measurements yielded the following results:

Velocity (determined for droplets)	$\pm 5$ per cent
Density of steam	normally $< \pm 10 - 12$ per cent
Density of air	from about $\pm 10$ per cent early in the blowdowns to the order of a factor of ten in the later part of the blowdowns
Concentration of liquid droplets	errors are too large for a meaningful evaluation of water flow rate

#### 2.5 Choice of test for ISP17

In six of the blowdowns in the Marviken II tests most of the air in the drywell was transferred to the wetwell by a prepurging process before the main blowdown took place. It means that essentially no pool swell was encountered in these six experiments. Therefore one of the remaining three experiments BD17, BD18 and BD21 was preferred as basis for a standard problem.

In BD21 the pool was subdivided into two parts. BD17 and BD18 were relatively similar to each other. The main differences between them were

- The flow area was larger in BD17 than in BD18.

- The initial temperature profiles in the pressure vessel were different, giving BD18 a longer period of subcooled flow through the discharge pipe than BD17.
- BD17 has been used by many code developers as a reference case.

With these points in mind, BD18 was finally chosen to be the basis of the standard problem ISP17.

### 3. BRIEF PRESENTATION OF THE SELECTED STANDARD PROBLEM

In this chapter we will first give a brief summary of the data for the Marviken blowdown 18, focussing on the data most important for the evaluation of the standard problem, and then briefly relate the requested computations for ISP17.

The standard problem covers only the thermal-hydraulic part of the experiment, but not the dynamic part (oscillations). The reason is that general containment codes normally are not capable of handling the oscillatory phenomena correctly. For such purpose special codes are used.

#### 3.1 Basic data for Marviken Blowdown 18

The relevant data for Marviken Blowdown 18 are described in a set of reports, of which the most important are given in this report as Ref 11 through Ref 17. Below will be given a brief summary of the most important data for the ISP17 computations.

##### 3.1.1 The containment

The Marviken containment is of the pressure-suppression type, divided basically into two compartments, the drywell and the wetwell. The latter did contain a condensation water pool, connected to the drywell by a vent system (see Figure B.2).

The drywell, consisting of several subcompartments, had a total active air volume of 1 972 m<sup>3</sup> in BD18 (see Table A.4). In this volume is included the air in the open vent pipes, but not in the plugged vent pipes. The air volume of the drywell openings is also included.

The wetwell is located beneath the drywell. The initial depth of the wetwell water pool in BD18 was 4.51 m, giving an initial active water volume of 556 m<sup>3</sup> and an initial air space volume of 1 583 m<sup>3</sup>. In the active water volume is included 5.6 m<sup>3</sup> of water in the open vent pipes.

A schematic drawing of the containment is shown in Figure B.7. A possible subdivision into a 5-node model, used by two of the participants in ISP17, is also indicated in that figure.

The active cross-sectional area of the wetwell varies considerably for different distances above the wetwell floor (see Figure B.8). For the pool surface levels relevant for BD18, the variation is between 45 m<sup>2</sup> and 119 m<sup>2</sup>, being 108 m<sup>2</sup> for most of the pool swell distance.

### 3.1.2 Vent system

The vent system consists of 4 steel pipes, with a 1.2 m inside diameter, which connect the lower drywell to a header located in the wetwell air space. From this header a total of 58 vent pipes, around 5.5 m long (inside) and with a 0.3 m inside diameter, lead vertically downwards into the wetwell water pool. Thirty of the vent pipes were blocked (see Figure 9) during BD18, leaving 28 active vent pipes, i.e. totally 1.98 m<sup>2</sup> flow area. The initial submergence depth was 2.81 m.

### 3.1.3 Drywell openings

The minimum flow areas for the drywell openings are listed in Table A.5. When lumped together for the 5-Room case in Figure B.7, the total flow areas become as in Table A.6.



### 3.1.4 Heat conducting structures

The Marviken containment contains a vast amount of structures that could conduct and absorb heat. These structures are described in the test report MXB-101 (Ref 11). A summary of the total surfaces areas is given in Table A.7 and suggested values for some heat soakage constants in Table A.8. Below follows a brief discussion of possible modelling of these structures. A more detailed discussion is given in Ref 18.

#### A. Aluminium

The aluminium present in the containment was very thin, usually around 1 mm thick, and could therefore be represented by its total heat capacity. The total amount in drywell was 1 969 kg, representing a heat capacity of 1.76 MJ/K if  $C_p = 896 \text{ J/kg/K}$  is used, see Table A.9. No aluminium was present in the wetwell.

#### B. Structures made of steel or concrete

The total steel content in the containment is listed in Table A.10. Some of this is thin and could probably be treated as an additional heat capacity, while some is thicker and the heat conductivity has to be considered.

The blowdown pipes and possibly the vent pipes are the only structures that in any significant amount could contribute to heat flow by conduction between rooms. Most of the concrete walls have a thickness of 0.5 m or more, which means that their interior will not be affected by short transients. The thicknesses used for concrete walls in the models are therefore of no great importance, except possibly for some of the thinnest walls.

### 3.1.5 The pressure vessel

The pressure vessel had a 5.22 m inside diameter and a height including the top-cupola of 24.55 m. The net volume of the vessel, i.e. the free water space was 420 m<sup>3</sup>. In BD18 the pressure vessel was filled with 278 tons of water which was heated and pressurized to 4.6 MPa. A temperature stratification was established with about 25°C subcooling in the lower region and with saturation temperature in the upper region (cf Figure B.10). The reason for establishing temperature stratification was to prolong the period of subcooled single-phase liquid flow into the containment and facilitate the measurements of the discharge flow rate in the early phase of the blowdowns.

The pressure vessel was thermally insulated from the containment during the blowdown.

### 3.1.6 The discharge pipe

The pipe rupture was simulated in Room 122 of the lower drywell (see Figure B.2).

The design of the discharge outlet is shown in Figure B.11.

### 3.1.7 Discharge flow

Measured and evaluated data for the discharge flow are shown on Figures 12, 13 and 14 (copies of Diagrams E:4 through E:6 in Ref 14).

In Table A.11 are given suggested values of mass flow and specific enthalpy, as manually extracted from these curves. No data were given for specific enthalpy after ~ 120 s, but a value of 1 140 kJ/K, corresponding to saturated liquid, appears appropriate to use.

### 3.1.8 Initial conditions

The initial conditions for BD18 are given in Ref 14. A summary of these data, relevant for 2-node models and for the 5-node model of Figure 7, is given in Table A.12.

### 3.2 Requested computations

The standard problem is intended to cover only the thermal-hydraulic part of the experiment, but not the dynamic part (oscillations). The reason is that general containment codes normally are not capable of handling the oscillatory phenomena correctly. For such purpose special codes are used.

Each participant in the standard problem was to perform the calculations with the computer code available to him and in such a way that the time history behaviour occurring in the experiment of pressures, temperatures, masses in the containment compartments, as well as the pressure differentials between the containment compartments, were precalculated as realistic as possible.

Calculations were suggested for 3 time intervals, 0 - 1.4 s, 0 - 4.4 s and 0 - 220 s. Since there was only one submittal for the 0 - 1.4 s interval, this submittal will be discussed together with the 0 - 4.4 s submittals.

For the representation of the containment two different approaches were offered, either

- Full representation of both drywell and wetwell

or

- Starting with the flow in the vents (vent pipe header), thereby avoiding the problems connected with representation of the quite complicated Marviken drywell.

The second alternative was not used by anyone, but instead a similar approach was used by some participants, controlling vent flow, in particular air flow, by input modifiers.

The variables for which results were requested are listed in Table A.13. The variables are indicated on basis of measuring positions, as shown in Figures B.4 through B.6.

#### 4. SUBMITTED RESULTS

Results were submitted for all three time-periods specified in Table A.13. Since there was only one submittal (ARIANNA-1, Italy) over the 0 - 1.4 s time period, this case will be discussed together with the 0 - 4.4 s cases. We will thus in the following discuss two time-periods, 0 - 4.4 s (from now on denoted by "short-time" period) and 0 - 220 s ("long-time" period).

##### 4.1 Computer codes used

Submitted results were obtained from the codes

- ARIANNA-1 (University of Pisa, Italy)
- CONTEMPT-LT/26 (University of Pisa, Italy)
- CONTEMPT-LT/28 (VTT, Finland)
- COPTA-7 (STUDSVIK, Sweden)
- ZOCO-V (ECN, Netherlands)

In Section 4.1.1 through 4.1.5 a brief description will be given of each of these codes, mainly as given in the submittal reports (Ref 19 through 22). Finally, in Section 4.1.6, the code differences of greatest importance to the standard problem will be shortly discussed.

#### 4.1.1 ARIANNA-1 Code

ARIANNA-1 is a code (23) for the analysis of thermal-hydraulic transients in a dry containment.

It can provide up to 100 volumes connected by 200 junctions, 20 of which may have time-dependent or  $\Delta p$ -dependent areas.

In each volume a stagnant homogeneous mixture of steam, air and water is assumed. The up-to-date version of the code includes a simplified model of deentrainment from which a pool results in each volume. This model takes into account only the effects of the fall-down of water droplets with low kinetic energy; the water impingement on internal structures is not taken into consideration by the ARIANNA-1 Code.

Mass and energy addition, into as many as five individual volumes, is provided.

The transient is described as a sequence of quasi-steady states. Mass and energy flows in each time-step are based on the thermodynamic conditions of the previous time-step.

The calculations are based on the following assumptions:

- stagnation pressures in the connected volumes give the  $\Delta p$  across the vent;
- fluid properties are assumed on the basis of the thermodynamic properties of the upstream volume and are frozen throughout the flow process.

The flow models used for the calculations are summarized in Table A.14.

Thermodynamic equilibrium is assumed in each volume; the state variables are determined by the solution of the state implicit equation with an iterative method.

For the calculation of the ISP17 a special compartment model has been introduced in ARIANNA-1. For this compartment the pressure is calculated by a time dependent input function and can be used to simulate the wet-well backpressure at the end of the vent pipes.

Particular care is given to the modelling of the heat structures and the heat transfer coefficients, so that it is possible:

- to provide up to 100 heat structures;
- to define up to 25 different materials;
- to choose from among three geometrical shapes (slab, cylindrical and spherical), described as one-dimensional;
- to define up to 25 constant, up to 25 time-dependent and 1 structure-temperature dependent heat transfer coefficients;
- to use the Uchida correlation, a natural convection model and/or the irradiation model.

ARIANNA-1 cannot presently\* predict the long-term behaviour of containment systems, because the compartments modelled with this code may contain two separated regions (vapor and liquid pool), but pool boiling, evaporation and steam condensation are not allowed.

---

\* A new version of the ARIANNA-2 Code which takes into account these phenomena and the carry-over of droplets between adjacent volumes is under development at DCMN.

4.1.2 CONTEMPT-LT/26 Code

CONTEMPT-LT/26 is a well known computer code (24) specifically written for the long-term analysis of the containment transient during a LOCA, particularly in pressure suppression systems (see Table A.15 ). The code can be used to model one to four compartments (vessel and suppression pool included), together with the engineered safety systems (as fan coolers and/or water sprays) present in the containment.

The code is not suitable for the analysis of the transient in a subdivided drywell, because the compartments are specialized; only compartment Number 3 can be used to simulate the drywell of a pressure suppression containment.



4.1.3 CONTEMPT-LT/28

The analyses have been performed using version 2 of the CONTEMPT-LT/28 code, revised by VTT. The additions and corrections made to the original program (25) are the same as presented in reference 28, excluding the subprogram HEAT which was recoded for the LT/28-version by the supporter. The main remedies of the version used, are the updatings of the volume and internal energy of vapor regions caused by changes of liquid region volume, and the addition of a model for steam flow through the wetwell pool. The version has also a new output routine, which allows to plot all variables existing in the common areas. A brief description of the code follows below.

CONTEMPT-LT/28 is a digital computer program, written in FORTRAN IV, developed to describe the long-term behaviour of water-cooled nuclear reactor containment systems subjected to postulated loss-of-coolant accident (LOCA) conditions. The program calculates the time variation of compartment pressures, temperatures mass and energy inventories, heat structure temperature distributions, and energy exchange with adjacent compartments. The program is capable of describing the effects of leakage on containment response. Models are provided to describe fan cooling and spray cooling engineering safety systems. Up to four compartments can be modeled with CONTEMPT-LT, and any compartment except the reactor system may have both a liquid pool region and an air-vapor atmosphere region above the pool. Each region is assumed to have a uniform temperature, but the temperatures of the two regions may be different. CONTEMPT-LT can be used to model all current boiling water reactor pressure suppression systems, including containments with either vertical or

horizontal vent systems. CONTEMPT-LT can also be used to model pressurized water reactor dry containments, subatmospheric containments, and dual volume containments with an annulus region, and can be used to describe containment responses in experimental containment systems.

As already mentioned the most significant changes in the code are directed to the vapor regions and steam condensing in the liquid pool. The influence of the volume (surface) changes of the liquid pool to the vapor region balance was not taken into account in the original version. As to the wetwell the updating of vent pipe submergence depth and static back pressure was failing also. These are now corrected in the VTT versions.

The original condensation model for vent steam assumed that the air rises from the wetwell pool fully dry. This has been replaced by a more natural model, which transfers air into the vapor region in the state of 100 % humidity, i.e. steam accompanying air has a partial pressure corresponding the saturated pressure of water in the pool temperature.

In connection with the wetwell vapor region heat balance it is possible to choose a use of  $c_p$  or  $c_v$  (specific heat at a constant pressure or at a constant volume) for energy increase caused by added air. Naturally  $c_p$ , i.e. enthalpy was used in these analyses. The use of  $c_v$  omits the compression work made by gas flowing into the control volume.

The CONTEMPT-LT program can model four compartments. The primary reactor compartment is, however, rather simple having one region only. The water

discharge rate from the reactor to the drywell has to be given by an input table. The primary model has not been utilized in the analyses under discussion.

Each of the remaining three compartments: drywell, annular (or dual) compartment and wetwell has two regions, a vapor region and a liquid region. These cannot be divided into subcompartments, and are assumed to be in thermal equilibrium. However, the temperatures of the two regions of each compartment can be different. In the energy and mass balance of the regions several activities can be taken into account. These include direct additions of water, steam, air and energy, heat transfer into structures and between compartments. There is no educated model for liquid water in the vapor regions. All water condensed from steam is dropped immediately on the bottom or, in the case of suppression containment, kept optionally floating in the gas region.

The vent model has a dynamic part for water clearing and a stationary part for choked or unchoked gas flow. It is possible to describe rather complicated flow systems with different elements and flow paths. However, only a multiple of a straight pipe is modelled in the present analyses. The irreversible energy losses in the other parts of drywell have been equivalenced and added to the entrance coefficient.

The code provides the capability to allow a user to modify the mixture composition of the flow through the vents. This can be achieved by vent flow mass fraction modifiers, which are used to calculate the final mass fractions. Modifiers are applicable for all mixture elements: liquid

water, steam and air. Liquid water can also be separated through a distinct input constant. Modifiers are time dependent and given by an input table.

The CONTEMPT-LT code applies a multilevel iteration process for numerical solution of balance equations. The process has also a certain trial procedure for temperature. Heat transfer to the structures is calculated by means of Crank-Nicholson implicit scheme. The vent clearing process utilizes a five step Runge-Kutta technique.

#### 4.1.4 COPTA-7

COPTA is a computer model for analyzing pressure and temperature transients in a multicompartment containment building, resulting from a postulated loss-of-coolant accident. Both pressurized water reactor dry containments and boiling water reactor pressure-suppression containments can be modelled.

The analysis is performed by dividing the containment into an arbitrary (but limited) number of compartment, connected by an arbitrary number of pipes and orifices. Each compartment is normally assumed to contain a gaseous and a liquid phase, the phases need not be in thermal equilibrium with each other. The two phases may exert influence on each other by mass and energy transport across the liquid surface - water drops falling into the liquid phase, air and steam bubbling up from the liquid and heat transfer across the surface. Simpler compartment models, assuming e.g. thermal equilibrium, are also available.

The gaseous phase will contain non-condensable gases (normally air) and either super-heated or saturated steam and may contain entrained droplets. Up to 5 different non-condensable gases may be treated at the same time. The entrained water droplets fall down to the liquid phase by gravity.

The liquid phase will contain subcooled or saturated water and may contain air/steam bubbles. The air bubbles formed e.g. after vent clearing in a BWR LOCA will rise to the pool surface and also carry steam, corresponding to saturation conditions, to the gaseous phase. There is a choice between two different vent clearing and pool swell models, one simple, based on a constant bubble rise velocity, and one more sophisticated. In other problem areas, boiling may occur, in which case steam bubbles are formed, and rise to the gaseous phase.

For each compartment the conservation equations for mass and energy are solved for each phase and each component. The flow between connected compartments is calculated using the linear momentum equation.

The computer model also considers such phenomena as heat transfer to internal structures and walls (using the one-dimensional heat equation), cooling of primary and secondary containment with fans or water spray (with optional heat exchangers), reversed flow through vacuum-breakers and arbitrary heat inputs (resulting e.g. from hydrogen burning).

Mathematically the problem is formulated as a system of non-linear differential equations and the program contains three different numerical

methods for solving these equations, two explicit methods which are used mainly for short-term transients and testing, and one implicit method based on the midpoint rule which is recommended for long-term transients.

The version COPTA-7 used for ISP17 differs from the version COPTA-6, described in the basic code description (26) mainly in the following aspects

- Extended flash models (allows interpolation between the two flash models contained in COPTA-6).
- Allows the user to specify that some given amount of air will not participate in the vent pipe flow (implemented specially for ISP17).

#### 4.1.5 ZOCO-V

The calculations for ISP17 are performed with the modified code ZOCO-V. A full description of the code is given in Ref 27. The ZOCO-code is a multi-node model and the communication between the nodes is done by a one-dimensional analytical model for the flow paths. In principle the following equations are used:

$$\text{mass balance} \quad \frac{d}{dt}m = F_i - F_o$$

$$\text{energy balance} \quad \frac{d}{dt}\mu = F_i h_i - F_o h_o + Q$$

$$\text{mass flow} \quad F = C_d A \sqrt{\frac{2\Delta P}{v}}$$

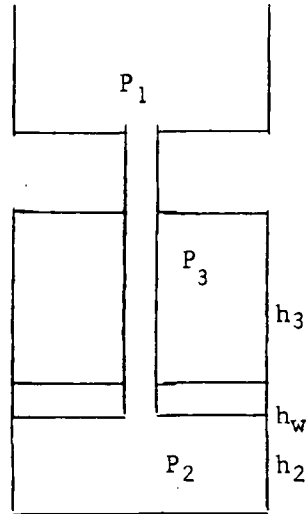
$$\text{equation of state} \quad P = f(\rho, T)$$

$$\text{heat transfer} \quad Q = \alpha A (T - T_{\text{wall}}).$$

Including a model for the wall temperature these equations represent the total model. The nodes may consist of water, steam and air in homogeneous thermal hydraulic equilibrium with each other. The following changes are made compared to the original ZOCO-V version:

- a An automatic switch from superheated steam to equilibrium conditions with water.
- b Heat transfer to walls. Instead of calculating the boundary wall temperature, the mean temperature of the outer wall is changed from  $Q = \alpha A(T - T_{\text{wall}})$  into  
$$Q = \alpha_t A(T - T_{\text{wall}})$$
 where  $1/\alpha_t = 1/\alpha + \sigma/2\lambda$ .
- c The carry-over factor is defined as that part of all the water in the room which is as particles in the steam-air mixture.

## d Waterlift-model.

 $A_v$  = vent area $A_p$  = pool area $k = \frac{c_p}{c_v}$  air $h_w$  = submerged length of the vent pipe $g = 9.81 \text{ m/s}^2$  $F_i$  = air flow $h_i = c_{p(\text{air})} T_i$  $D_v$  = vent diameter $V_s$  = pool surface velocity $V_v$  = velocity in the vent

The length of the vent pipe is extended with its diameter. Moment of vent clearance:

$$P_2 = P_1 \quad T_2 = T_1$$

$$h_2 = \frac{\pi D_v^2}{4} \times D_v / A$$

$$(\mu)_2 = P_2 V_2 / (k-1)$$

$$v_s = \frac{A_v V_v}{A_p}$$

After vent clearance:

$$\frac{d}{dt}(\mu)_2 = F_i h_i - P_2 A_v$$

$$\frac{d}{dt}(\mu)_3 = P_3 A_v$$

$$\frac{d}{dt} v_s = (P_2 - P_3) / (\rho_w h_w) - g$$

$$\frac{d}{dt} h_2 = v_s \quad \frac{d}{dt} h_3 = -v_s$$

$$\frac{d}{dt} m_{2\text{air}} = F_i$$



It is assumed that for the calculation of the waterlift the steam condensates immediately in the wetwell:

$$P_2 = (k - 1)(\mu)_2 / (h_2 A_p)$$

$$P_3 = (k - 1)(\mu)_3 / (h_3 A_p)$$

The range of application of the code ZOCO-V for the calculation of temperatures and pressures in the containment is:

pressure	.02 - 5.0 bar
temperature	18 - 152°C.

The maximum number of compartments is 11. The possible combinations are:

- a One wetwell compartment and 1 - 10 compartments of drywell type.
- b No wetwell compartment and 1 - 11 compartments of drywell type.

#### 4.2 Basic input data used

A summary of some of the basic input data used by the submittals is given in Tables A.16 through A.19.

The main differences concern

- Drywell heat absorbing areas (Table A.16)
- Heat transfer coefficients (Table A.17)
- Nodalization (Tables A.18 and A.19)
- Flashing (Tables A.18 and A.19)
- Air modifiers (Tables A.18 and A.19)

A brief discussion of these is intended to be included here later on.

#### 4.3 Main differences between codes and data as related to ISP17

A summary of some basic code characteristics is given in Table A.15.

ARIANNA-1 is a dry containment code. It can thus not treat the wetwell phenonema. The gas volume of the drywell did, however, increase due to the water plug movement only by less than 0.6 % up to vent clearing. Therefore it is quite possible to use such a program for the period up to vent clearing (0 - 1.4 s).

An advantage of ARIANNA-1 is that the drywell may be subdivided into a large amount of subcompartments (maximum 100), and therefore presumably give better results for pressure differences, flow composition etc in the drywell.

In the submitted run, a subdivision of the drywell into 17 subcompartments was used (see Figure B.7).

The code CONTEMPT-LT/26 does not allow subdivision of the drywell into subcompartments and therefore cannot be used to compute e.g. pressure differences in the drywell.

The code is also not capable of predicting the pool swell in its present version.

In order to correctly compute the air mass flow from the drywell to the wetwell, an input data table has been used to control this flow.

In the submitted calculations, an insufficiency was present in the code, meaning that no steam was carried to the wetwell gas phase by the air

rising through the wetwell pool. This was later corrected and results from the corrected version were added in the parameter study.

The version CONTEMPT-LT/28 similarly cannot compute pressure differences in the drywell and pool swell.

For the air mass flow an input data table has been used to modify the flow composition through the vent pipes in such a way that the evaluated air mass transfer was very closely approximated.

Both the CONTEMPT codes can make predictions on the steam evaporating from the pool surface, after that the flow of air has ceased, but this effect is practically negligible.

The COPTA-7 code has been run with a 4-node subdivision of the drywell in the short-time case and with a single node for drywell in the long-time case.

In order to get the right final value of air transferred to the wetwell, some amount of air has been assumed retained in the drywell, participating in the thermo-dynamics but not in the vent pipe flow.

Different flashing models have been used for the two geometrical subdivisions, in order to get approximately the same flow of liquid water into the vent pipes, and at the same time approximating the pressure differences in the drywell sufficiently well.

The ZOCO-V code uses the 4-node subdivision also in the long-time run.

The code assumes thermal equilibrium in all compartments, i.e. also in wetwell, and therefore underpredicts wetwell gas temperatures in roughly the first half of the transient.

No specific assumptions have been made concerning air flow modifiers, which means that the final amount of air transferred to the wetwell will be overpredicted.

The assumption of thermal equilibrium and the slightly too large flow of air to some extent balance in the first part of the long-time transient.

## 5. COMPARISON OF CALCULATED RESULTS AND EXPERIMENTAL DATA

In this chapter we will discuss the results obtained by the participants in relation to the experimental data. We will start with the short-time behaviour and then continue with the long-time behaviour. A summary of the submitted results is given in Table A.20.

Curves for submitted results as well as for measured or evaluated experimental data are plotted in Diagrams C.1 through C.35. The same symbols have been used throughout in these diagrams, with dashed lines for experimental results, chain-dashed for the two Swedish submittals, chain-dotted for the two Italian and solid lines for the Finnish and Dutch submittals.

### 5.1 Short-time behaviour

Six sets of results, produced by five computer codes were submitted for the short-time period. These sets of results are

- ARIANNA-1, 17 nodes
- CONTEMPT-LT/26, 2 nodes
- CONTEMPT-LT/28, 2 nodes
- COPTA-7, 2 nodes
- COPTA-7, 5 nodes
- ZOCO-V, 5 nodes

Two types of diagrams, A and B, have been produced for the short-time period.

The A-type diagrams (Diagram C.1A through C.17A) contain results produced by runs with drywell subdivided into subcompartments. A run with the COPTA

code using only one node for drywell is also included in order to illustrate the influence of drywell subdivision (see Table A.20).

The B-type diagrams (Diagram C.1B through C.17B) contain results produced by runs using only one node for drywell. The results produced by the ZOCO Code, using 4 subcompartments for drywell, is also included, mainly because it is the only multi-compartment run that continues into the long-time case, as the other B-type runs do.

In some cases either A or B type diagrams are missing, since they have been considered of less interest. Some of the key results for the short-time cases are listed in Table A.21.

5.1.1 Short-time pressure difference between drywell and wetwell (Diagrams C.1A and C.1B)

-----

Curves for the short-time pressure difference between compartment 110 (lower drywell) and 105 (wetwell) are plotted in Diagrams C.1A and C.1B. Most submittals approximate the measured curve quite well, as a rule with a slight overestimate. The main exception is the Finnish submittal that overestimates the pressure difference by roughly 50 %. The main reason for this is probably (see Section 5.1.8) that the standard heat transfer coefficient used (Uchida) is too low for this case, giving too fast pressurization of the drywell. Another reason is the influence of the omission of rooms 123 and 124 and their heat soaking structures.

5.1.2 Short-time pressure difference between  
-----header and wetwell-----

The same statements as for drywell to wetwell hold for the short-time pressure difference between header and wetwell as shown in Diagrams C.2A and C.2B. Of the submitted results only the multi-node submittals differ from the previous two diagrams.

5.1.3 Short-time pressure difference between  
-----compartments 122 and 124-----

The short-time pressure difference between the break compartment 122 and the top compartment 124 is shown in Diagram C.3A, comparing the three multinode submittals with experimental values. Note, that in this diagram, as well as in the two following, the zero level is not at the bottom of the diagram. Note also, that the experimental pressure difference for these three diagrams (C.3A - C.5A) is obtained as the difference between measured data by probe 122M144 and appropriate probes for the other compartments. Any error in the 122M144 data will thus be present in all of these three diagrams.

5.1.4 Short-time pressure difference between  
-----compartments 122 and 110-----

The short-time pressure difference between the break compartment 122 and lower drywell (110) is shown in Diagram C.4A. All three submittals approximate the experimental results fairly well, the Swedish submittal slightly overestimating and the Dutch slightly underestimating for most of the transients, while the Italian submittal is quite close.

5.1.5 Short-time pressure difference between  
----- compartments 122 and 106 -----

The short-time pressure difference between the break compartment 122 and the header 106 is shown in Diagram C.5A. All three submittals approximate this quantity quite well. The Italian submittal, using 17 nodes for drywell, even appears to approximate the oscillatory behaviour of the pressure difference.

A final point to make is that there appears to be an initial negative pressure difference for the measured data in all three Diagrams C.3A through C.5A. This emanates from an initial decrease in the measured pressure for the break compartment 122 (see Diagram C.7A). Whether this is real or not is hard to say. It could have some connection with the initial cold water plug in the discharge pipe (which has not been modelled by the participants) or it could be some measuring error. None of the submittals exhibits this initial negative peak.

5.1.6 Short-time pressure transient for com-  
----- partment 124 -----

The short-time pressure transients for the top compartment 124 are shown in Diagram C.6A. All the submittals approximate the experimental curve quite well with a slight overestimate for the two 5-node submittals. The Italian submittal fits the experimental curve quite well.

5.1.7 Short-time pressure transient for com-  
----- partment 122 -----

The short-time pressure transients for the break compartment 122 are shown in Diagram C.7A. As for the top compartment, all submittals fit the experi-



mental curve quite well, with slight overpredictions for the 5-node submittals and quite good fit for the ARIANNA run.

5.1.8 Short-time pressure transient for compartment 110  
-----

The short-time pressure transients for compartment 110 in lower drywell are shown in Diagrams C.8A and C.8B. All the submittals approximate the experimental curve quite well, except the Finnish submittal, which somewhat overestimates the experiment. The main reason for this overestimate is that the standard heat transfer coefficient (Uchida) has been used for the drywell structures, giving a too fast heating of the drywell and therefore too fast pressurization of the drywell. It also leads to an overestimate of the steam flow rate into the pool, the heating rate of the pool, and therefore also to some extent increases the drywell pressure through increased wetwell pressure and increased pressure difference over the vent pipes. In a parameter study (case SF3), a much higher value (up to  $5 \text{ kW/m}^2, \text{K}$  compared to the Uchida maximum of  $1.6 \text{ kW/m}^2, \text{K}$ ) has been used for the heat transfer coefficient in drywell, and that run shows considerably better correspondance with the experimental curve. Another, but less important reason is that in the Finnish submittal, the uppermost subcompartments have not been included, giving slightly smaller compressible volume and heat soakage area, and therefore faster pressurization.

The two 5-node runs (Italy and Sweden) show a similar, but much smaller, overestimate.

5.1.9 Short-time pressure transient for com-  
partment 106  
-----

The short-time pressure transients for compartment 106, the header, are shown in Diagrams C.9A and C.9B. Essentially the same comments are valid as for Diagrams C.8A and C.8B.

5.1.10 Short-time pressure transient for  
wetwell  
-----

The short-time transient for wetwell are shown in Diagram C.10B. The correspondance with the measured curve is fairly good, with the Finnish and Dutch submittals slightly overestimating and the Swedish and Italian submittals slightly underestimating the pressure rise. The reasons are slightly different.

For the Finnish submittal, the main reason is probably that the heat transfer between the pool and the wetwell atmosphere, which is quite large between approximately 2 and 20 s due to water splashing, has been ignored. The initially too high steam flow rate gives an overestimate of the pool temperature, which influences the wetwell pressure through the rising air/steam bubbles. Another contributing factor could be overestimation of the initial air flow in connection with too fast vent clearing (see Diagrams C.27 and C.30). Overestimate of the flow of air is probably also the main cause of the overestimate by the Dutch submittal. Since ZOCO-V uses thermal equilibrium for the wetwell compartment, corresponding to an infinite heat transfer coefficient between the pool and the wetwell atmosphere, one should in fact have expected an underestimate of the pressure rise, instead of an overestimate.

The underestimates by the Swedish and Italian submittals are probably mainly caused by underestimates of the initial air flow. This underestimate, which to a large extent emanates from the use of a 1-room model for drywell, more than compensates the effect of the omission of heat transfer between pool and wetwell atmosphere.

5.1.11 Short-time temperature transient in  
-----compartment 124-----

The short-time temperature transients for the top compartment 124 are shown in Diagram C.11A. Apart from the initial transient the correspondence is very good. The initial transient is mainly of theoretical interest, but it could be of some value to discuss the possible reasons for the different shapes of the curves.

The ARIANNA and COPTA curves both exhibit a minimum after some tenths of a second. The reason for this is that water drops enter from the break compartment 122 in the slightly superheated top compartment 124 and are instantaneously evaporated according to the equilibrium models used. This process requires so much energy that the temperature drops, even though the entering mixture is hotter than the compartment 124. When compartment 124 has reached saturation, the temperature starts to rise.

The behaviour of the ZOCO transient is somewhat hard to explain.

5.1.12 Short-time temperature transient in  
-----compartment 122-----

The short-time temperature transients for the break compartment 122 are shown in Diagram C.12A. The correspondence with measured values is quite

good. For the initial 0.1 s transient similar arguments hold as for Diagram C.11A. It also appears from Diagram C.12A that the temperature measurements are some 0.2 s slow. In the "Zero time" section of Chapter 4 of MXB-218 (14) it is stated that all the PCM-data (i.e. data in M-tables and M-diagrams) were slow by 187 ms due to incorrect zero signal conversion. This delay has however been corrected when plotting the "MX-data" in the present report.

5.1.13 Short-time temperature transient in  
----- compartment 111 -----

The short-time temperature transients for compartment 111 in lower drywell are shown in Diagrams C.13A and C.13B. Essentially the same arguments hold as for Diagram C.12A.

5.1.14 Short-time temperature transient in  
----- compartment 106 -----

The short-time temperature transients for compartment 106, the header, are shown in Diagrams C.14A and C.14B. The submittals using a single node for drywell, for that reason, deviate fairly much from the measured values. This has, however, only small effect on the other results, since this excess heat is mainly stored in the wetwell pool. The submittals using four nodes for drywell show fairly good correspondence to the measured values.

5.1.15 Short-time temperature transient in  
----- wetwell vapor -----

The short-time temperature transients for the wetwell vapor are shown in Diagrams C.15A and C.15B. All the submittals show a considerably faster temperature increase than the curve for measured data. One possible reason for this could

be that the heat transfer coefficient for the temperature transducers is quite small up to the break-through of the pool water surface at around 3 s (see Diagram C.17), slowing down the temperature response of the probes. After break-through, the furiously splashing water will tend to retain the vapor phase at the temperature of the pool, until the air flow rate is decreased sufficiently (from around 10 s, compare Diagrams C.25 and C.27).

The differences between the submittals are mainly due to different vent clearing time and initial air flow, to some extent also to other effects, such as heat transfer to solid structures in the wetwell vapor.

#### 5.1.16 Water plug size

Curves showing the sizes of the water plugs in the vent pipes are given in Diagrams C.16A and C.16B. If the dynamics of the water plugs are modelled similarly for the codes involved, these curves should be closely related to the curves for header pressures shown in Diagrams C.9A and C.9B. A check reveals that this appears to be true for the computed curves. Compared to the measured curve, the computed curves give a slightly too fast vent clearing time, though the difference is fairly small.

#### 5.1.17 Pool swell

Only two of the codes contain special models for pool swell, COPTA and ZOCO. The submitted results from these two codes are shown in Diagram C.17A, together with measured curves for different vertical location in the Marviken wetwell. The bottom of the header, which drastically changes the available cross-sectional area, is roughly 4.8 m

above the vent pipe outlet (zero point of level scale). Therefore one should not pay too much attention to the behaviour above that level for the measured data.

Anyhow, the pool swell models give a roughly correct picture of the pool swell and for COPTA also for the break-through time (ZOCO does not indicate break-through within the time period studied).

## 5.2 Long-time behaviour

Results produced by four computer codes are compared for long-time behaviour. The results compared are produced by

- CONTEMPT-LT/26, 2 nodes
- CONTEMPT-LT/28, 2 nodes
- COPTA-7, 2 nodes
- ZOCO-V, 5 nodes

The ZOCO-V run uses a subdivision of drywell into 4 subcompartments, all the others use a single node to represent drywell. The ZOCO-V run also, unlike the other runs, does not make any attempt to artificially control the flow of air through the vent pipes.

Therefore the ZOCO run is stopped at around 75 s when the amount of air transferred to the wetwell exceeds the total amount transferred at the end of the experiment.

The COPTA run specifies the amount of air retained in drywell at the end of the test and is therefore approximatively correct concerning the total amount

of air transferred to wetwell at the end of the blowdown, while the time history differs from the actual one.

Both of the CONTEMPT runs control the flow composition in such a way that also the time history of air transfer is approximatively correct.

The transfer of air into the wetwell is of quite great importance for the long-time behaviour, and therefore the results for many other parameters (pressures, differential pressures, temperatures) depend to a large extent on the assumptions made for the air transfer.

#### 5.2.1 Long-time pressure difference drywell - ----- wetwell -----

In Diagram C.18 the test data are represented by two dashed lines, corresponding approximately to the minimum and maximum values of the pressure oscillations. Thus they do not represent error limits or confidence intervals, although for much of the transient they might be of roughly the same order of magnitude as these.

The peak pressure difference at around 30 s is quite exactly predicted by all runs (although the Finnish submittal also does exhibit a substantially larger peak at around 7 s).

Most parts of the submitted results fall between the minimum and maximum of the oscillations. Exceptions are

- The early transient from 5 s or less to between 10 s and 20 s, where most runs overpredict the pressure difference, Italy the least and Finland the most. As discussed earlier, the deviation

for the Finnish submittal is mainly due to a too low heat transfer coefficient in drywell.

- The Italian submittal slightly underpredicts in the later phase of the blowdown.
- After the cessation of the blowdown the decrease of pressure difference for the Italian submittal stops at around the hydrostatic pressure corresponding to the submergence depth, while the Finnish and Swedish submittals continue below this value, fairly close to the experimental curve.

The behaviour after the cessation of the blowdown should not be given too much attention in this standard problem, since most participants probably have not tried to fit this part by choosing correct heat transfer values etc, but it could all the same be worthwhile for the participants to think about the information that this "tail" may give on some input parameters.

#### 5.2.2 Long-time pressure difference header - -----wetwell-----

Many of the comments made for the previous diagram (pressure difference drywell - wetwell) are valid also for Diagram C.19 (pressure difference header - wetwell). The pressure oscillations in the header were considerably larger than in the drywell, which is reflected by the larger distance between the dashed test curves. Of the submitted results naturally only the ZOCO results differ from those in the previous diagram. We can see, for instance, that all results overpredict the pressure difference up to 15 s or more.

#### 5.2.3 Long-time drywell pressure

The drywell pressure (Diagram C.20) depends to a large extent on the wetwell pressure and the



pressure difference required to maintain the flow through the vent pipes. The correspondence with measured data is on the whole quite good, with a few exceptions:

- o The Finnish submittal overpredicts the drywell pressure up to 30 s, as discussed earlier mainly due to the use of a too low heat transfer coefficient in drywell.
- o The Swedish submittal overpredicts the drywell pressure between 10 s and 120 s mainly due to overprediction of the wetwell pressure, which arises from the overprediction of the rate of transfer of air to the wetwell atmosphere.
- o The Dutch submittal predicts the drywell pressure quite well until 40 s, when it starts to overpredict due to overprediction of the wetwell pressure (see discussion in Section 5.2.5).
- o The "tail" after 170 s is fairly well predicted by the Finnish and Swedish submittals, but less well (not attempted?) by the Italian submittal.

#### 5.2.4 Long-time header pressure

Mainly the same comments as for Diagram C.20 are valid also for Diagram C.21.

In fact, among the submittals, only the ZOCO-V curve differs from those for the drywell pressure.

#### 5.2.5 Long-time wetwell pressure

The long-time wetwell pressure, shown in Diagram 22, depends to a very large extent on the amount of air transferred to the wetwell. Other parameters with large influence are mainly heat transfer to and from the wetwell atmosphere and steam addition to the atmosphere. The Marviken containment is somewhat strange in the aspect that use of a high heat transfer coefficient in the

wetwell atmosphere could increase the wetwell pressure, since the heat transfer from drywell through the large steel walled blowdown pipes could increase faster than the heat soakage of the concrete walls in wetwell for some range of HTC values. This, however, happens for fairly high HTC values, which normally are not used for the wetwell atmosphere.

Comparing Diagram C.22 with Diagram C.30 we see that the tendencies for the wetwell pressure quite closely follow the tendencies for the amount of air in the wetwell. The only exception is ZOCO-V, where overprediction of air in the wetwell still gives a very close approximation of the wetwell pressure up to 40 s or more. The reason is here that the equilibrium assumption of equal temperatures for pool water and wetwell atmosphere counteracts the larger amount of air.

Since the Finnish submittal has an almost perfect fit of air and steam transfer to the wetwell atmosphere, the main cause for the deviations, which in fact are very small, is most certainly an underestimate of the heat transfer to the pool water in the "splashing period".

For the other two submittals (Sweden and Italy), the possible inaccuracies in the models used for heat transfer to and from the wetwell atmosphere, as well as the steam addition to the wetwell atmosphere, are so small, that the inaccuracies in the rate of air flow to the wetwell dominates over other effects. This does not mean that these models are correct, only that the main deviation is caused by deviations in air mass.

The influence of the rate of steam addition to the wetwell atmosphere (compare Diagram C.34) could possibly be observed for the last 100 s of the transients. There the wetwell pressures of the Italian submittal, and to some extent also the Swedish submittal, are slightly lower than would be expected from the comparisons for amount of air in the wetwell.

#### 5.2.6 Long-time drywell temperatures

The drywell temperatures (Diagram C.23) are quite accurately predicted in all submittals. Slight underpredictions of the drywell temperature could be noticed for the two CONTEMPT runs after 10 s and for the COPTA run in the last part of the transient. These effects are small and are probably explained by the choices made of heat transfer and heat conduction parameters.

#### 5.2.7 Long-time header temperatures

The header temperature curve is quite close to the drywell temperature curve and three of the four submitted curves are identical for drywell and header. Therefore most of what is said for the drywell temperature comparison is also valid for the header temperature, (Diagram C.24), although the differences are perhaps even smaller here.

#### 5.2.8 Long-time wetwell gas temperature

The wetwell gas temperature curve shown in Diagram 25 is an average over values from some 30 different thermocouples that were located in the wetwell gas space.

None of the submittals approximates this curve very well for the first 20 - 30 s. Differences in the order of tenths of degrees are noticed.

For the ZOCO-V run the reason is quite evident, the assumption of thermal equilibrium inevitably leads to an underestimate of the wetwell gas temperature for such cases as ISP17.

For the other runs, the main reason is presumably that the influence of the large contact area between the pool water and the wetwell atmosphere during the period of high air flow and water splashing has been underestimated or deliberately neglected.

It should be noticed, however, that the seemingly large differences do not have that large effect on the pressures or other parameters, since the main influence is through the state equation for air  $P_a V_a = m_a R_a T_k$ , where  $T_k$  is the temperature in Kelvin. Thus an error of say 15 K corresponds to a relative error in  $P_a$  or  $m_a$  of around 5 %.

In the later part of the transient the curve for the Swedish submittal decreases faster than the experimental curve and the CONTEMPT curves. The reason for this is partly because the transfer of air to the wetwell occurred faster in the Swedish submittal. There could also be some influence from the choice of heat transfer and heat conduction parameters, but this influence is hard to estimate.

There are two more points of some theoretical interest, although a thorough evaluation is perhaps not feasible. The first is that there is a crossover between wetwell gas temperature and pool temperature at roughly 150 s. The second is that the end of the blowdown at 170 s leads to a decompression of the drywell, leading to a reentry of the water plug in the vent pipes. The volume of this water plug, which is of the order of some

meter (or meters) times  $2 \text{ m}^2$ , corresponds to an adiabatic expansion of the wetwell atmosphere, in addition to the ongoing thermal exchange with pool water and solid structures. This effect is possible to detect on the experimental curve and also on the CONTEMPT runs (although perhaps over-estimated?).

#### 5.2.9 Long-time average pool temperature

The experimental value of the pool temperature (Diagram C.26) has been evaluated from several thermocouples in the pool.

This temperature is strongly connected with the amount of steam condensed in the pool. The MX curve for the total amount of steam through the vent pipes (Diagram C.31) has in fact been computed from the temperature rise of the pool water. Therefore it is not any surprise that Diagrams C.26 and C.31 show the same tendencies. On the contrary this indicates some degree of consistency, concerning condensation of the steam, between the codes used for the submitted runs, and the code used to compute the steam flow through the vent pipes. The fact that the IRE curve for steam flow is fairly close to the MX curve (see Diagram C.28 and C.31) indicates that this is also true vis-a-vis the experiment.

We can therefore use Diagram C.26 together with Diagrams C.28 and C.31 to comment both on total steam flow and on pool temperature.

The three runs with a single node for drywell slightly overpredict the steam flow and consequently the pool temperature, while the ZOCO-V run with four nodes for drywell quite closely predicts the steam flow, but somewhat underpredicts the pool temperature.

The last point is somewhat surprising, since the ZOCO-V run also underpredicts the wetwell gas temperature (Diagram C.25).

The reason why the models with one node for drywell overpredict the steam flow is not quite clear, whether it has to do with the number of nodes and questions attached to that (water separation, condensation etc) or whether it has to do with choice of flashing models and heat soakage in the drywell.

#### 5.2.10 Long-time air flow

Curves for the air flow through the vent pipes are shown in Diagram C.27. Note, that in this diagram the time span is only 0 - 55 s (compared to 0 - 220 s for the other diagrams) and that the zero level is not at the bottom of the page.

The picture is quite messy and even the two curves representing the test data (MX and IRE) are quite different.

The MX data are not actually measured, but computed through use of the ideal gas law on the measured pressures and temperatures of the wetwell gas phase. The resulting curve for total amount of air transferred has then been differentiated and smoothed. The Finnish submittal is based on this curve but using slightly different values, essentially neglecting the smoothing for the first 10 - 20 s.

It is therefore hard to claim any certainty for "measured values", but it seems fairly probable that the correct curve should fall somewhere between the Finnish submittal and the IRE curve, presumably closer to the Finnish submittal.

If we turn to integrated air flow (Diagram C.30) the picture is considerably clearer.

We see that the two "measured" curves are fairly close to each other and that the Finnish submittal almost exactly matches the "MX-DATA".

The Italian submittal somewhat underpredicts the air transferred in the beginning and overpredicts in the last part of the transient.

Both the Dutch and the Swedish submittal overpredict the air transferred in the beginning. The Dutch submittal stops when essentially all of the drywell air has been transferred, while the Swedish submittal discontinues the air flow when approximately the right amount of air has been transferred.

All these tendencies are direct consequences of the input data chosen and the differences thus do not depend on differences in the codes but on differences in approach.

As commented earlier, the amount of air transferred has a great impact on the wetwell pressure (Diagram 22) and also to some extent on the drywell pressures and the wetwell gas temperature.

#### 5.2.11 Long-time steam flow

Two curves representing experimental data for steam flow through the vent pipes are shown in Diagram C.28. The IRE curve is a smoothed (by hand) representation of results from the infrared measurements. The curve denoted "MX-DATA" is obtained from measurements of the pool temperature. The fact that these two curves, obtained in

totally different ways agree fairly well gives us some confidence to use them and also indicates roughly the possible errors associated with them. The "IRE-DATA" curve is probably closer to the correct values, at least close to the steep parts (due to the smoothing method used for the "MX-DATA"). From the integrated values (Diagram C.31) we see that the total amount of steam added to the wetwell is predicted almost identically by the two methods.

Returning to Diagram C.28, we see that the Dutch submittal very closely predicts the steam flow up to 75 s.

The other three submittals overpredict the steam flow for most of the transient. The total overprediction is of the order of 20 % for the Italian and Swedish submittals and slightly larger for the Finnish submittal.

Possible causes for this overprediction could be the use of a one-node representation of drywell or the models and values used for flashing and condensation.

The prediction of the steam flow has a close relation to the prediction of pressure differences between drywell and wetwell (Diagrams C.18 and C.19).

#### 5.2.12 Long-time flow of water

As for the flow of air and steam there are two curves representing the flow of liquid water through the vent pipes (see Diagram C.29). The curve "IRE-DATA" has been measured by infra-red technique and then smoothed "by hand". The "MX-



DATA" curve has been obtained from the steam flow curve by using an assumption of constant steam quality adjusted as to satisfy the mass and energy balance for the pool water.

The "IRE-DATA" and "MX-DATA" curves differ enormously, the "MX-DATA" implying a transfer of totally 19 tons of liquid water, while the "IRE-DATA" imply only 0.8 tons. At least one of these must be totally wrong and it seems reasonable from different reasons to conclude that the "MX-DATA" curve is wrong. We cannot, however, claim that the "IRE-DATA" curve is right. The correct values could be somewhere between those two curves. In fact, the mass balance measurements (see Figure B.15) indicate that the computations and the IRE measurements could have underestimated the total water and/or steam flow by as much as 8 - 10 tons. Therefore the comparison is mainly between the codes and not so much code to experiment.

The submittals from Italy and Sweden indicate results of the same order of magnitude as the IRE-DATA. There are some significant differences, but since we cannot rely on the test data, no definite conclusions may be given. In the CONTEMPT code a choice has to be made between two extreme vapor region models. Either is all liquid water contained in the vapor region or is all liquid water immediately transferred to the floor. Since the drywell model used in the Finnish submittal does not allow liquid water (water drops) in the vapor region, the flow of liquid water is caused by a numerical residual only, which explains this apparently strange curve.

The same arguments may be used for the integrated mass flow of liquid water, Diagram C.32.

5.2.13 Total flow of air through vents

These data have been discussed earlier (see e.g. 5.2.10).

5.2.14 Total flow of steam through vents

These data have been discussed earlier (see e.g. 5.2.11).

5.2.15 Total flow of liquid water through vents

These data have been discussed earlier (see e.g. 5.2.12).

5.2.16 Mass of sump water

The reported mass of sump water (Diagram C.33) is evidently wrong, since the final amount, 260 tons, exceeds the amount expelled from the pressure vessel. A possible reason for this could be temperature drift in the differential pressure transducers used to measure water levels. If similar errors are present for the pool water measurements, this could explain much of the differences also for the measured flow of liquid water through the vent pipes.

Disregarding the experimental curve, we see in Diagram C.33 that all the four submittals give approximately the same sump water amounts. Although not a proof, this gives a strong indication that all the computed values are at least approximately correct, and certainly more correct than the experimental curve.

Measurements made after the blowdown (Figure 7:3 in Ref 11) did in fact give a final value of approximately 160 tons, and parameter studies made by Sweden cover a range of 148 - 175 tons.

5.2.17 Long-time total mass of steam in wetwell  
----- atmosphere -----

The experimental value ("MX-DATA") for the mass of steam in the wetwell atmosphere in Diagram C.34 was computed in the following way: The initial value was computed assuming 100 % relative humidity in the wetwell, and the air entering the wetwell atmosphere was assumed to carry steam corresponding to 100 % humidity at the temperature of the pool water. No steam evaporation was added to this.

Similar methods are used also by the codes for the Finnish and Swedish submittals, and the differences compared to the experimental curve arises mainly due to differences in pool water temperature (both submittals), timing of air transfer (Sweden) and initial humidity (86 % used by Sweden).

The results for the Dutch submittal are completely different due to the equilibrium assumption in the ZOCO-V Code.

Finally, the Italian submittal was run by a code version that did not account for mass transport of steam together with air into the wetwell atmosphere and therefore gives a constant value for the steam content. In a revised version of the code this facility has been implemented.

5.2.18 Total mass of steam + water through the  
----- vent -----

The curves shown in Diagram C.35 are the sums of the individual curves for steam and water, shown in Diagrams C.31 and C.32 respectively. Therefore the discussion is quite similar as for these diagrams. We can see that all the submitted curves for most of the transient fall between the "MX-DATA" curve and the "IRE-DATA" curve.

#### 5.2.19 Mass and energy balance

The mass and energy balances for some of the codes at 171 s is shown in Figure B.15.

#### 5.3 Concluding remarks

The correspondence between calculated results and measured data is in general good. Quite different approaches have been used by the participants, which means that the comparisons to a high degree are between the approaches chosen and measurements as well as between codes and measurements. Most of the existing differences may be explained by reference to the approaches and models used by the participants. For some parameters (mainly flow of water and to some extent also steam to the wetwell pool) the measured data are quite uncertain, precluding definite and exact judgements on submitted results.

6. COMMENTS BY PARTICIPANTS

This chapter is intended to include comments received by participants, as given in the planned workshop or in written contributions.

## 7.           PARAMETER STUDIES

This chapter is intended to comment upon parameter studies submitted by the participants and presented in appendices. Parameter studies have been made by three of the participants; Italy, Finland and Sweden.

## 8. REFERENCES

1. WINKLER  
CSNI report No 41.  
Comparison report on OECD-CSNI Containment  
Standard Problem No 1.  
May 1980.
2. NGUYEN and WINKLER  
CSNI report No 65.  
Comparison report on OECD-CSNI Containment  
Standard Problem No 2.  
May 1982.
3. MARSHALL and WOODMAN  
CSNI report No 77.  
Comparison report on Containment Analysis  
Standard Problem No 3.
4. Design report for the HDR containment  
experiments V21.1 to V21.3 and V42 to  
V44 with specifications for the pre-  
test computations.  
Report No 3, 280/82 KfK, Karlsruhe,  
Jan 82.
5. Working Group on Water Reactor Contain-  
ment Safety.  
Summary record of the Third Meeting held  
at the Chateau de La Muette, Paris on  
24th - 26th February, 1982.  
SEN/SIN (82) 11.
6. MARKLUND, J-E  
Proposal for an international contain-  
ment standard problem based on the Mar-  
viken full scale pressure suppression  
experiment SD-82/128, 82-09-06.
7. The Marviken Full Scale Containment Ex-  
periments.  
First series.  
Summary report MXA-1-301.  
October 1974.
8. The Marviken Full Scale Containment Ex-  
periments.  
Second series.  
Summary report MXB-301.  
March 1977.
9. MARKLUND, J-E  
Specifications for TBISP17 - An inter-  
national standard problem based on the  
Marviken full scale pressure suppression  
experiment BD18.  
STUDSVIK Technical Report SD-83/12,  
1983-03-23.

10. MARKLUND, J-E  
Preparatory meeting for ISP17.  
STUDSVIK Technical Report SD-83/24,  
1983-08-18.
11. The Marviken full scale Containment Ex-  
periments.  
Description of the test facility. MXB-101.
12. The Marviken full scale Containment Ex-  
periments.  
Measurement system. MXB-102.
13. The Marviken full scale Containment Ex-  
periments.  
Data accuracy. MXB-105.
14. The Marviken full scale Containment Ex-  
periments.  
Blowdown 18 results. MXB-218.
15. The Marviken full scale Containment Ex-  
periments.  
Appendix to Blowdown 18 results. MXB-  
218 App.
16. The Marviken full scale Containment Ex-  
periments.  
Summary report MXB-301.
17. The Marviken full scale Containment Ex-  
periments.  
Report abstracts. MXB-401.
18. MARKLUND, J-E  
Representation of walls and other struc-  
tures in a 5-room model of the Marviken II  
containment.  
Studsvik report SD-83/17.
19. BELLUCCI, L, MAZZINI, M, ORIOLI, F,  
PACI, S and ROMANACCI, R  
OECD-CSNI International Standard Problem  
No 17: Marviken Full Scale Pressure Sup-  
pression Experiment BD18. Calculation re-  
sults using ARIANNA and CONTEMPT-LT/26  
computer codes.  
Univ of Pisa, RL 082(84).
20. WOULDSTRA, A  
Calculational results of OECD Standard  
Problem ISP17 by means of the modified  
code ZOCO-V.  
ECN, Memo No 0.375.03-GR38 (OB79-24).



21. EERIKÄINEN, L  
TBISP17 - International Containment  
Safety Standard Problem on the Marviken  
Full Scale Pressure Suppression experi-  
ment BD18.  
Finnish calculations with the CON-  
TEMPT-LT/28 program.
22. MARKLUND, J-E  
Calculations by the code COPTA on OECD-  
CSNI International Standard Problem No 17,  
based on Marviken Blowdown 18.
23. CERULLO, N, GORLANDI, A M, ORIOLO, F  
ARIANNA: Un codici di calcolo per  
l'Analisi del Transitorio Termoidraulico  
in Sistemi di Contenimento Compartmentali  
XXXVI Congresso Nazionale  
dell'Associazione Termotecnica Italiana  
(ATI).  
Viareggio, 5 - 8 Ottobre 1982.
24. MINGS, W J  
Version 26 Modifications to the CONTEMPT-  
LT Program.  
SRD-83-76, April 1979.
25. CONTEMPT-LT/028. A computer program for  
predicting containment pressure - tempera-  
ture response to a loss of coolant acci-  
dent.  
NUREG/CR-0255. Idaho, March, 1979.
26. MARKLUND, J-E and JOHANSSON, Å  
Model description of containment program  
COPTA-6.  
Studsvik report AE-RD-105, 1979-07-12.
27. ZOCO-V, Ein Rechenmodell zur Berechnung  
von zeitlichen und örtlichen Druck-  
verteilung in Reaktorsicherheitsbehältern.
28. EERIKÄINEN, L  
Corrections and additions to CONTEMPT-LT  
computer codes for containment analysis.  
Revised version of CONTEMPT-LT/26.  
Helsinki 1980, Technical Research Center  
of Finland, Nuclear Engineering Labora-  
tory, Report 44, 24 p.

## LIST OF TABLES

- A.1 Test conditions for the blowdown tests in the second Marviken test series
- A.2 Survey of the data channels
- A.3 Error limits of pressure channels, DP-channels and temperature channels
- A.4 Containment volumes for Blowdown 18
- A.5 Flow areas in drywell
- A.6 Flow paths for the 4-node drywell
- A.7 Summary of heat soakage areas
- A.8 Suggested values of heat soakage constants
- A.9 Aluminium content in the containment
- A.10 Total steel content in the containment
- A.11 Suggested discharge flow data for Blowdown 18
- A.12 Summary of geometry and initial conditions for BD18
- A.13 Requested computations for ISP17
- A.14 Flow models in ARIANNA computer code
- A.15 Some basic computer code characteristics
- A.16 Summary of surface areas for heat absorbing structures
- A.17 Models used for heat soakage
- A.18 Some computer run details for short-time cases
- A.19 Some computer run details for long-time cases
- A.20 Submitted results for ISP17
- A.21 Some key results for short-time cases

Table A.1

Test conditions for the blowdown tests in the second Marviken test series.

BLOW-DOWN number	DISCHARGE CONDITIONS				VESSEL CONDITIONS		CONTAINMENT CONDITIONS						SPECIFIC FEATURE
	top pipe pre-purging	main discharge line orifice diam mm	flow reduction from sec	time of blow-down sec	pressure MPa	mass of water and steam Mg	depth wetwell pool m	vent pipe subm m	pool volume m <sup>3</sup>	number of open vent pipes	vent pipe flow area m <sup>3</sup>	wetwell pool temperature °C	
17	no	330	-	163	4.77	277	4.50	2.80	560	57	4.03	12	As BD 10 in MX-I
18	no	280	-	171	4.64	288	4.51	2.81	561	28	1.98	16	Reduced VP flow area
19	yes	280	-	146	4.71	289	4.54	2.84	564	28	1.98	16	As BD 18 except prepurging
20	yes	280	-	143	4.82	290	2.20	0.50	277	28	1.98	9	As BD 19 except lower pool depth
21	no	280	200	211	4.71	290	4.50	2.80	257/294	27/1	1.91/ 0.07	15	As BD 18 except pool partition
22	yes	280	125	340	4.73	290	4.48	2.78	256/293	27/1	1.91/ 0.07	17	As BD 19 except pool part and red flow after 125 s
23	yes	280	15	520	4.82	284	4.50	2.80	257/294	27/1	1.91/ 0.07	18	As BD 22 except low disch flow rate after 15 s
24	yes	280	80	220	4.80	284	4.50	2.80	257/294	27/1	1.91/ 0.07	16	As BD 22 except detuning of vent system
25	yes	330	70	180	4.89	286	5.51	3.81	314/344	27/1	1.91/ 0.07	13	As BD 24 except larger pool depth and single cell studies

TABLE A.2

Survey of the data channels.

Measurement position	Parameter	Scanning rate			Remarks
		10 Hz	952 Hz	contin- uous	
Pressure vessel	Pressure Temperature Mass of water Water level	2 10 4		1  1 10	DP-over-vessel Special type of probe
Main discharge line (Original steam line system)	Pressure Temperature Mass flow	5 3 2	1 1		Pitot tube
Top pipe (Prepurging line)	Pressure Temperature	1 2			
Drywell	Pressure Diff pressure Temperature Water level	9 2 16 1	8  7	1	DP-channel
Downcomers and vent pipe header	Pressure Temperature Flow velocity Mass composition	1 3	5 7 6	11	Radioactive tracer method and infrared attenuation technique
Vent pipes and around vent pipes	Pressure Temperature Water level Phase boundary	10	4 17 13 39		Level probes of spark plug type Level probes of spark plug type
Wetwell	Pressure Temperature Mass of water Water level Impact load Visualization	2 100 2	10  43 6	1	DP-channels Level probes of spark plug type Strain gauges Two TV-cameras
<u>Miscellaneous</u>					
Drywell-wetwell	Diff pressure	2	2		
Header-wetwell	"-		2		
DP-over-vessel, lead tubes	Temperature	4			

Table A.3

Error limits of pressure channels, DP-channels and temperature channels.

Parameter	Type	Location	Max error	Probable error
Pressure	VARIAN	Vessel and discharge pipe	$\pm 70$ kPa	$\pm 6$ kPa
Pressure	PCM	Vessel and discharge pipe	$\pm 90$ kPa	$\approx \pm 50$ kPa
Pressure	VARIAN	Containment	$\pm 6.3$ kPa	$\pm 0.4$ kPa
Pressure	PCM	Containment	$\pm 8.1$ kPa	$\pm 1.2$ kPa
DP	VARIAN	DP-over-vessel	$< \pm 4.8$ kPa	$\pm 1.0$ kPa
DP	VARIAN	Containment	$\pm 1.8$ kPa	$\pm 1.0$ kPa
DP	PCM	Containment	$\pm 2.1$ kPa	$\pm 2.0$ kPa
Temperature	VARIAN	Vessel, pipes and containment	$\pm 2.9^{\circ}\text{C}$	$\pm 1^{\circ}\text{C}$
Temperature	PCM	Vessel, pipes and containment	$\pm 4.3^{\circ}\text{C}$	$\pm 1^{\circ}\text{C}$

Table A.4

Containment volumes for BD18.

Room	Volume, m <sup>3</sup>
124	312.0
A	102.0
B	133.5
123	43.9
123.1	10.6
123.2	70.9
123.3	10.3
122	175.5
121	298.5
114	16.7
113	63.7 <sup>1</sup>
112	115.9
111	100.2
111.1	185.1
110	121.0
104	66.5
106	140.8
Drywell, excl v p	1967.1
Vent pipes <sup>2</sup>	5.3
DW, active volume	1972.4
Wetwell, excl v p	2133.0
Water plugs <sup>3</sup>	5.6
WW, active volume	2138.6
Inactive vent pipes <sup>4</sup>	10.9

<sup>1</sup> The drain pipe valve just below the floor of room 113 is assumed to be closed during blowdown

<sup>2</sup> 28 pipes, 1.98 m<sup>2</sup>, 5.5 - 2.81 = 2.69 m length

<sup>3</sup> 28 pipes, 1.98 m<sup>2</sup>, 2.81 m submergence depth

<sup>4</sup> 29 pipes, 1.98 m<sup>2</sup>, 5.5 m length

Table A.5

Flow areas in drywell.

Connection	Description	Area (m <sup>2</sup> )
124 - B	18 Ducts by-passing the floor of room 124	3.55
124 - 122	4 ventilation pipes, $\emptyset$ 0.48 m x 28 m	0.60 <sup>a)</sup>
B - A	Inlet gap to radiation shield tank	6.05
B - 122	3 pipes $\emptyset$ 0.7 m x 5.90 m, with butterfly valves in the ceiling of room 122	1.0 <sup>b)</sup>
	1 pipe from the original ventilation drum, $\emptyset$ 0.8 m x 6.5 m	0.50
123.8 - 123.3	48 openings, 0.1 m x 0.7 m, in the reactor skirt	3.36
123.8 - 121	Pipe, $\emptyset$ 0.7 m x 5.90 m, with one-way flapper valve max opening 0.26 m	0.29
123.3 - 123.1	Part of annulus	1.60
123.3 - 123	Annular, rectangular and trapezoidal openings	0.94
123.1 - 123	Rectangular openings	0.41
123 - 123.2	4 doors in the insulation box (max opening)	1.25 <sup>c)</sup>
123 - 121	2 shafts	2.98
123.1 - 121	Trapezoidal duct	0.44
123.1 - 122	10 rectangular ventilation openings, 0.8 m x 0.05 m	0.40
122 - 121	Circular opening	0.78
	Rectangular opening at the optional water break position	0.67
	Circular opening around the main discharge line	0.20
	Square opening	0.12
	Gap around steam break valve	0.47
	Minor holes and gaps	0.54
122 - 111.1	Entrance opening with stairs	3.80
121 - 111.1	Rectangular door opening and two minor holes.	2.50
121 - 113	Annulus along the containment wall	1.54
121 - 112	Annulus along the containment wall	2.0
	3 rectangular and square openings	0.32
121 - 110	Annulus along the containment wall	2.90
	3 rectangular openings	1.75
111.1 - 111	Imaginary boundary at the grating below the door to room 121	24.5
111 - 110	Rectangular opening	11.4
112 - 110	Rectangular openings, one of them along the containment wall	1.70
113 - 112	Rectangular opening	10.0
113 - 114	Entrance and rectangular openings in the ceiling	2.60
111 - 112	Rectangular entrance opening plus minor holes in the wall	2.20

Table A.5 (cont'd)

Connection	Description	Area (m <sup>2</sup> )
111 - 113	Rectangular opening	4.94
113 - 105	Drain pipe	0 <sup>d)</sup>
110 - 105	3 pipes with vacuum breaker check valves	0 <sup>e)</sup>
111.1 - 104	2 rectangular openings	5.92
104 - 106	4 blowdown pipes	4.60
106 - 105	57 open vent pipes, $\emptyset$ 0.30 m	4.03 <sup>f)</sup>
106 - 105	28 open vent pipes (alternatively)	1.98 <sup>g)</sup>

- a) One of the ventilation pipes is partly closed at the exit in room 122
- b) The flow area in one of the valves is slightly reduced because of damage
- c) The doors were closed before the majority of the blowdowns
- d) An orifice plate and a valve are installed in the drain pipe
- e) Closed during blowdown. The valves begin to open at a pressure difference between wetwell and drywell of 0.22 bar and are fully open at a pressure difference of 0.28 bar (max flow area through all four valves: 0.45 m<sup>2</sup>)
- f) Only valid for Blowdown 17 (only the permanently blocked vent pipe)
- g) The distribution of the open vent pipes for the particular blowdowns is shown in the corresponding test results report (MXB-218 to -225).



Table A.6

Flow paths for the 4-node drywell.

<u>Between rooms</u>	<u>Between rooms</u>	<u>A (m<sup>2</sup>)</u>
	124 - 122	0.60
	B - 120	1.50
	123.1 - 122	<u>0.40</u>
1 - 2		2.50
	122 - 111.1	3.80
	122 - 121	<u>2.78</u>
2 - 3		6.58
	123.2 - 121	0.29
	123 - 121	2.98
	123.1 - 121	<u>0.44</u>
1 - 3		3.71
3 - 4	111.1 - 104	5.92
4 - 5	106 - 105	1.98

Table A.7

Summary of heat soakage areas.

	Areas m <sup>2</sup>			Totally
	Drywell	Pool	Above pool	
Concrete only	951.5	213.5	683.3	1 848.3
Painted	1 184.3	-	133.5	1 317.8
Steel lined	1 606.8	369.5	-	1 976.3
Steel only	1 984.7	3.7	678.1	2 666.5
Subtotal	5 727.3	586.7	1 494.9	7 808.9
Aluminium	1 021.4	-	-	1 021.4
Grand total	6 748.7	586.7	1 494.9	8.830.3

Table A.8

Suggested values of heat soakage constants.

	$\lambda$ W/(m <sup>2</sup> *K)	$\rho$ kg/m <sup>3</sup>	$c_p$ J/(kg*K)
Concrete	1.63	2 400	880
Steel	55	7 800	460
Aluminium	210	2 690	896

The value of  $\lambda$  for concrete may be too low, taking reinforcements into account.

Table A.9

Aluminium content in the containment.

Room*	mC <sub>p</sub> , MJ/K
1:5	1.20
2:5	0.01
3:5	0.55
Drywell	1.76

\* See Figure 7

Table A.10

Total steel content in the containment.

	Total heat capacity, MJ/K			Totally
	Drywell	Pool	Above pool	
Steel liner	50.9	12.6	-	63.5
Steel only	91.0	0	7.3	98.3
Steel total	141.9	12.6	7.3	161.8

Table A.11

Suggested discharge flow data for Blowdown 18.

Time (s)	Mass flow kg/s	Spec enth kJ/kg	Integrated Mass, tons	Integrated m*H, GJ
0.00	0.	0.	0.000	0.000
0.00	0.	765.	0.000	0.000
.12	1 800.	765.	.108	.083
.25	3 060.	765.	.424	.324
.50	3 000.	765.	1.181	.904
.70	2 800.	765.	1.761	1.347
.90	2 370.	765.	2.278	1.743
1.20	2 070.	765.	2.944	2.252
2.00	2 050.	818.	4.592	3.557
3.00	2 040.	885.	6.637	5.298
4.00	2 060.	933.	8.687	7.161
4.40	2 068.	940.	9.513	7.935
5.00	2 080.	956.	10.757	9.114
6.00	2 140.	970.	12.867	11.147
8.00	1 800.	985.	16.807	14.995
10.00	1 840.	995.	20.447	18.599
11.00	1 880.	998.	22.307	20.453
14.00	1 740.	1 000.	27.737	25.877
20.00	1 700.	1 006.	38.057	36.228
30.00	1 660.	1 012.	54.857	53.178
42.00	1 580.	1 013.	74.297	72.861
50.00	1 540.	1 023.	86.777	85.565
58.00	1 210.	1 039.	97.777	96.895
65.00	1 370.	1 049.	106.807	106.325
74.00	1 160.	1 060.	118.192	118.326
80.00	1 140.	1 068.	125.092	125.667
85.00	1 120.	1 075.	130.742	131.721
120.00	1 000.	1 075.	167.842	171.603
137.00	1 000.	1 140.	184.842	190.431
140.00	1 000.	1 140.	187.842	193.851
164.00	960.	1 140.	211.362	220.664
171.00	280.	1 140.	215.702	225.611
175.00	80.	1 140.	216.422	226.432
190.00	0.	1 140.	217.022	227.116

Input data acc to Diagram E.4, E.5, E.6 in MXB-218.

Table A.12

Summary of geometry and initial conditions for BD 18.

Room no	Volume m <sup>3</sup>	Temp °C	Initial conditions		
			Humidity g/kg	Pressure bar	Water tons
1:5	683	61.0	12	1.045	-
2:5	175	49.5	9	1.045	-
3:5	901	21.9	4	1.045	-
4:5	213*	19.0	4	1.045	-
Drywell	1 972*	37.5	7	1.045	-
Wetwell	2 133**	16.0	-	1.045	549
WW, gas	1 583	16.0	12	1.045	-
WW, liq	550**	16.0	-	1.045	549**
Header	146*	18.5	?	1.045	-

\* Incl 5.3 m<sup>3</sup> of air in 28 open vent pipes, but excl 5.5 m<sup>3</sup> of air in blocked vent pipes.

\*\* Excl 5.6 m<sup>3</sup> of water in 28 open vent pipes and 5.4 m<sup>3</sup> of water in blocked vent pipes.

Table A.13

Requested computations for ISP17.

Quantity	Unit	EUC code	Compartment	Measurement position	Compare diagram in MXB-218	Case <sup>1)</sup> (1.4s)		Remarks
						4.4s	220s	
Δp	kPa	70	110-105	110M213	M:22	C	C	Slightly high
		"	106-105	106M215	M:23	(B) <sup>4)</sup>	(B)	
		"	122-124	122M144-124M142	M:6,4	(A)		
		"	122-110	" -110M147	M:6,9	(A)		
		"	122-106	" -106M163	M:6,14	(A)		
p	MPa	87	124	124M142	M:4	(A)		Smoothed (1-2 kPa high)
		"	122	122M144	M:6	A		
		"	110	110M147	M:9	A	C	
		"	106	106M163	M:14	B	B	
		"	105	105M122	M:18	C	C	
T	K	84	124, vapor	124M572	M:24	A		
		"	122 "	122M574	M:24	A		
		"	111 "	111M576	M:25	A	C	
		"	106 "	106M586	M:28	B	B	
		"	105 "	Average	E:16	C	C	
"	105, liquid	"	E:16		C			
G <sub>a</sub>	kg/s	78	Vents	Evaluated	E:12,40		B	Flow of air
G <sub>s</sub>	"	"	"	"	E:10,41		B	"- vapor
G <sub>w</sub>	"	"	"	"	E:11,39		B	"- liquid
Δm <sub>a</sub> <sup>v</sup>	kg	80	Vents	Evaluated	E:15,25		B	Integrated flows of air, steam and liquid
Δm <sub>s</sub> <sup>v</sup>	"	"	"	"	E:13		B	
Δm <sub>w</sub> <sup>v</sup>	"	"	"	"	E:14		B	
Δm <sub>w</sub> <sup>DW</sup>	kg	80	Drywell	Evaluated	-		B	Sump water <sup>3)</sup>
m <sub>s</sub> <sup>WW</sup>	kg	80	105, vapor	Evaluated	E:26		C	
Z <sub>v</sub> <sup>2)</sup>	m	83	Vents	Evaluated	E:29	C		Water plug level
Z <sub>p</sub> <sup>2)</sup>	"	"	105,G1	Evaluated	E:27	C		Pool swell
	"	"	105,G3	"	E:27	C		"

$$9A + 0A = 9A$$

$$3B + 10B = 13B$$

$$6C + 7C = 13C$$

Totally: 18 + 17 = 35 diagrams

- 1) "PWR programs": Only A (up to 1.4s)  
 "Starting from header": C + some of B (B normally = input data, but interesting for comparison purpose)  
 "Full representation of drywell": A+B+C
- 2) Relative vent pipe outlet
- 3) Water on drywell floor, cf Table E:7 in MXB-218
- 4) Brackets indicate variables of less interest for the evaluation.

Table A.14

Flow models in ARIANNA Computer Code.

Thermodynamic state	Junction geometry	Subcritical flow	Critical flow
Superheated Steam	Orifice (L/A=0)	Ideal Gas Model ( $G_{id}$ )	Ideal Gas Model ( $G_{id}^{cr}$ )
	Pipe (L/A>0)	Momentum Equation ( $G_{ME}$ )	$\min (G_{id}^{cr}, G_{ME}^{cr})$
Saturated Steam	Orifice (L/A=0)	( $G_{id} \cdot \frac{G_{moody}}{G_{id}^{er}}$ )	Moody Model ( $G_{moody}$ )
	Pipe (L/A>0)	Momentum Equation ( $G_{ME}$ )	$\min (G_{moody}, G_{ME}^{cr})$

Table A.15

Some basic computer code characteristics.

1. Code	ARIANNA-1	CONTEMPT-LT/26	CONTEMPT-LT/28	COPTA-7	ZOCO-V
2. Basic code description	Ref 23	Ref 24	Ref 25	Ref 26	Ref 27
3. Changes made to the code compared to basic code description	Simplified wetwell model (backpressure)	No*	See Ref 28 (Volume change effect, steam in air bubbles)	Extended flash model Possibility to retain air in drywell	Automatic swith superheat to saturation Heat transfer Carryover
4. Maximum possible number of compartments					
a Drywell type	100	1 - 2	1 - 2	10	11
b Wetwell type	-	1	1	10	1
c Totally	100	2 - 3	2 - 3	10	11
5. Contains press-vessel model?		Simplified	Simplified	Yes	
6. Pool swell model	-	No	No	Yes	Yes
7. Compartment thermodynamics	Equilibrium	Non-Eq	Non-Eq	Non-Eq	Equilibrium

\* Changes made in parameter studies.



Table A.16

Summary of surface areas for heat absorbing structures.

Code	CONTEMPT LT/26	CONTEMPT LT/28	COPTA-7	ZOCO-V	ARIANNA
1. Drywell					
a) Concrete only	1 138	1 653	951	950	288
b) Painted concrete	-		765	765	1 158
c) Lined concrete	1 606	711 <sup>1</sup>	1 607	1 607	1 607
d) Totally concrete	2 744	2 364	3 323	3 323	3 053
e) Downcomers	26	195	198	-	-
f) Other steel	1 809	799	1 787	2 037	1 901
g) Aluminum	1 021		(1 021) <sup>2</sup>	606	635
h) Totally, DW	5 592	3 358	6 329	5 966	5 589
2. Wetwell, gas phase					
a) Concrete only	1 357.5	1 152	683	683	
b) Painted concrete	-	120	553	553	
c) Lined concrete	23.3	-	-	-	
d) Totally concrete	1 298.8	1 262	1 236	1 236	
e) Downcomers	148.4	195	193	-	
f) Other steel	471.0	485	485	625	
g) Aluminum	-	-	-	-	
h) Totally, WW gas	2 018.2	1 943	1 914	1 861	
3. Wetwell, pool					
a) Totally concrete	330.5	479	584	-	
b) Steel	-	479	4	-	
Totally, WW pool	330.5	959	587	-	
4. Drywell + Wetwell	7 904.6	6 260	8 830	7 827	
5. Additional mC <sub>p</sub> , kJ/K					
a) Drywell		-	1.8		
b) Wetwell vapor		-	-		

<sup>1</sup> Structures of rooms 123 and 124 excluded<sup>2</sup> Treated as mC<sub>p</sub>

Table A.17

Models used for heat soakage.

Code	CONTEMPT LT/26	CONTEMPT LT/28	COPTA-7	ZOCO-V	ARIANNA
1. Condensation model <sup>1</sup>					
a) Drywell	Cond	Cond/Bulk	Bulk	Bulk	?
b) Wetwell, vapor	Bulk	Bulk	Bulk	Bulk	-
c) Pool	Bulk	Bulk	Bulk	Bulk	-
2. HTC, W/(m <sup>2</sup> *K)					
a) Drywell	DCMN <sup>2</sup>	Uchida	5 000		DCMN
b) Wetwell, vapor	Nat conv <sup>3</sup>	Nat conv	Uchida		-
c) Pool	2.27	5 000	500		-

<sup>1</sup> Cond = Condensation on walls, Bulk = Bulk heat transfer from the volume.

<sup>2</sup> DCMN = Correlation developed by DCMN (Dipartimento di Costruzioni Meccaniche E Nucleari).

<sup>3</sup> Natural convection = 0 - 10 W/(m<sup>2</sup>\*K).

Table A.18

Some computer run details for short-time cases.

Item						
1. Computer code	CONTEMPT LT/26	CONTEMPT LT/28	COPTA-7	COPTA-7	ZOCO-V	ARIANNA-1 0 - 1.45 S
2. Computer utilized	IBM370/168	CYBER173	CYBER 170/835	CYBER 170/835	CYBER173	IBM370/168
3. CPU time (s)	47	-	42	112	120	485
4. Maximum time-step (s)	.01	-	.02	.005	.00125	.001
5. Number of drywell compartments	1	1	1	4	4	17
6. Flashing model for break flow (Equilibrium/pressure model)	Eq	Eq	Pressure flashing	80 % Eq 20 % flash	(Eq)	Eq
7. Model for mass concentrations at vent flow entrance	Air mod	Air mod	383 kg air locked	As gas phase	As gas phase	-
a) Air						
b) Steam						
c) Water						
8. Vent flow model. In particular						-
a) Dynamic/Steady state	SS	SS	SS	SS	SS	
b) Comp/Incompressible	Compr	Compr	Compr	Compr	Compr	
9. Pool model. In particular						-
a) Surface area (m <sup>2</sup> )	141.0	118	113.5	113.5	107.7	
b) Surface HTC (W/m <sup>2</sup> -K)	Evap-cond	0-1.35	0	0		
c) Temp of rising air	As pool	As pool	As pool	As pool	Eq	
d) Steam content of rising air	0	Sat	Sat	Sat		
e) Air rise velocity	∞	∞	Pool swell model		Pool swell model	

Table A.19

Some computer run details for long-time cases.

Item				
1. Computer code	CONTEMPT-LT/26	CONTEMPT-LT/28	COPTA-7	ZOCO-V*
2. Computer utilized	IBM 370/168	CYBER173	CYBER170-835	CYBER175
3. CPU time (s)	1 477	600	269	496
4. Maximum time-step (s)	.02	0.2	5	.005
5. Number of drywell compartments	1	1	1	4
6. Flashing model for break flow (Equilibrium/pressure model)	Equilibrium	Equilibrium	Pressure flashing	Eq model
8. Model for mass concentrations at vent flow entrance a) Air b) Steam c) Water	Air flow modifiers	Air flow modifiers	383 kg of air locked in DW	Header composition
8. Vent flow model after vent clearing	Steady state Compr	SS Compr	SS Compr	SS Compr
9. Pool model. In particular				
a) Surface area (m <sup>2</sup> )	141	118	113.5	107.7
b) Surface HTC (W/m <sup>2</sup> -K)	Evap-cond	0 to 1.35	0	
c) Temp of rising air	As pool	As pool	As pool	
d) Steam content of rising air	None	Sat	Sat	Eq model
e) Air rise velocity, m/s	∞	∞	1	

\* Up to 75 s.

Table A.20

Submitted results for ISP17.

Code	Number of dry- well subcom- partments	Type of diagram		
		A	B	C
		0 - 1.4 s 0 - 4.4 s	0 - 4.4 s	0 - 220 s
ARIANNA-1	17	x		
CONTEMPT-LT/26	1		x	x
CONTEMPT-LT/28	1		x	x
COPTA-7	1	(x) <sup>1</sup>	x	x
COPTA-7	4	x		
ZOCO-V	4	x	x	x <sup>2</sup>

<sup>1</sup> As parameter study<sup>2</sup> 0 - 75 s

Table A.21

Some key results for short-time cases.

Item	CONTEMPT LT/26	CONTEMPT LT/28	COPTA-7 2 nodes	COPTA-7 5 nodes	ZOCO-V 5 nodes	MX-DATA
1. Time for vent clearing (v.c.), s	1.26	0.89	1.25	1.11	1.08	1.36
2. Header pressure at v.c., MPa	.147	.166	.138	.145	.144	.135-.140
3. Water plug speed at v.c., m/s	8.53	19.3	7.15	11.4	31.8	5.5-6.5
4. Drywell pressure at 4.4S, MPa	.168	.210	.171	.193	.194	.168-.172
5. Peak pool swell, m (above initial level)			3.43	4.17	3.15	2.0-3.5
6. At time =			2.70	2.39	4.4	2.7-3.2
7. Maximum pool surface velocity, m/s			4.39	5.54	1.44	2.0-5.0
8. At time =			2.70	2.39	1.75	2.0-3.2

## LIST OF FIGURES

- B.1 The exterior of the Marviken Plant
- B.2 Cross-section of the Marviken containment
- B.3 Layout of the measurement system
- B.4 Pressure and differential pressure measurement positions
- B.5 Temperature, flow velocity and mass composition measurement positions
- B.6 Locations of the level probes in the wetwell
- B.7 Schematic representation of the Marviken containment
- B.8 Cross-sectional area and volume for lower wetwell in Blowdown 18
- B.9 Vent pipe blocking for Blowdown 18
- B.10 Initial temperature profile versus height in the pressure vessel
- B.11 Discharge outlet of main discharge pipe with rupture disc arrangement
- B.12 Discharge flow rates calculated from DP-over-vessel data and from the flow pressure drop
- B.13 Discharge flow rate at the beginning of Blowdown 18
- B.14 Specific enthalpy of the discharge flow in Blowdown 18
- B.15 Mass and energy balance fro ISP17, 0 - 171 s

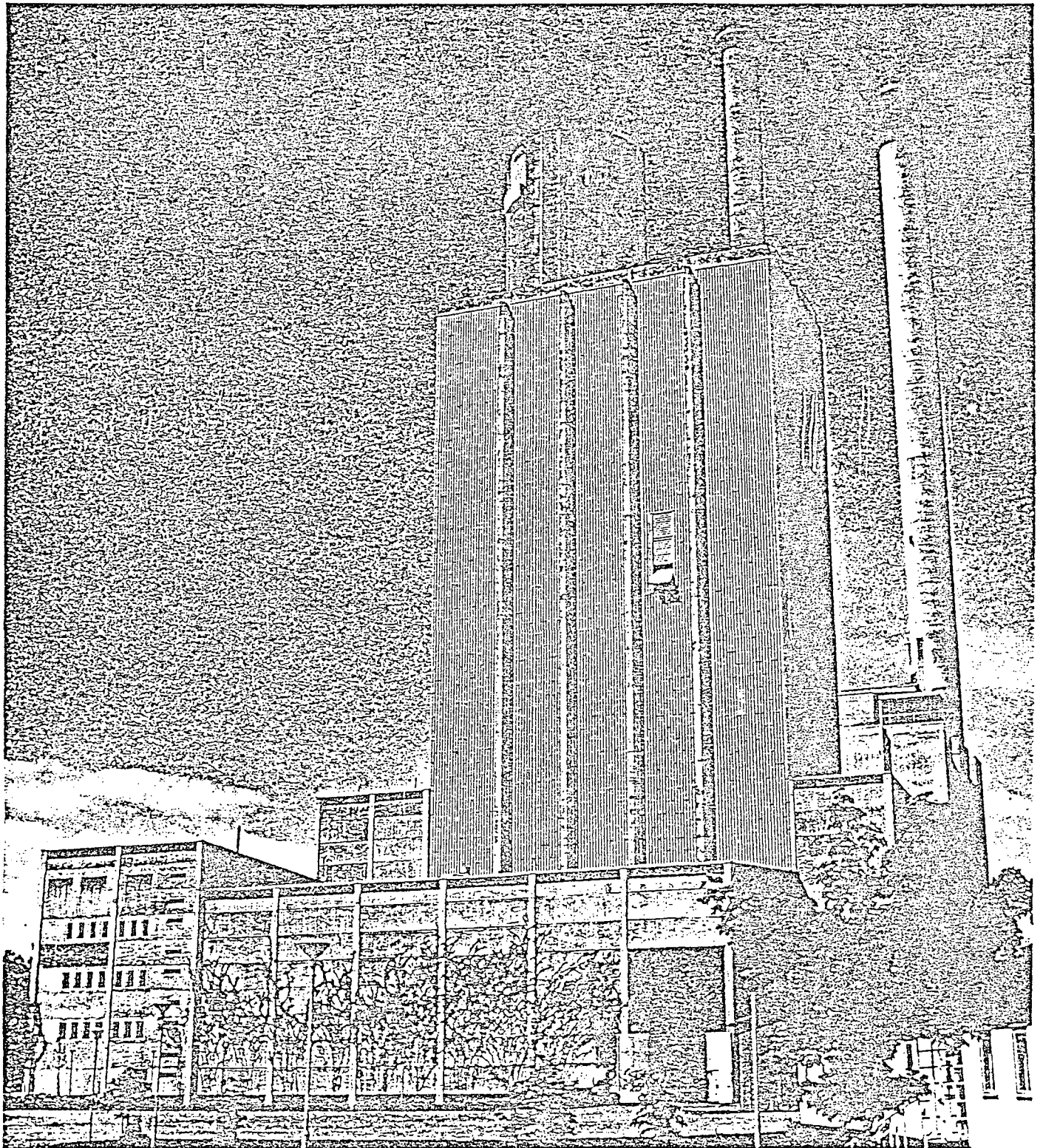


Figure B.1

The exterior of the Marviken Power Plant.



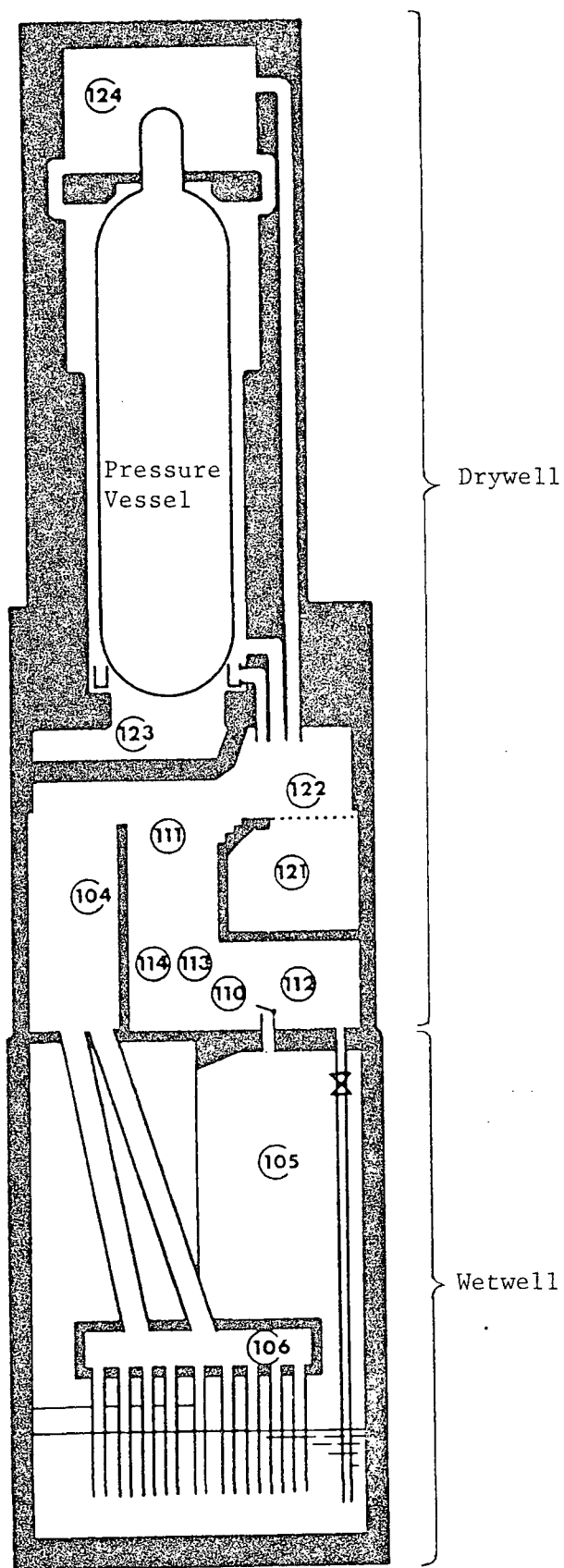


Figure B.2

Cross-sectional view of the containment.

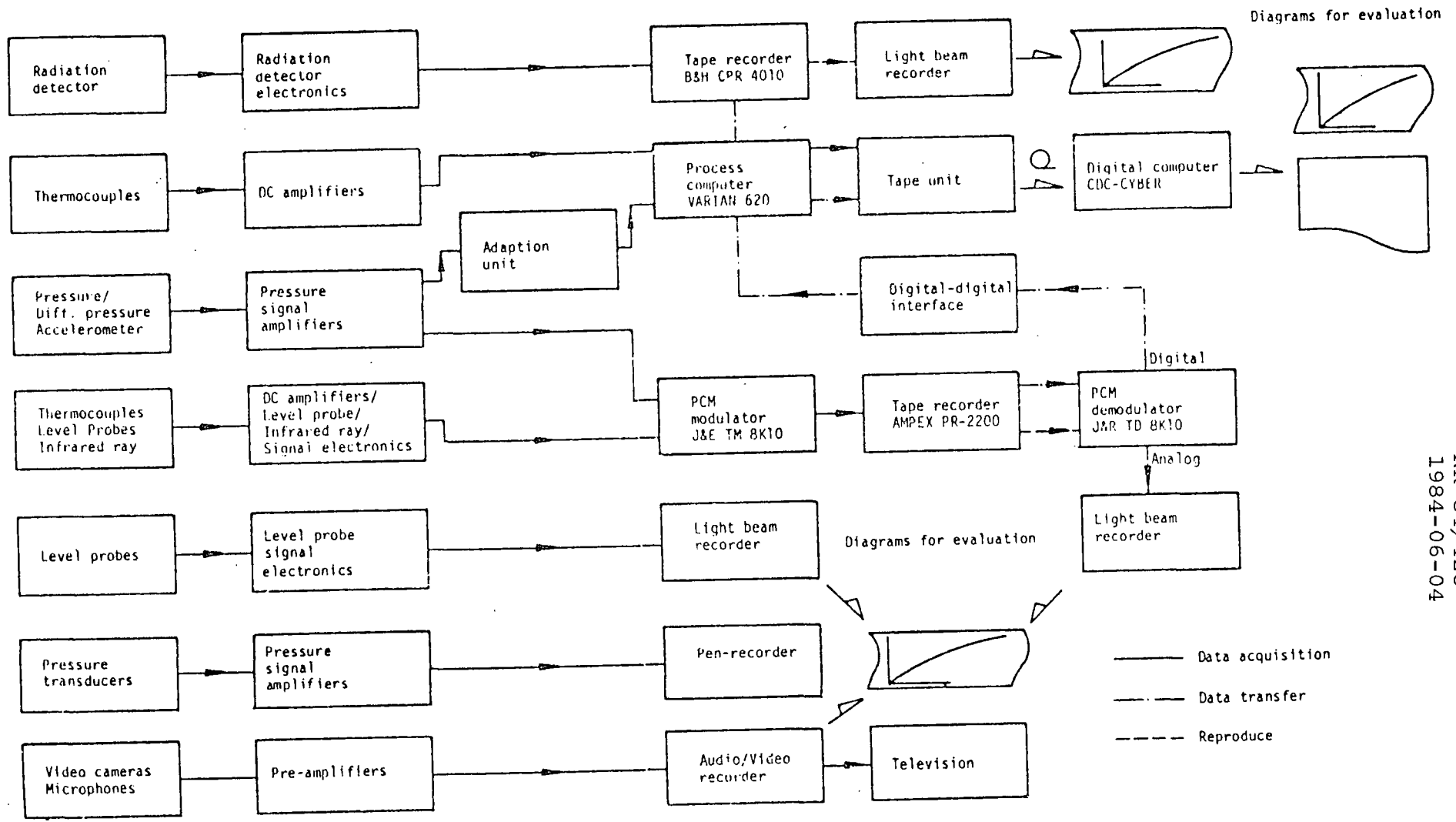


Figure B.3  
Lay-out of the measurement system.



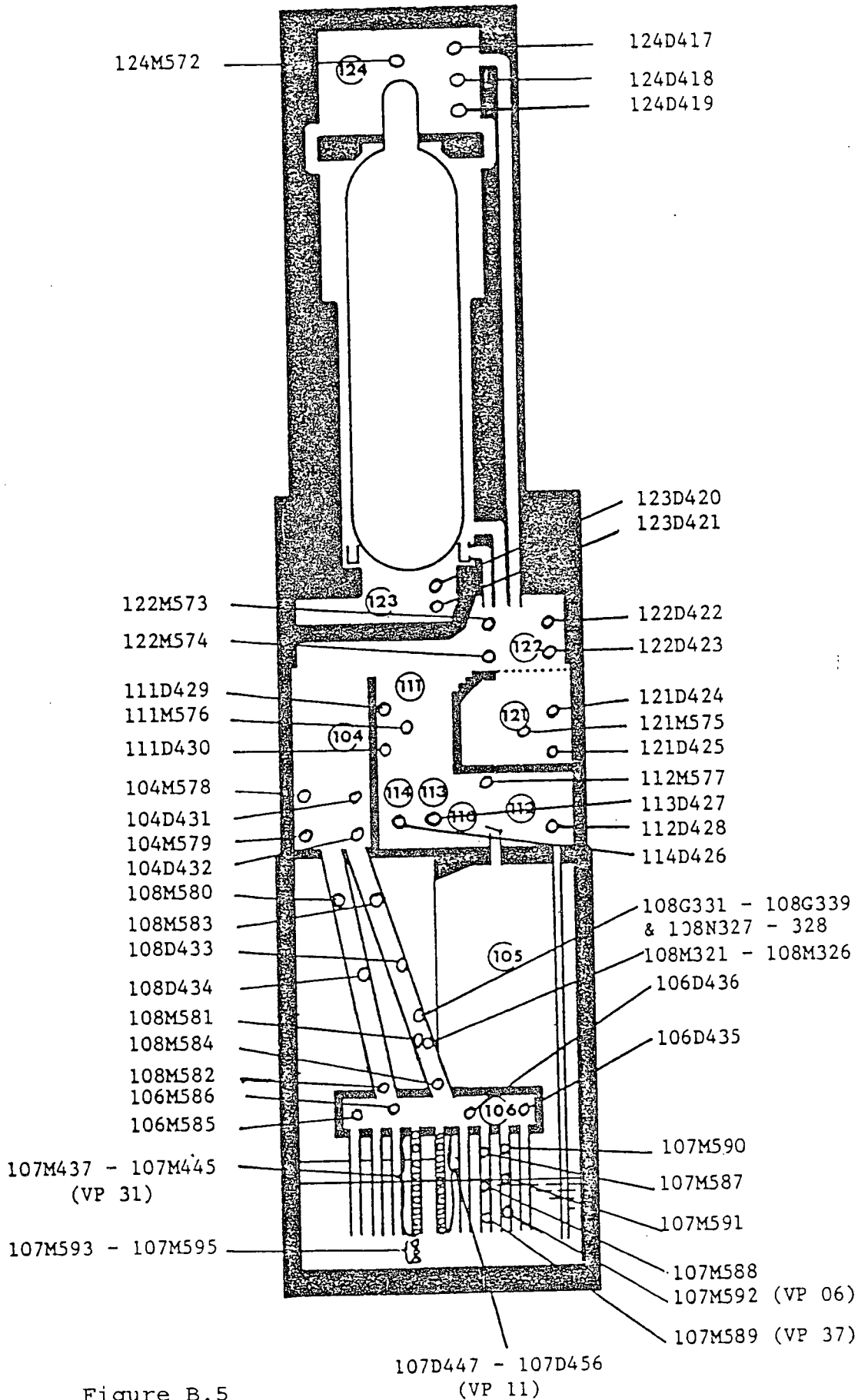


Figure B.5

Temperature flow velocity and mass composition measurement positions.

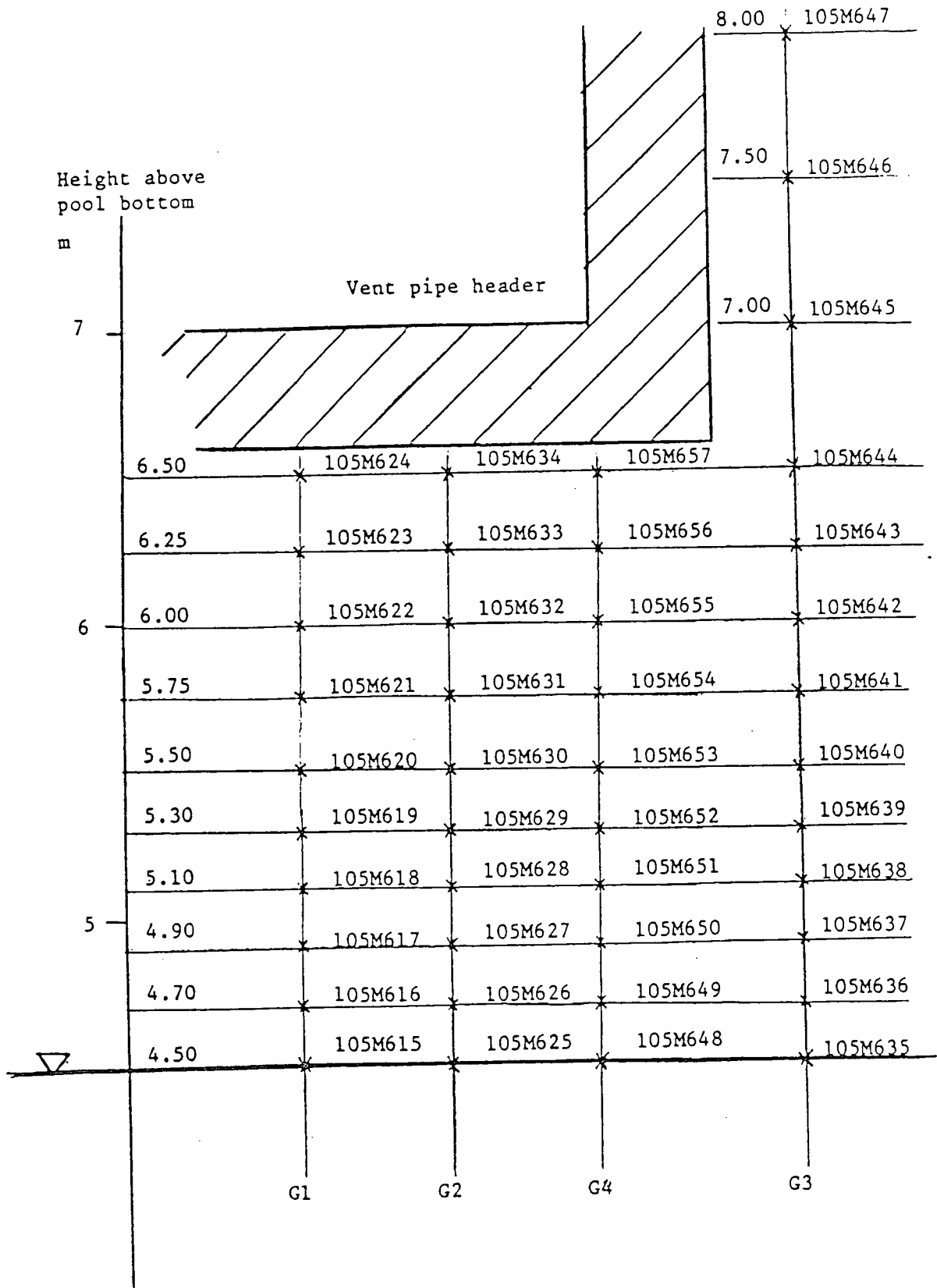


Figure B.6

Locations of level probes in the wetwell.

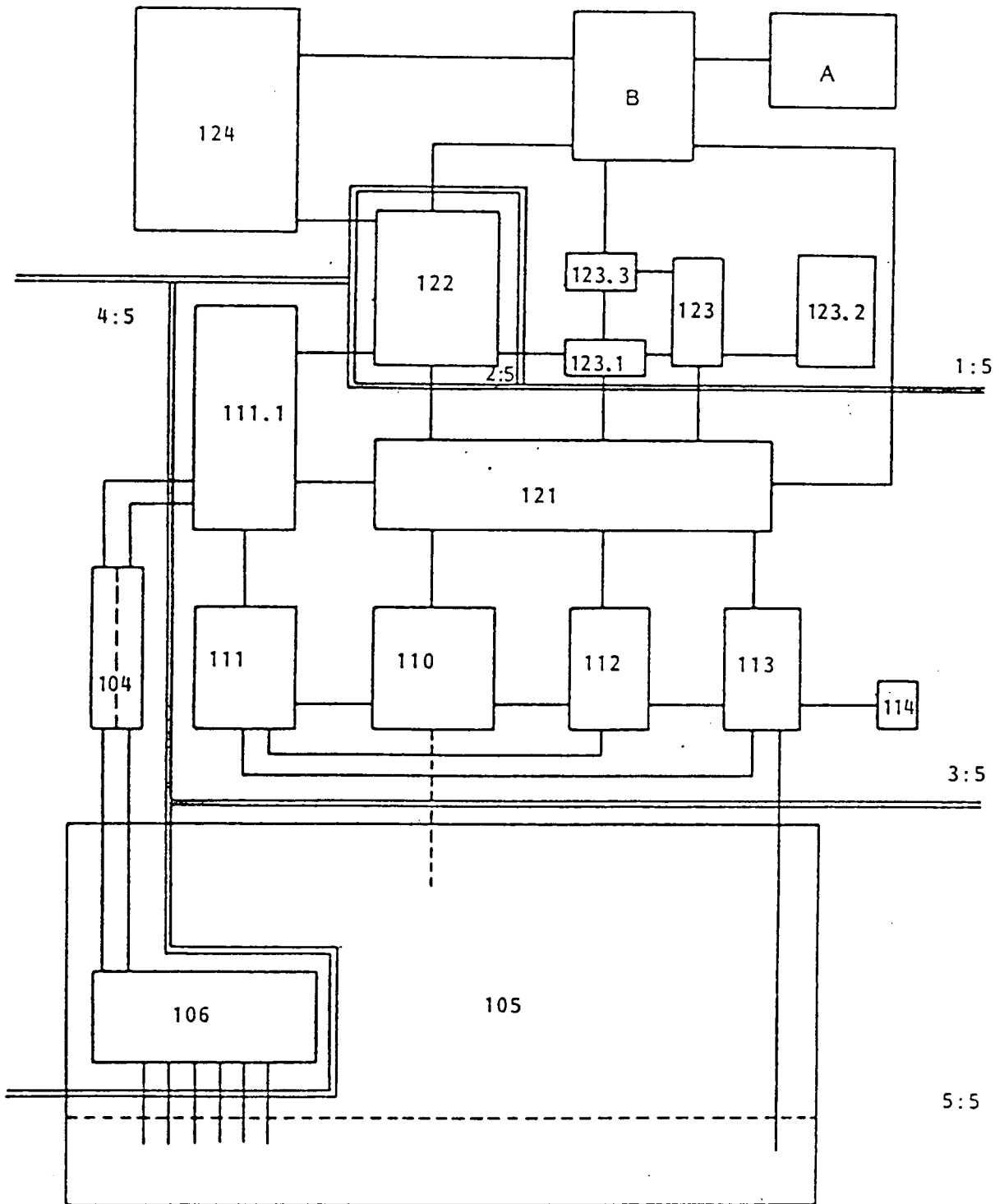
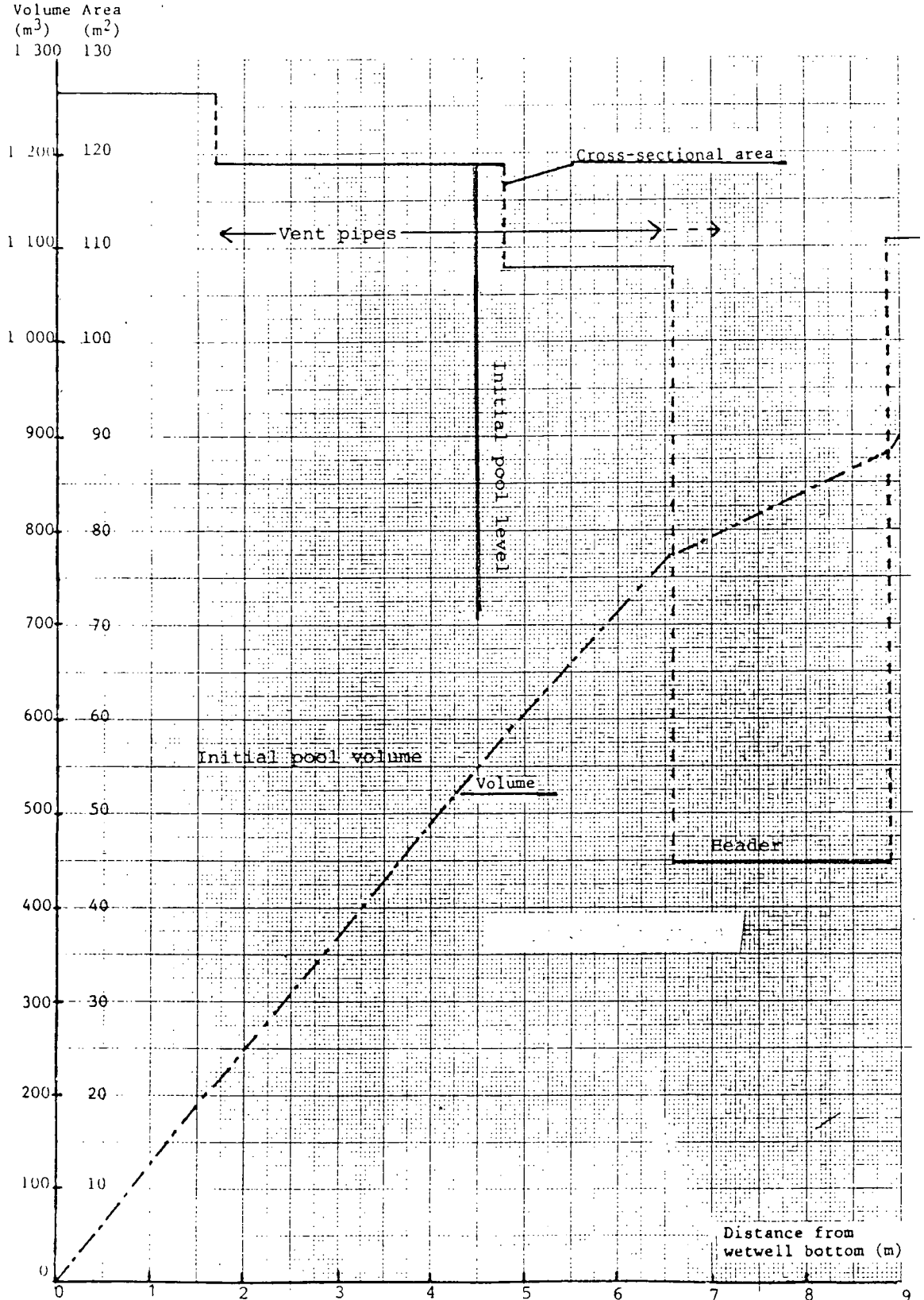


Figure B.7

Schematic diagram of rooms and connections in the Marviken containment ( $50 \text{ cm}^2 \hat{=} 1\,000 \text{ m}^3$ ).

Figure B.8

Cross-sectional area and volume for lower wetwell in BD 18.



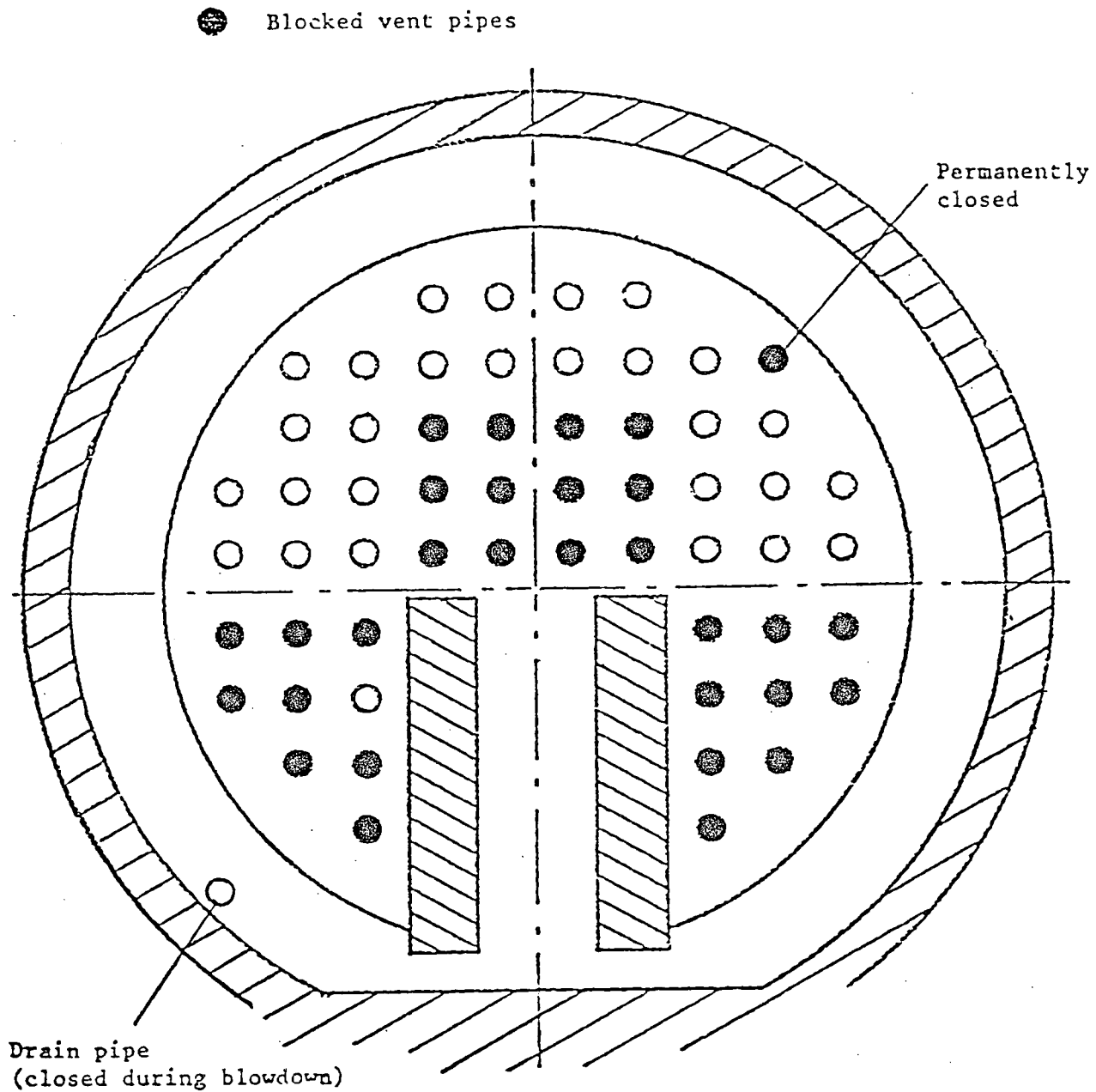


Figure B.9

Vent pipe blocking for Blowdown 18.



BLOWDOWN 18

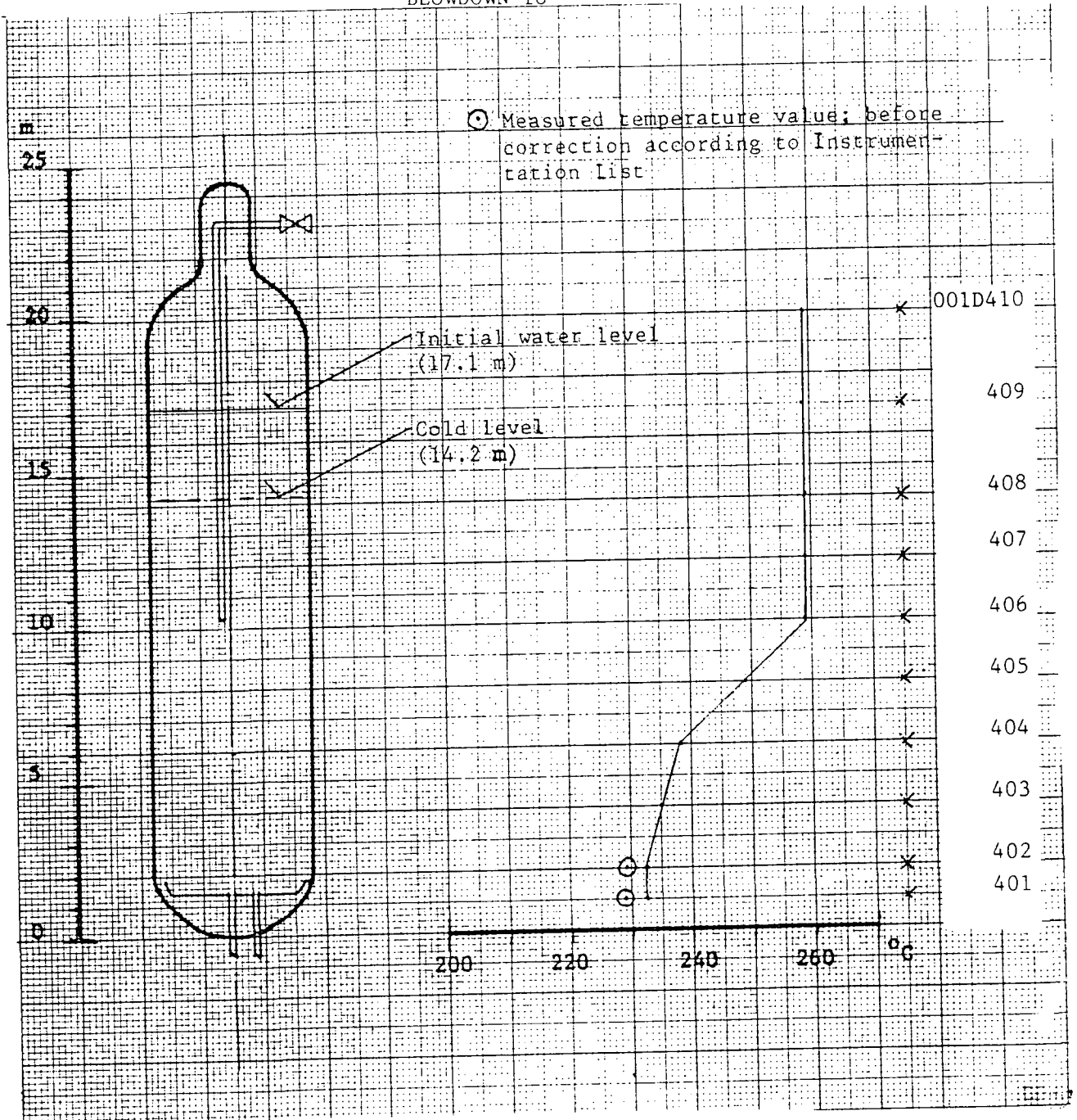


Figure B.10

Initial temperature profile versus height in the pressure vessel.



Figure B.12

Discharge flow rates calculated from DP-over-vessel data and from the flow pressure drop.

BLOWDOWN 18

○ MASS FLOW FROM THE VESSEL  
--- based on pressure drop (003D108-003D107)  
in the discharge pipe

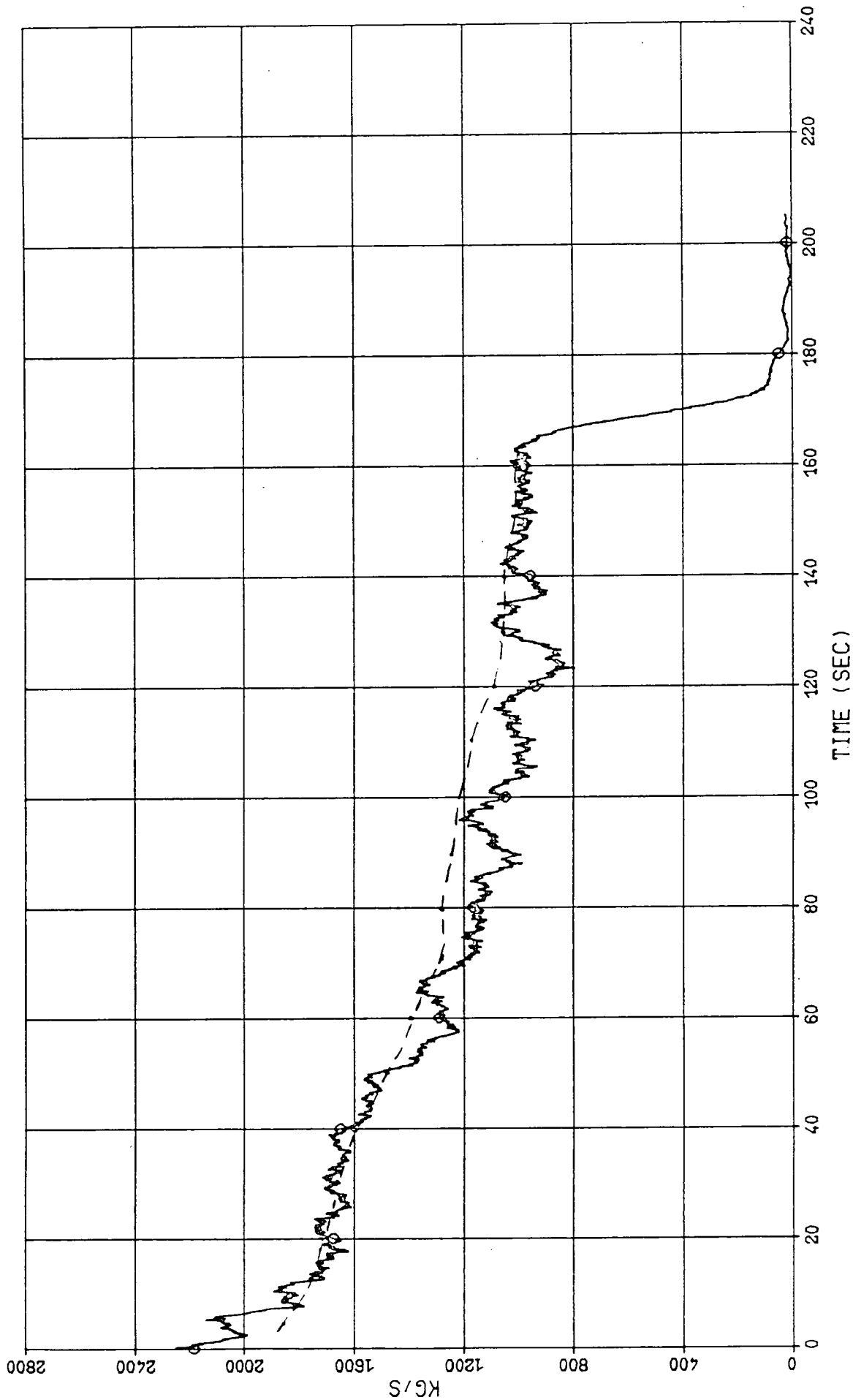


Figure B.13

Discharge flow rate at the beginning of blowdown 18.

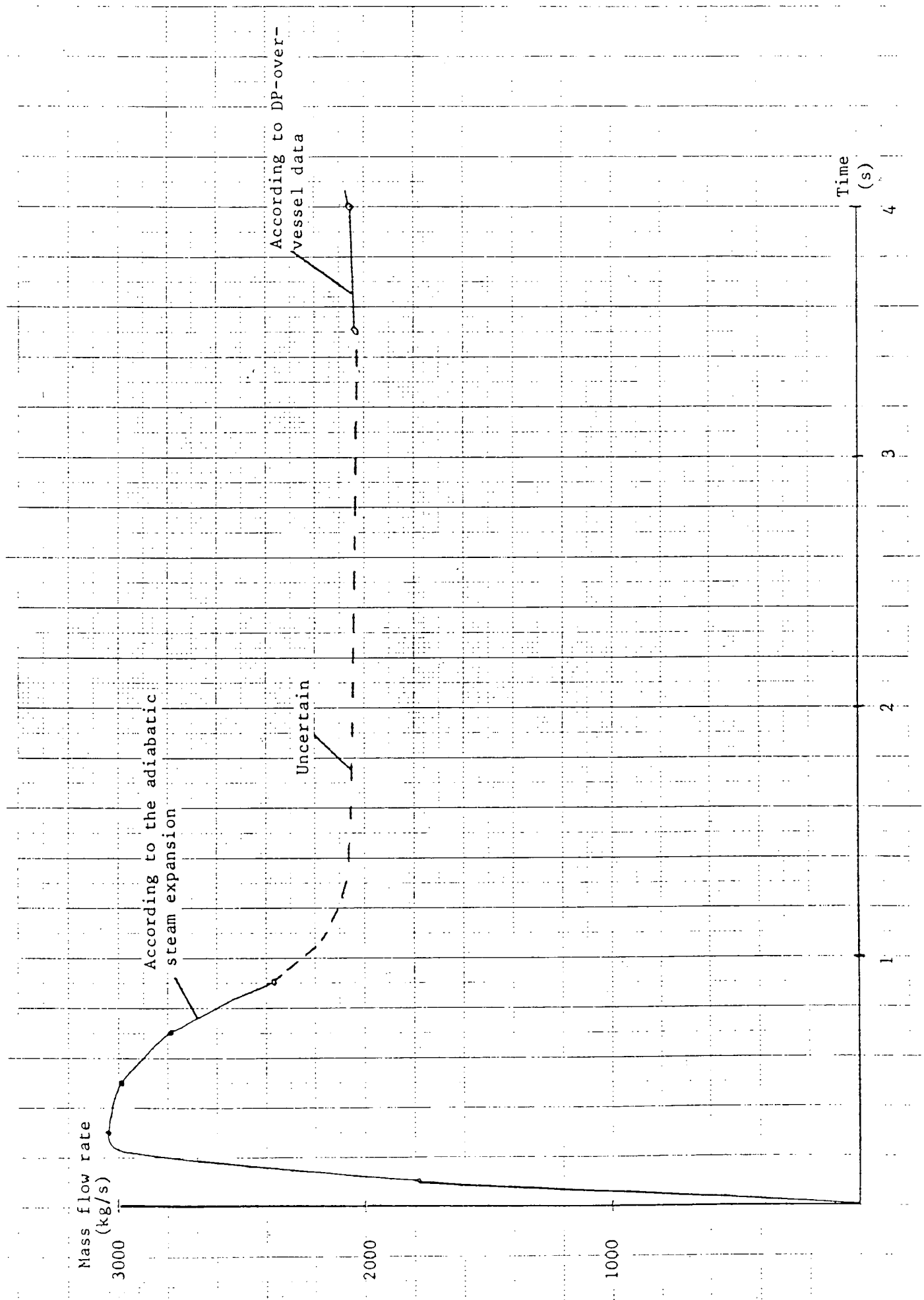


Figure B.14

Specific enthalpy of the discharge flow in Blowdown 18.

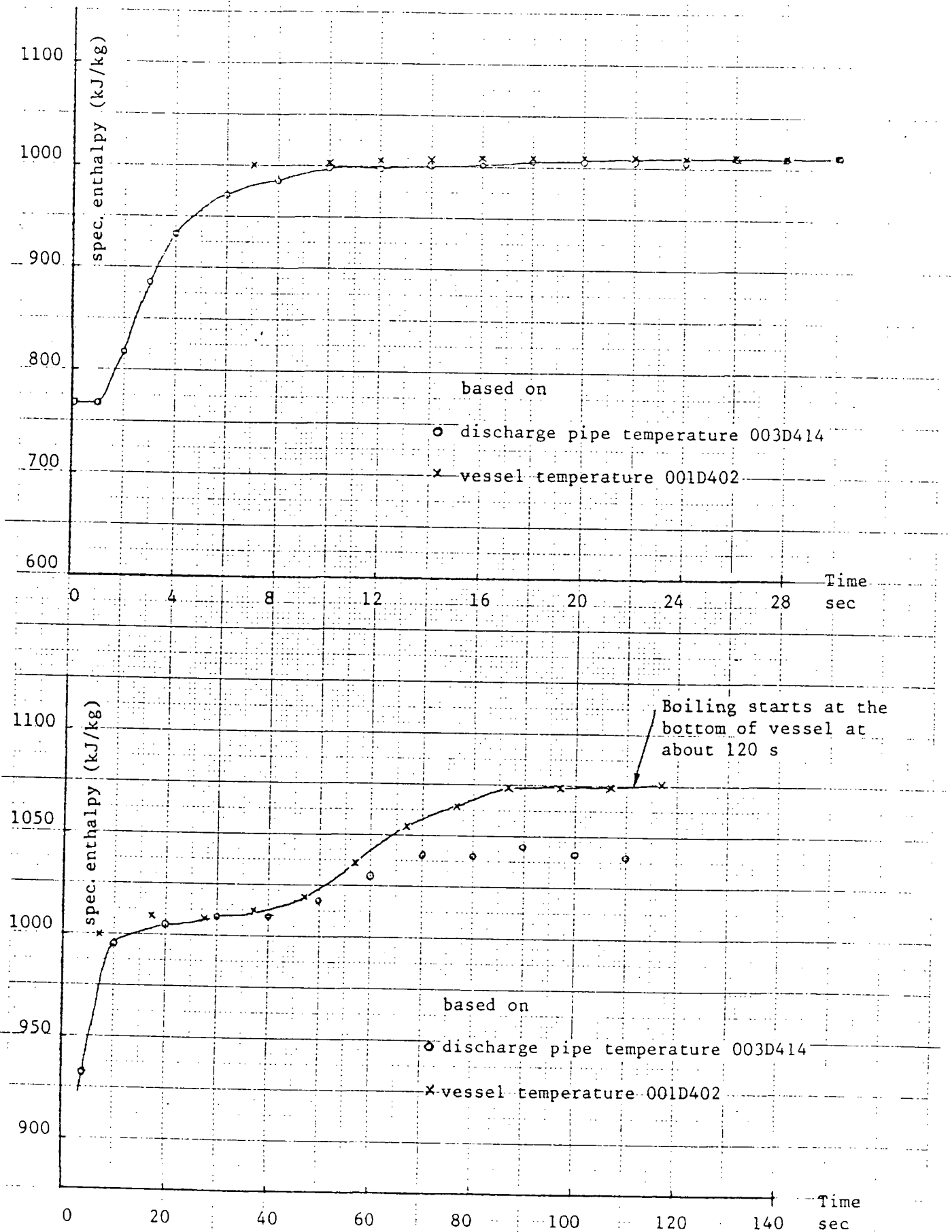
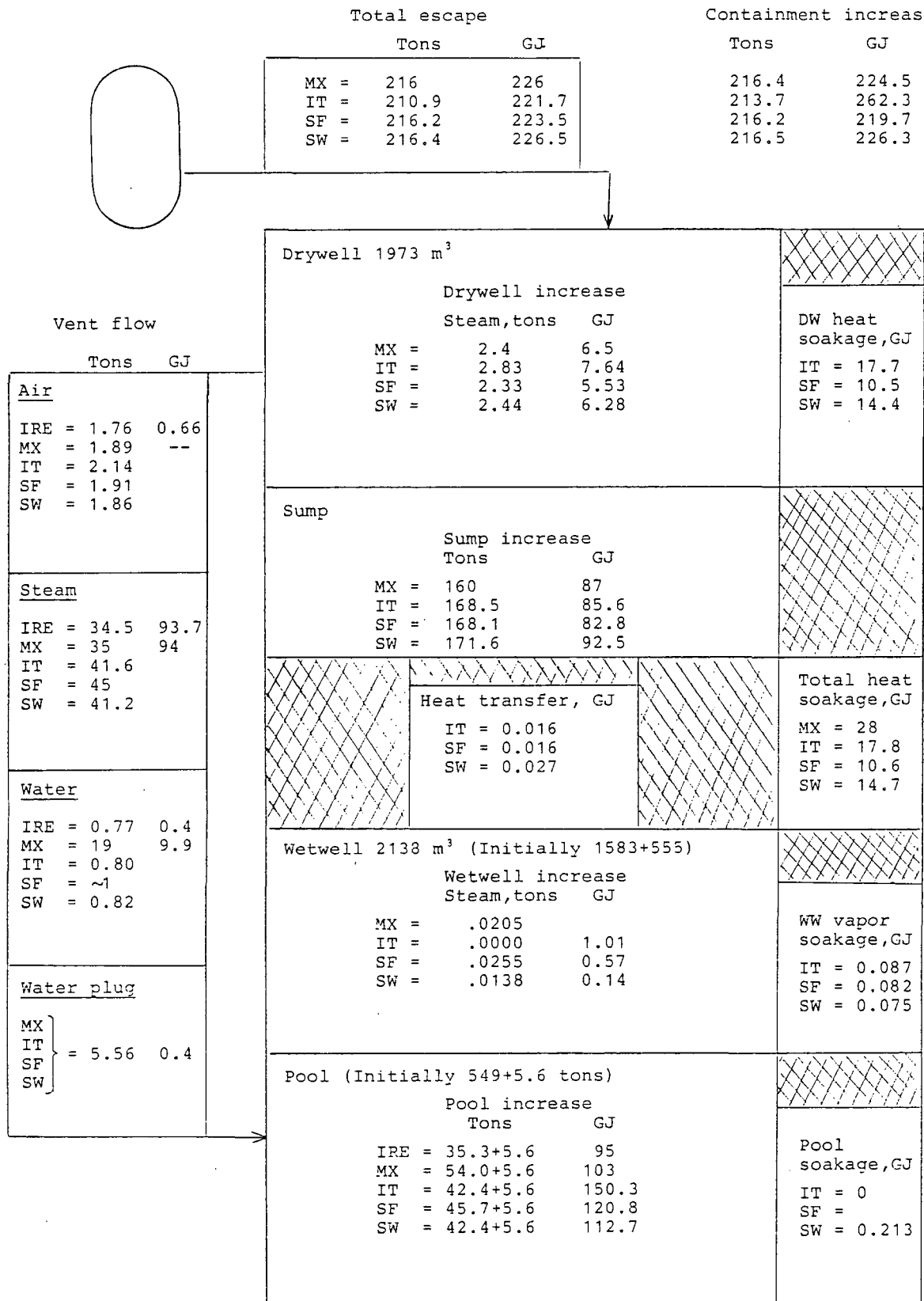


Figure B.15

Mass and energy balance for ISP17, 0 - 171 s.



IRE = Acc. to infra-red measurements, MX = Acc. to Fig 7:3 in ref 11

IT = Italy, SF = Finland, SW = Sweden

## LIST OF DIAGRAMS

Short-time transient, 0 - 4.4 s

C.1A, C.1B	Pressure difference	110 - 105
C.2A, C.2B	Pressure difference	106 - 105
C.3A	Pressure difference	122 - 124
C.4A	Pressure difference	122 - 110
C.5A	Pressure difference	122 - 106
C.6A	Pressure in room	124
C.7A	Pressure in room	122
C.8A, C.8B	Pressure in room	110
C.9A, C.9B	Pressure in room	106
C.10B	Pressure in	wetwell
C.11A	Temperature in room	124
C.12A	Temperature in room	122
C.13A, C.13B	Temperature in room	111
C.14A, C.14B	Temperature in room	106
C.15A, C.15B	Temperature in	wetwell vapor
C.16A, C.16B	Water plug size	
C.17A	Pool level	

Long-time transient, 0 - 220 s

C.18	Pressure difference drywell-wetwell	
C.19	Pressure difference header-wetwell	
C.20	Drywell pressure	
C.21	Header pressure	
C.22	Wetwell pressure	

## LIST OF DIAGRAMS (cont'd)

- C.23 Drywell temperature
- C.24 Header temperature
- C.25 Wetwell gas temperature, average
- C.26 Average pool temperatur
- C.27 Vent pipe air flow
- C.28 Vent pipe steam flow
- C.29 Vent pipe flow of liquid water
- C.30 Total air through vents
- C.31 Total steam through vents
- C.32 Total liquid water through vents
- C.33 Mass of sump water
- C.34 Mass of steam in wetwell gas
- C.35 Total mass of steam + water through vents



ISP17,PRESSURE DIFF 110-105,110M213,DIAG M.22,TABLE M.4

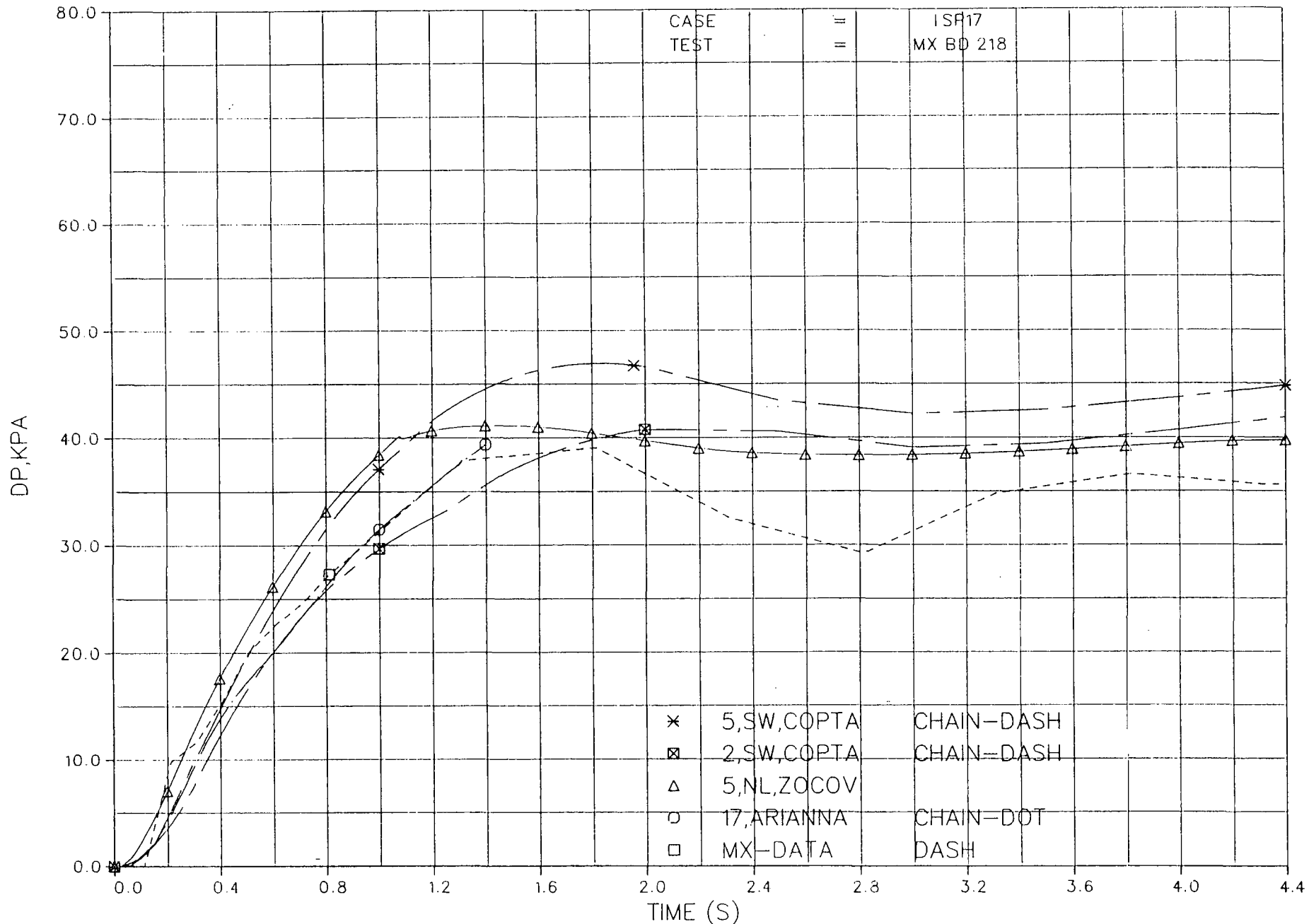


Diagram 1A. Short-time pressure difference, 110-105

ISP17,PRESSURE DIFF 110-105,110M213,DIAG M.22,TABLE M.4

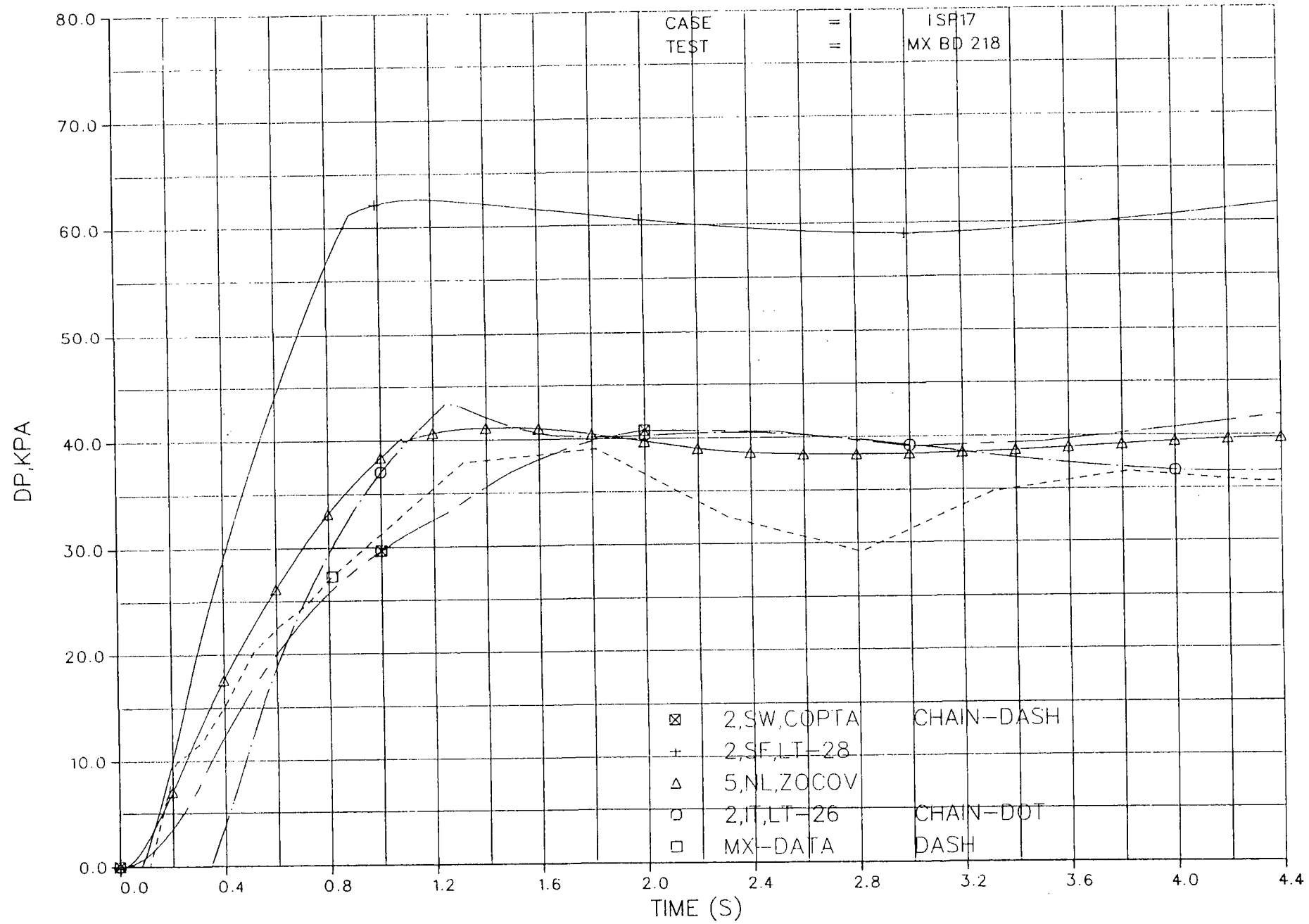


Diagram 1B. Short-time pressure difference, 110-105

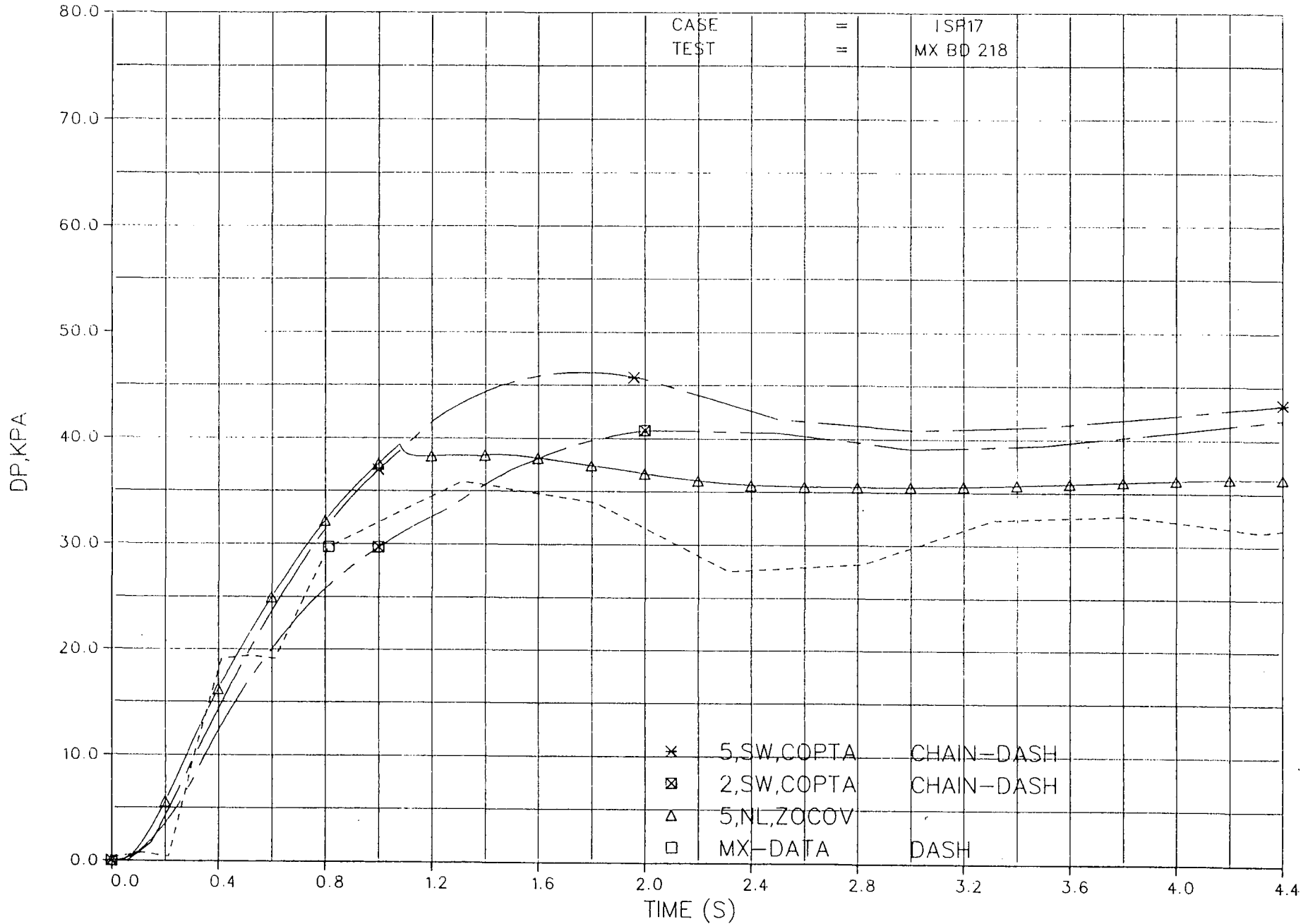


Diagram 2A. Short-time pressure difference, 106-105

ISP17,PRESSURE DIFF 106-105,106M215,DIAG M.23,TABLE M.4

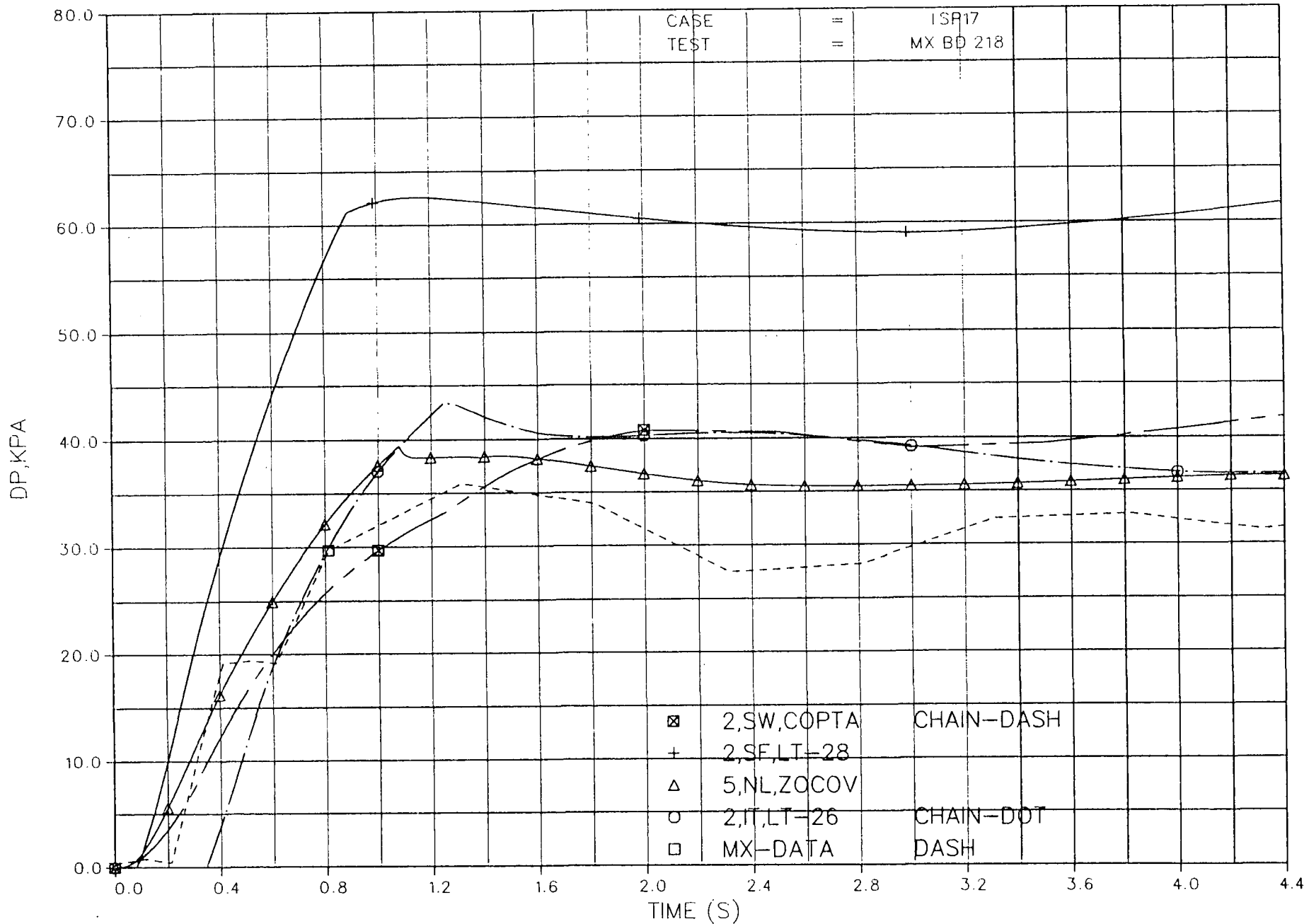


Diagram 2B. Short-time pressure difference, 106-105

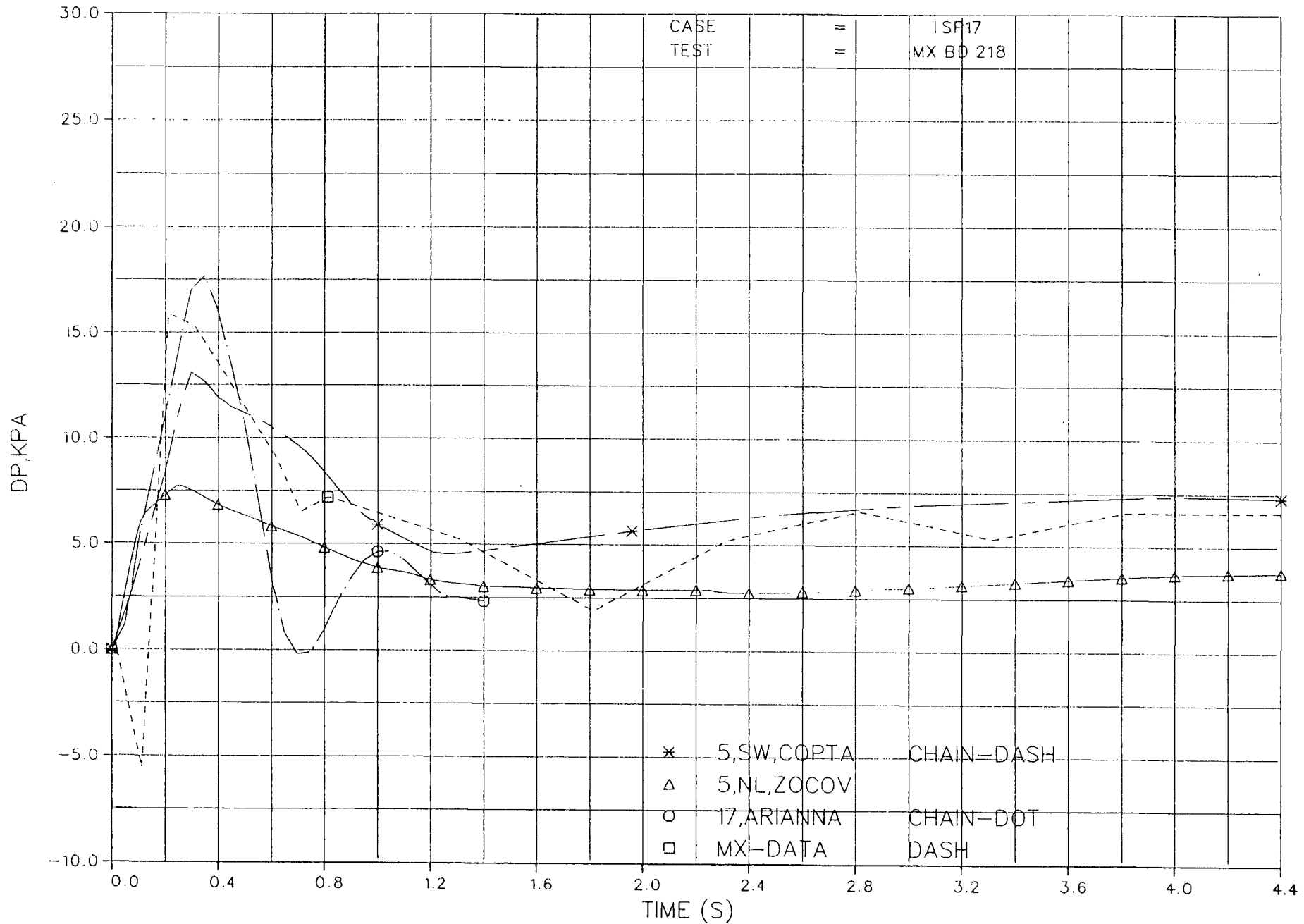


Diagram 3A. Short-time pressure difference, 122-124

Diagram 3B. Intentionally omitted

ISP17,PRESSURE DIFF 122-110,122M144-110M147,DIAG M.6,9,TABLE M.2

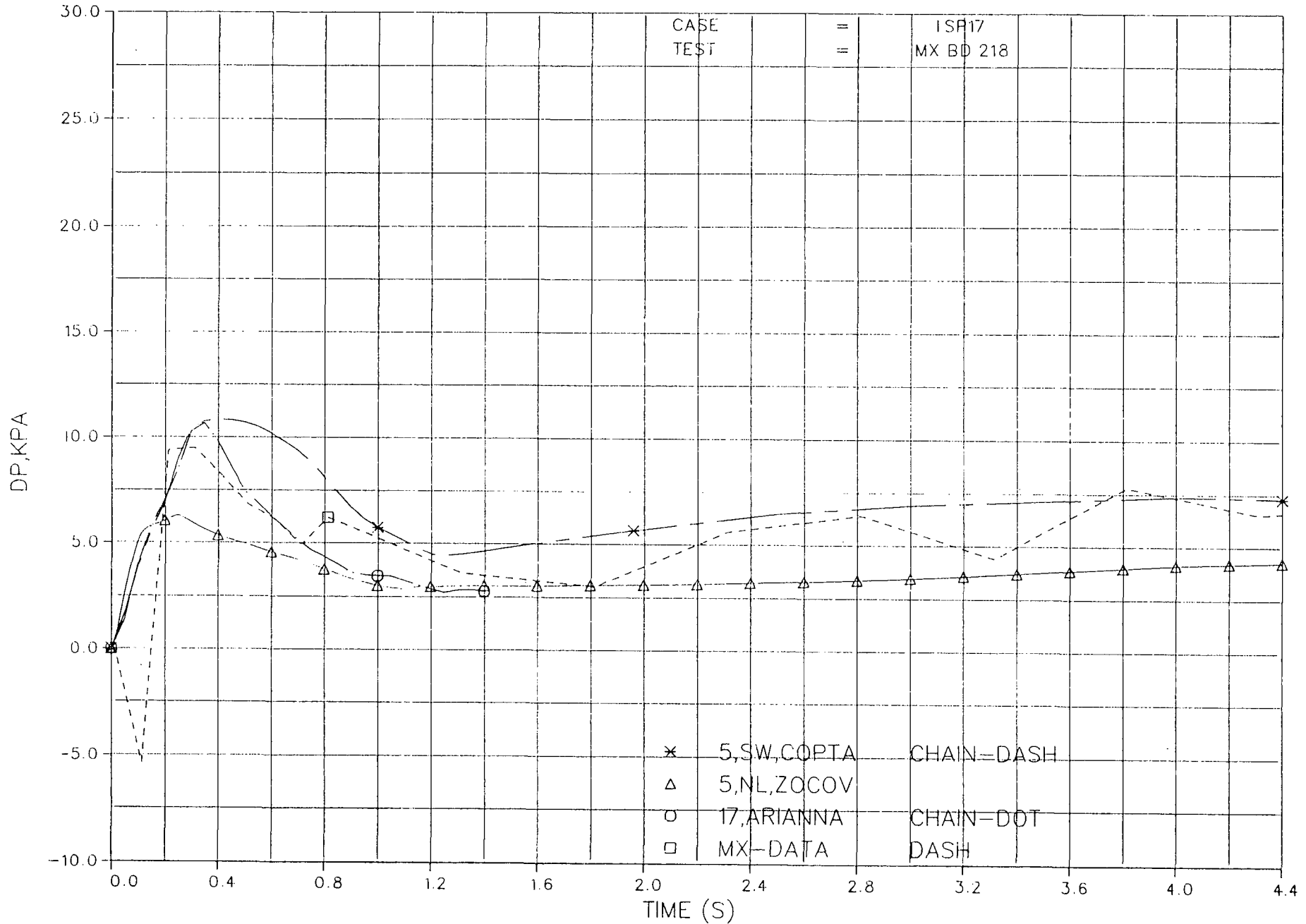


Diagram 4A. Short-time pressure difference, 122-110

Diagram 4B. Intentionally omitted



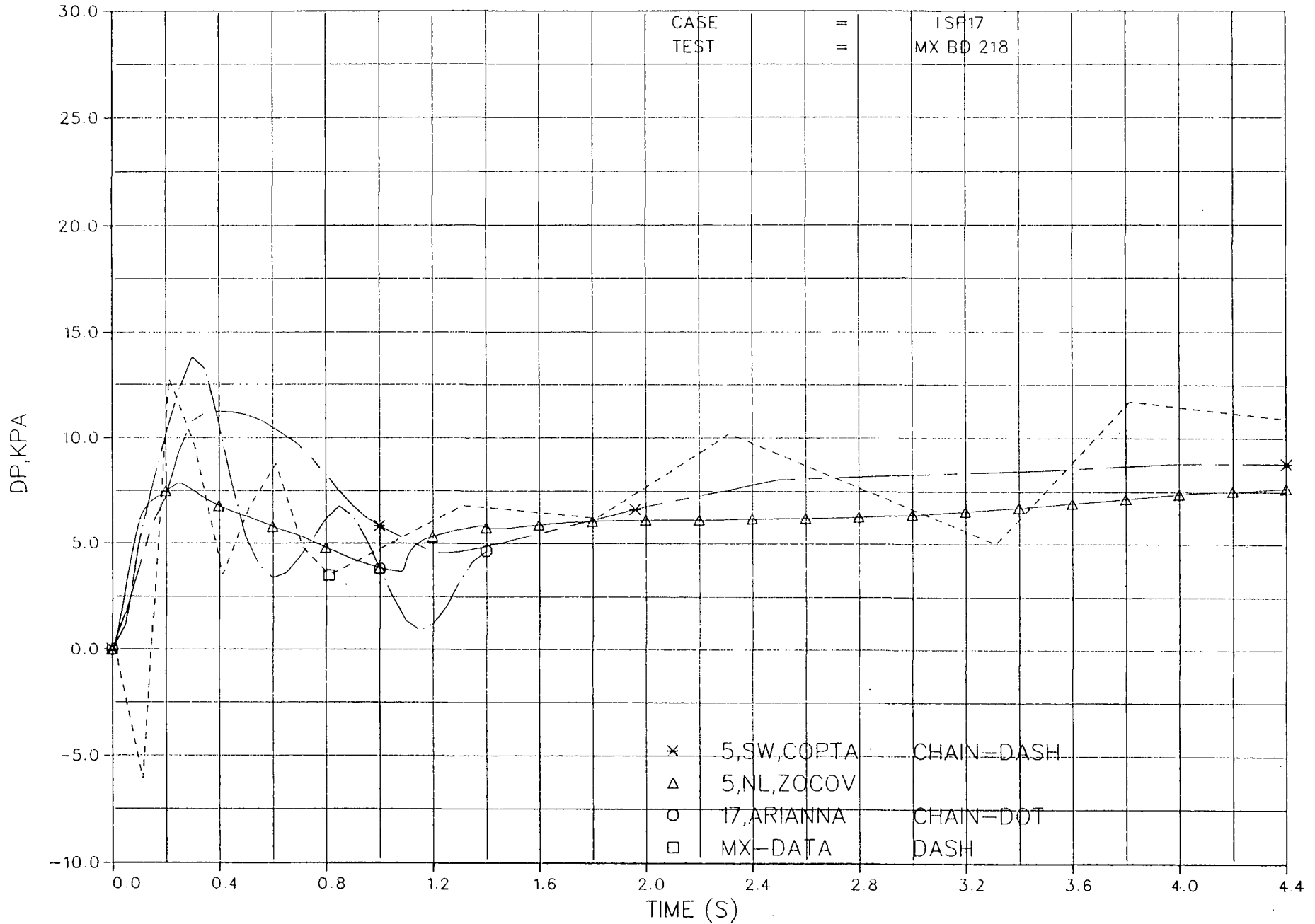


Diagram 5A. Short-time pressure difference, 122-106

Diagram 5B. Intentionally omitted

ISP17, PRESSURE IN ROOM 124,124M142,DIAG M.4,TABLE M.2

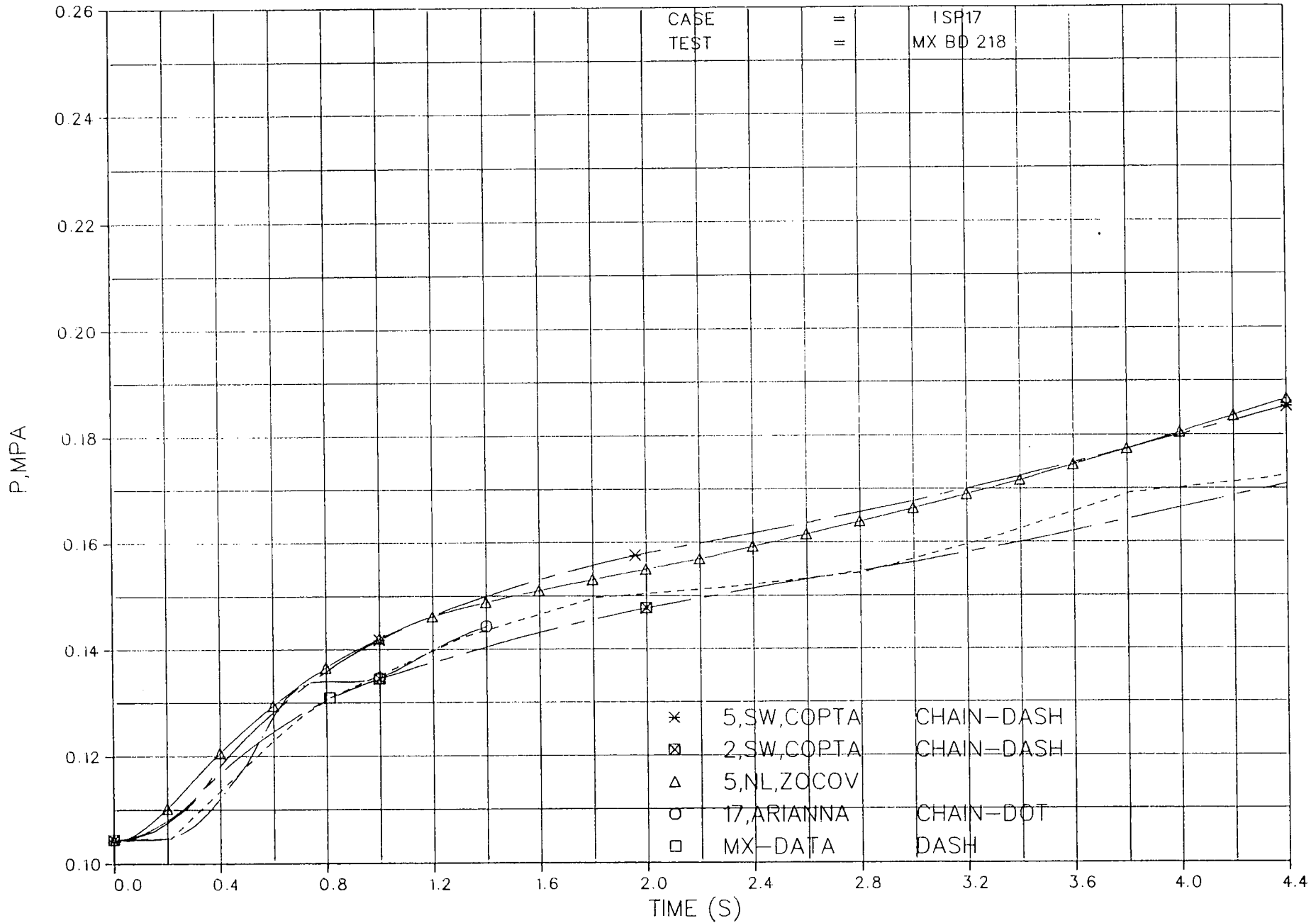


Diagram 6A. Short-time pressure transient in room 124

Diagram 6B. Intentionally omitted

ISP17, PRESSURE IN ROOM 122,122M144,DIAG M.6,TABLE M.2

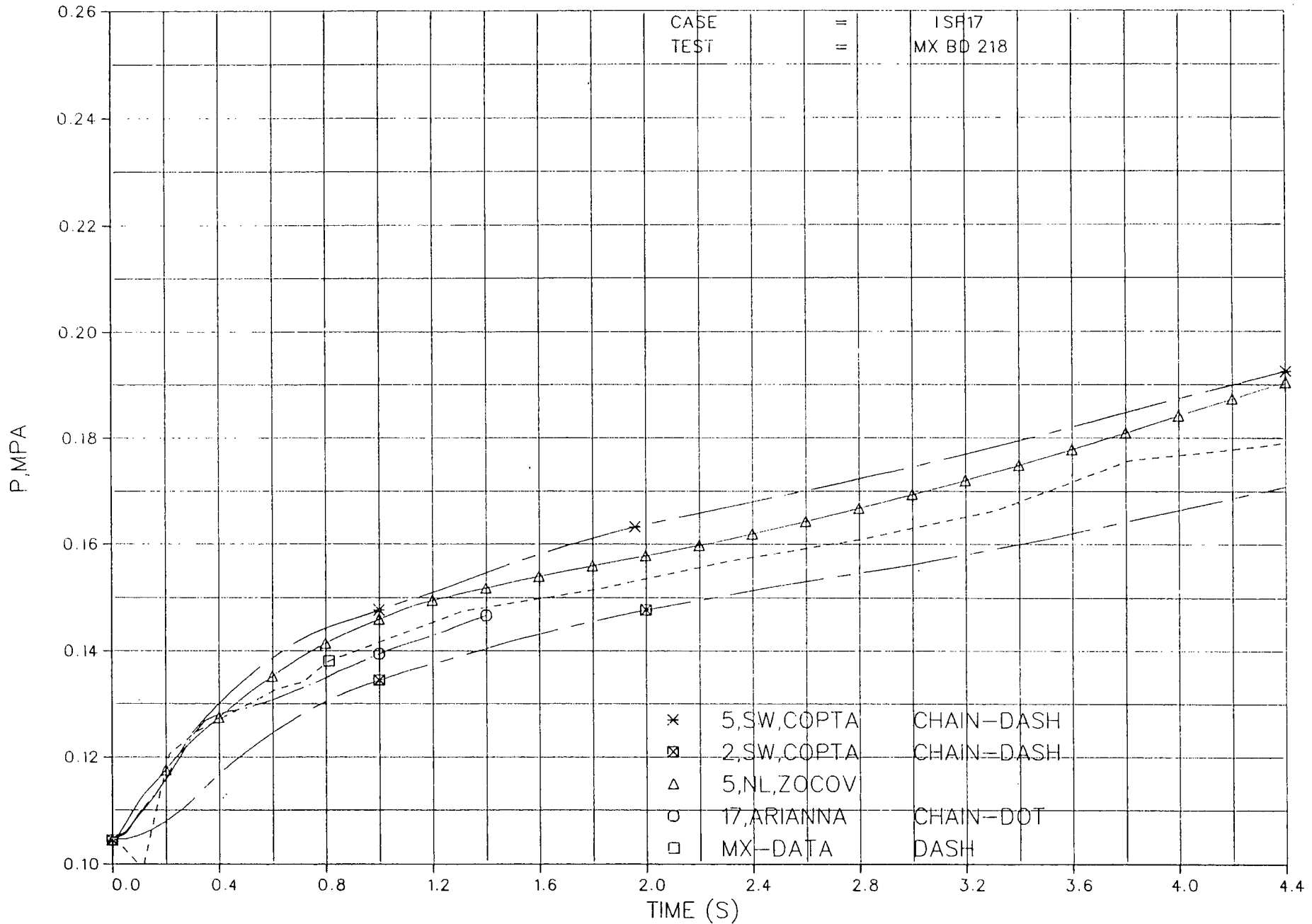


Diagram 7A. Short-time pressure transient in room 122

Diagram 7B. Intentionally omitted

ISP17, PRESSURE IN ROOM 110,110M147,DIAG M.9,TABLE M.2

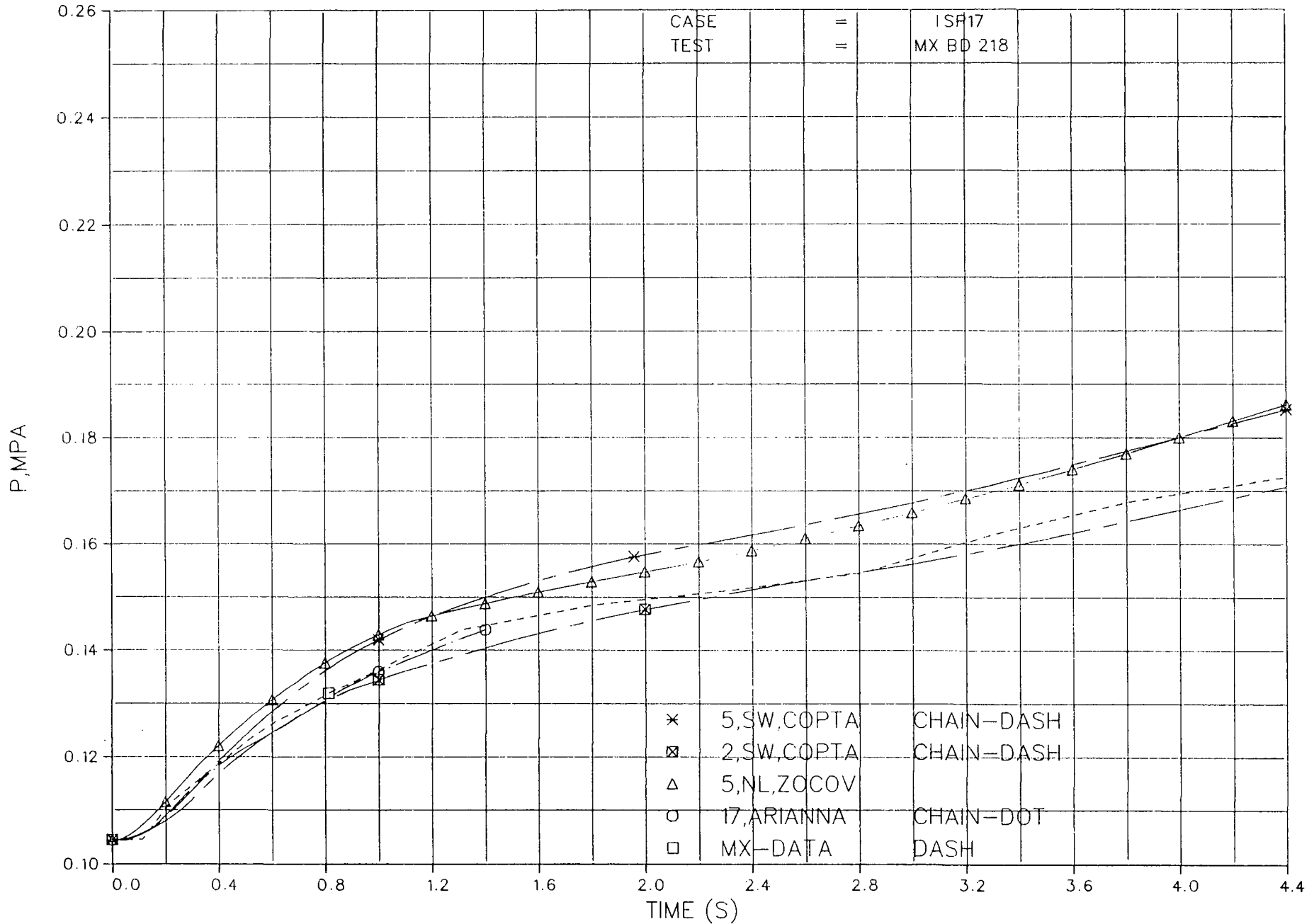


Diagram 8A. Short-time pressure transient in room 110

ISP17, PRESSURE IN ROOM 110,110M147,DIAG M.9,TABLE M.2

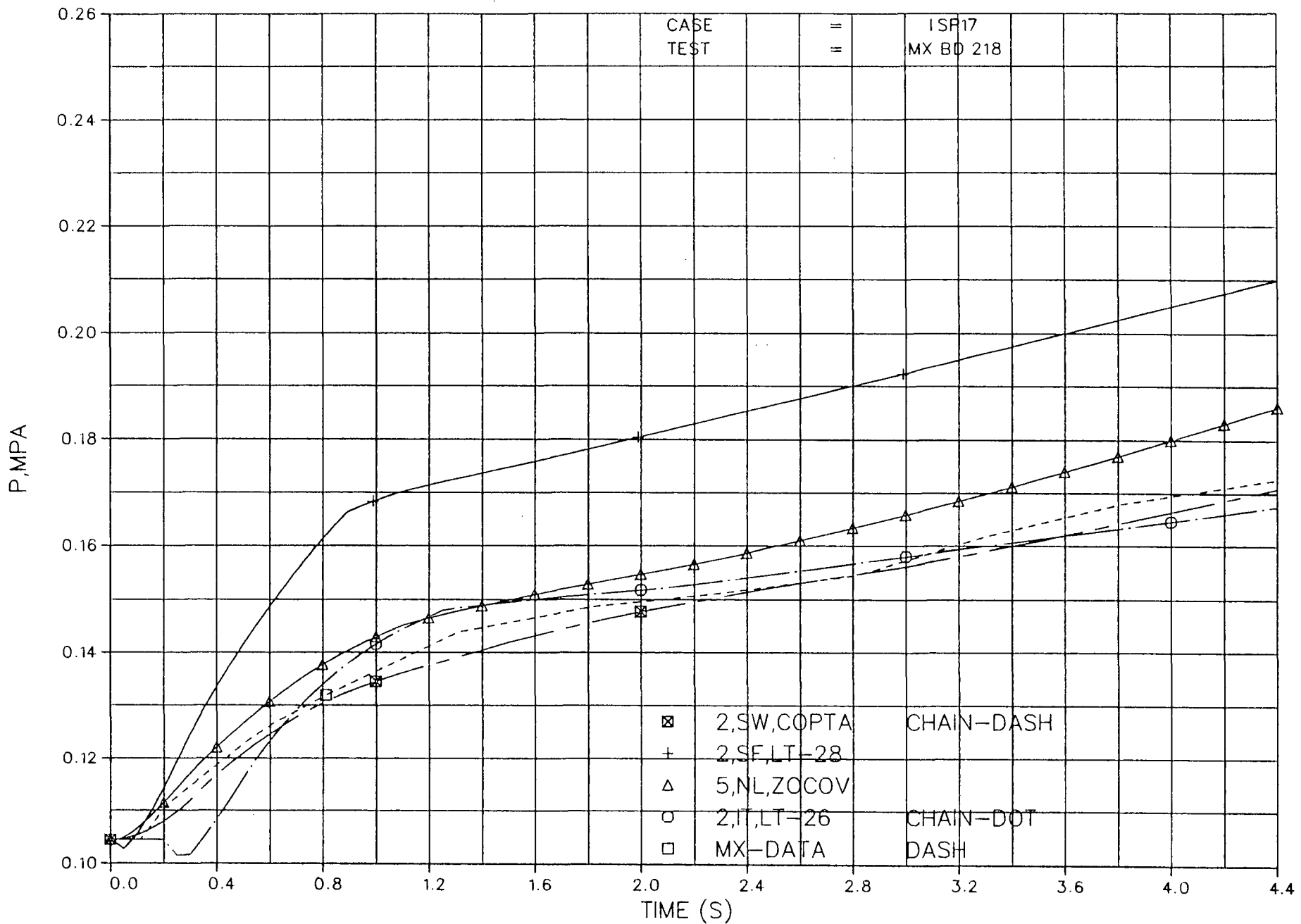


Diagram 8B. Short-time pressure transient in room 110



ISP17, PRESSURE IN ROOM 106,106M163,DIAG M.14,TABLE M.5

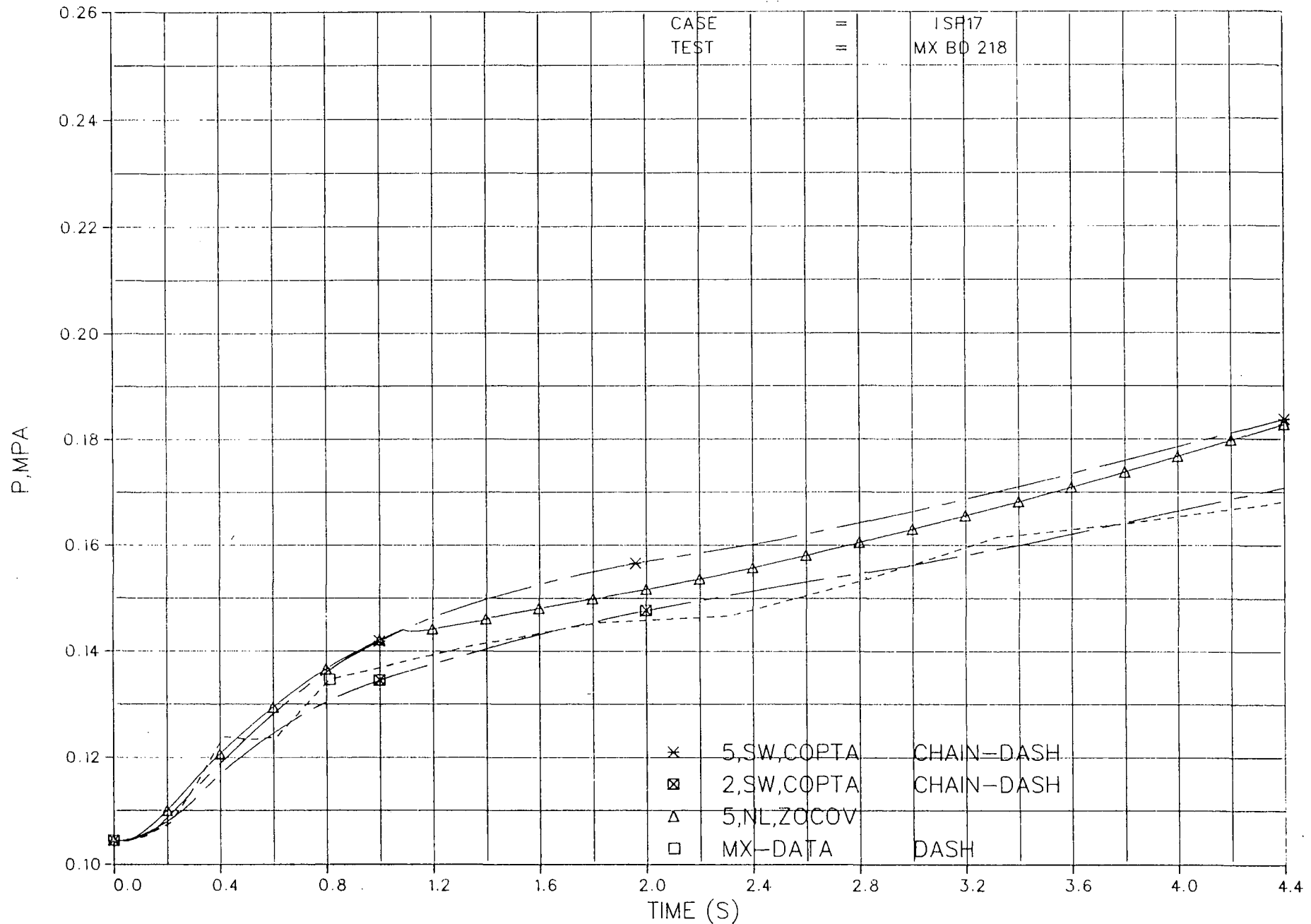


Diagram 9A. Short-time pressure transient in room 106

ISP17, PRESSURE IN ROOM 106,106M163,DIAG M.14, TABLE M.5

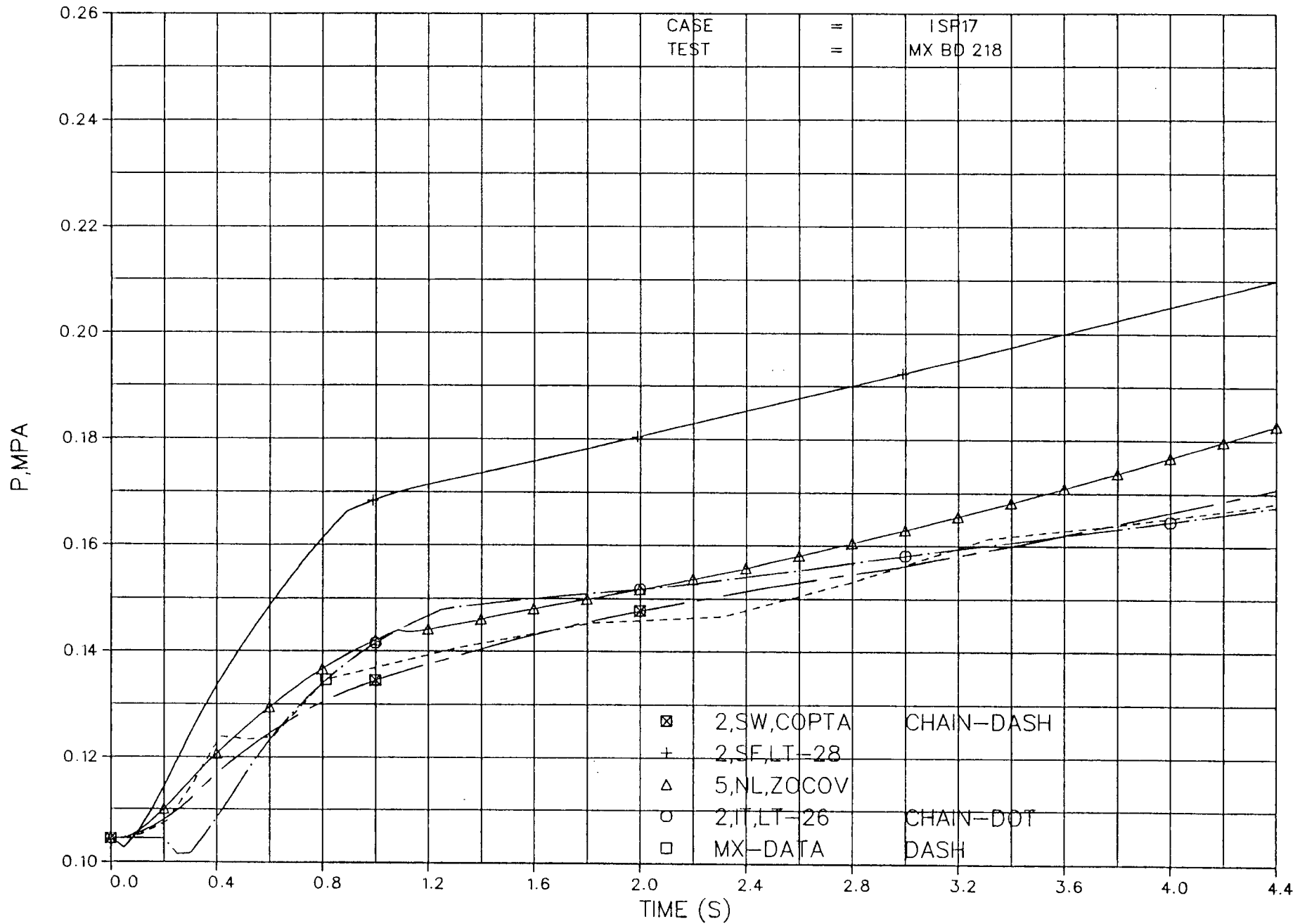


Diagram 9B. Short-time pressure transient in room 106

Diagram 10A. Intentionally omitted

ISP17,WETWELL PRESSURE,105M122,DIAG M.18,TABLE M.4

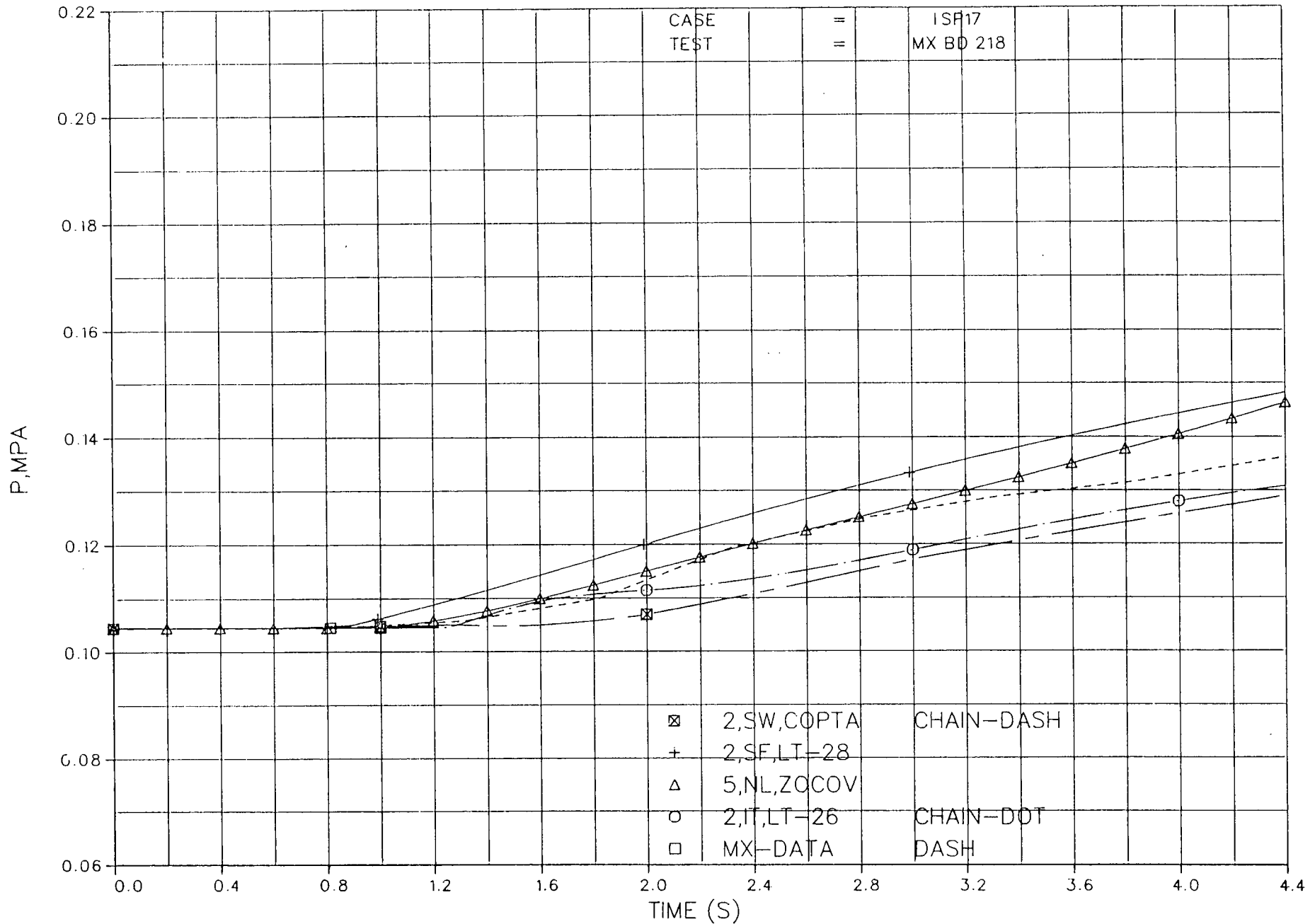


Diagram 10B. Short-time pressure transient in wetwell

ISP17,TEMPERATURE IN ROOM 124,VAPOR,124M572,DIAG M.24,TABLE M.6

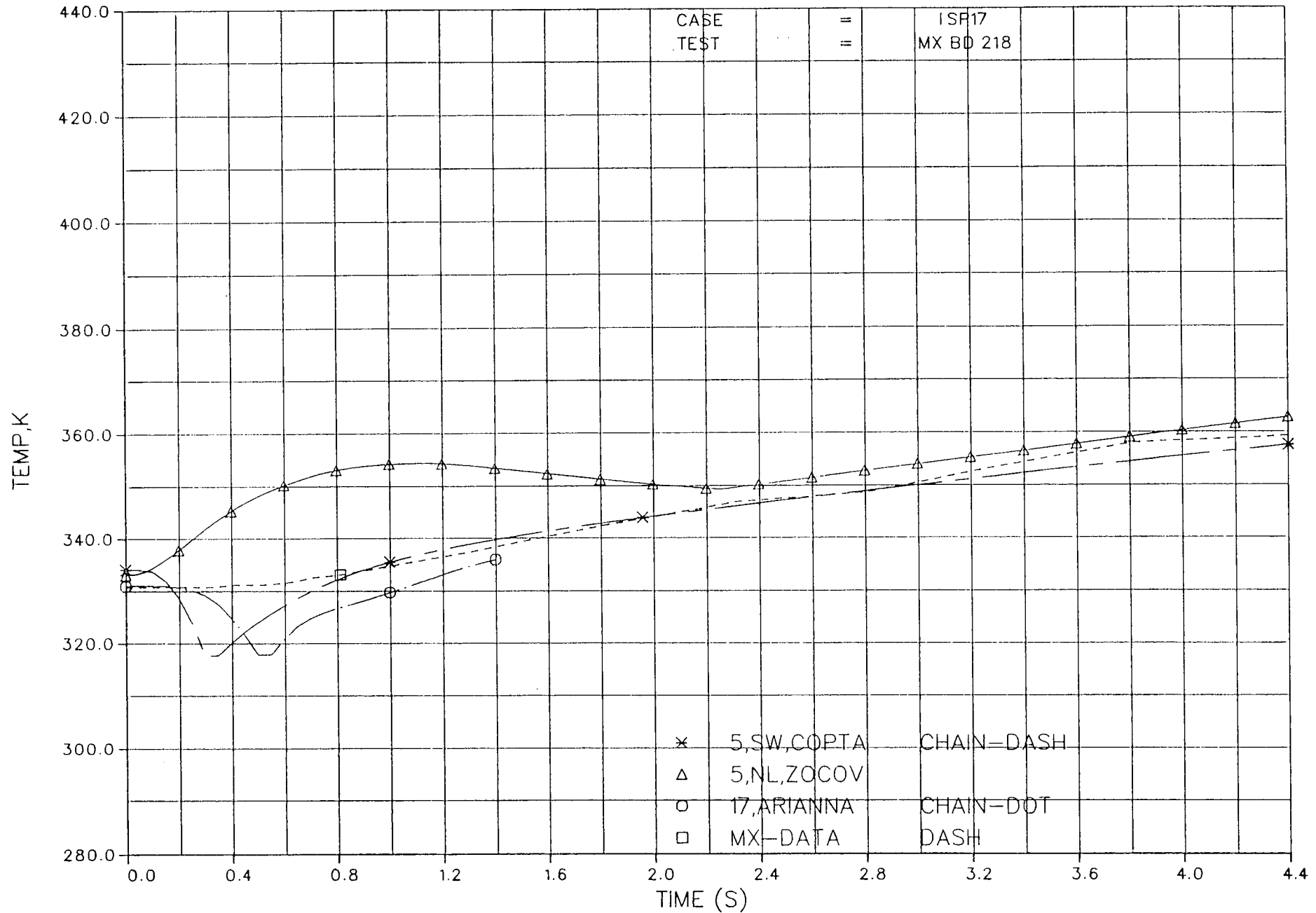


Diagram 11A. Short-time temperature transient in room 124

Diagram 11B. Intentionally omitted

ISP17,TEMPERATURE IN ROOM 122,VAPOR,122M574,DIAG M.24,TABLE M.6

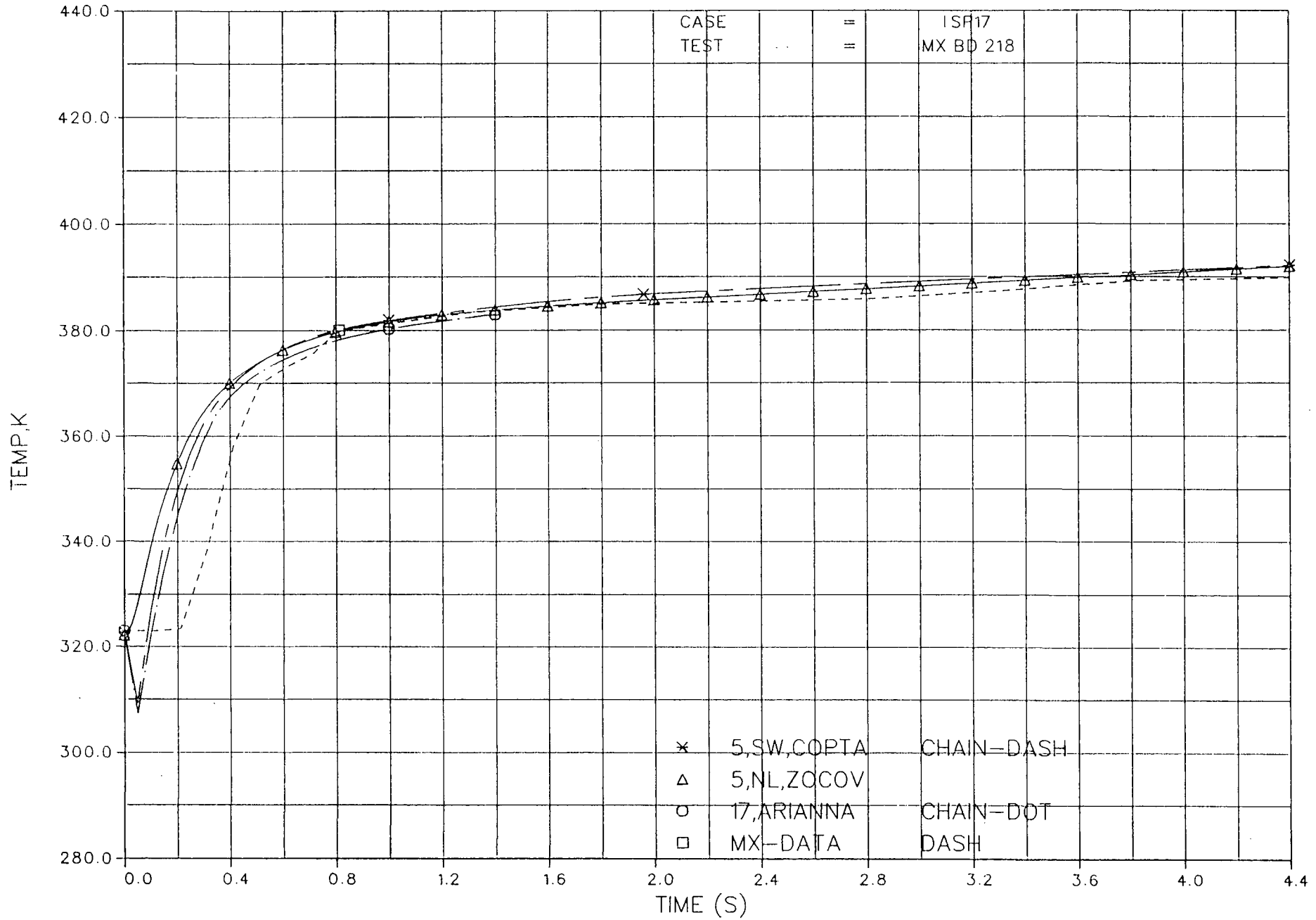


Diagram 12A. Short-time temperature transient in room 122

Diagram 12B. Intentionally omitted



ISP17,TEMPERATURE IN ROOM 111,VAPOR,111M576,DIAG M.25,TABLE M.6

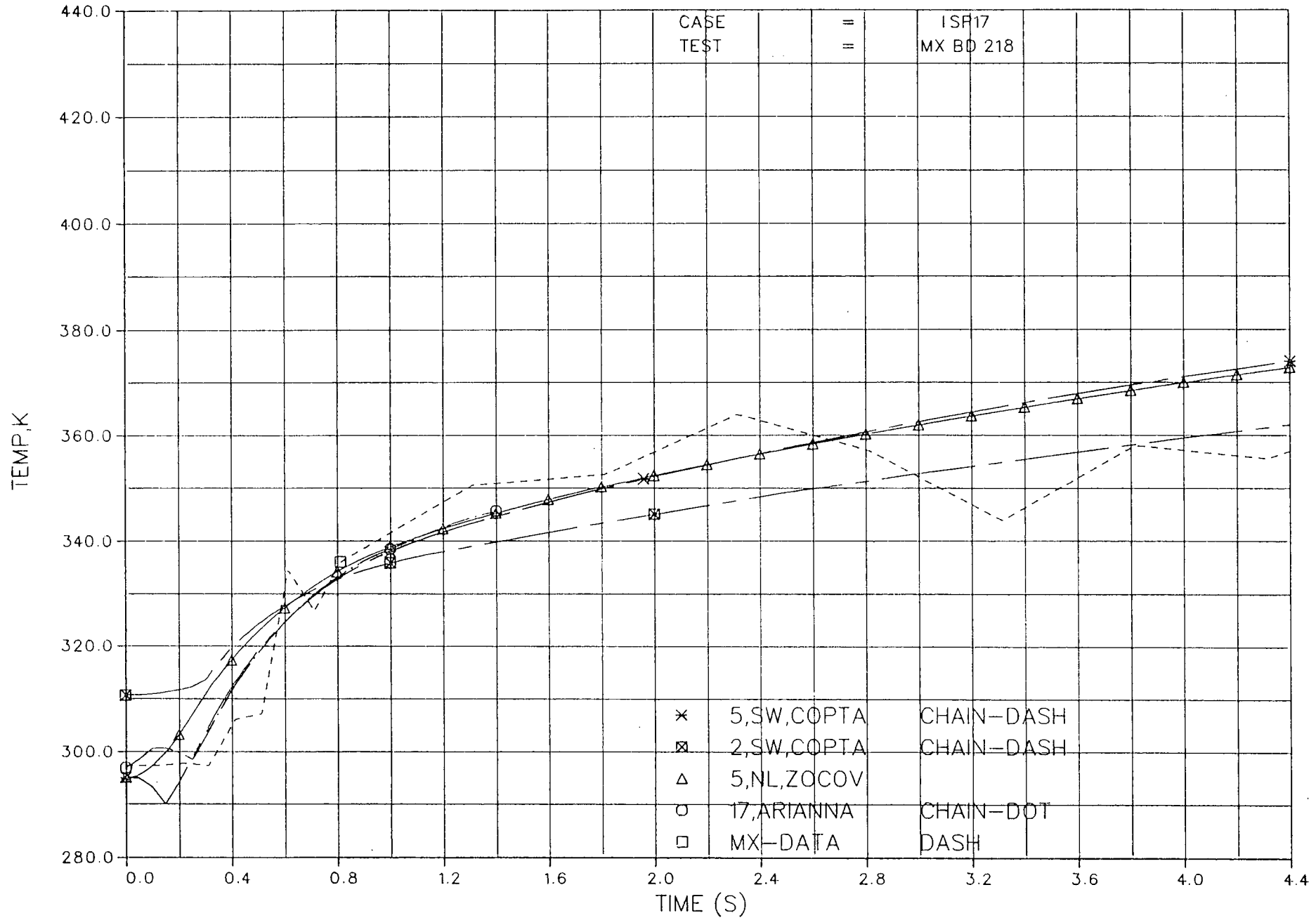


Diagram 13A. Short-time temperature transient in room 111

ISP17,TEMPERATURE IN ROOM 111,VAPOR,111M576,DIAG M.25,TABLE M.6

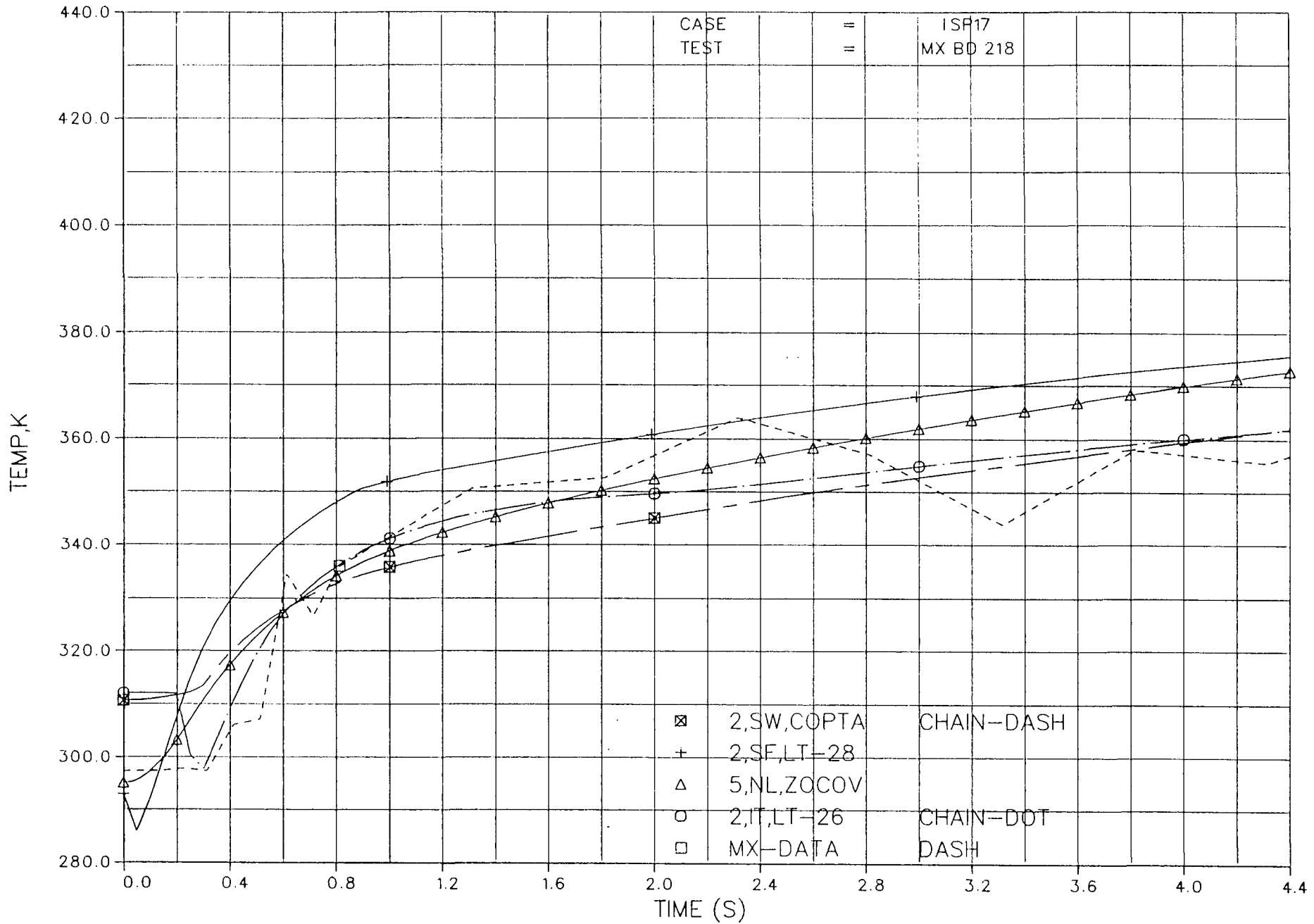


Diagram 13B. Short-time temperature transient in room 111

ISP17,TEMPERATURE IN ROOM 106,VAPOR,106M586,DIAG M.28,TABLE M.7

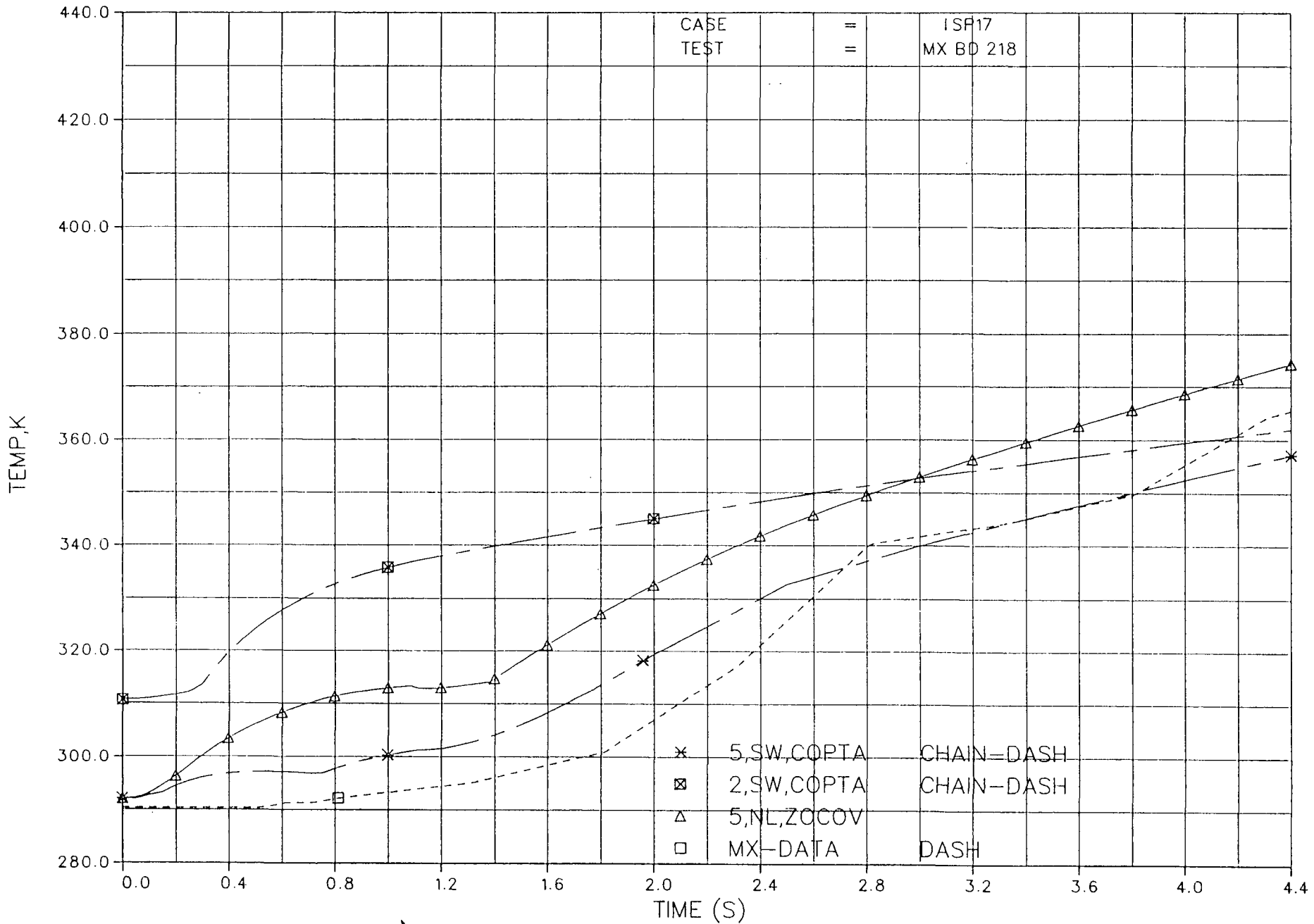


Diagram 14A. Short-time temperature transient in room 106

ISP17,TEMPERATURE IN ROOM 106,VAPOR,106M586,DIAG M.28,TABLE M.7

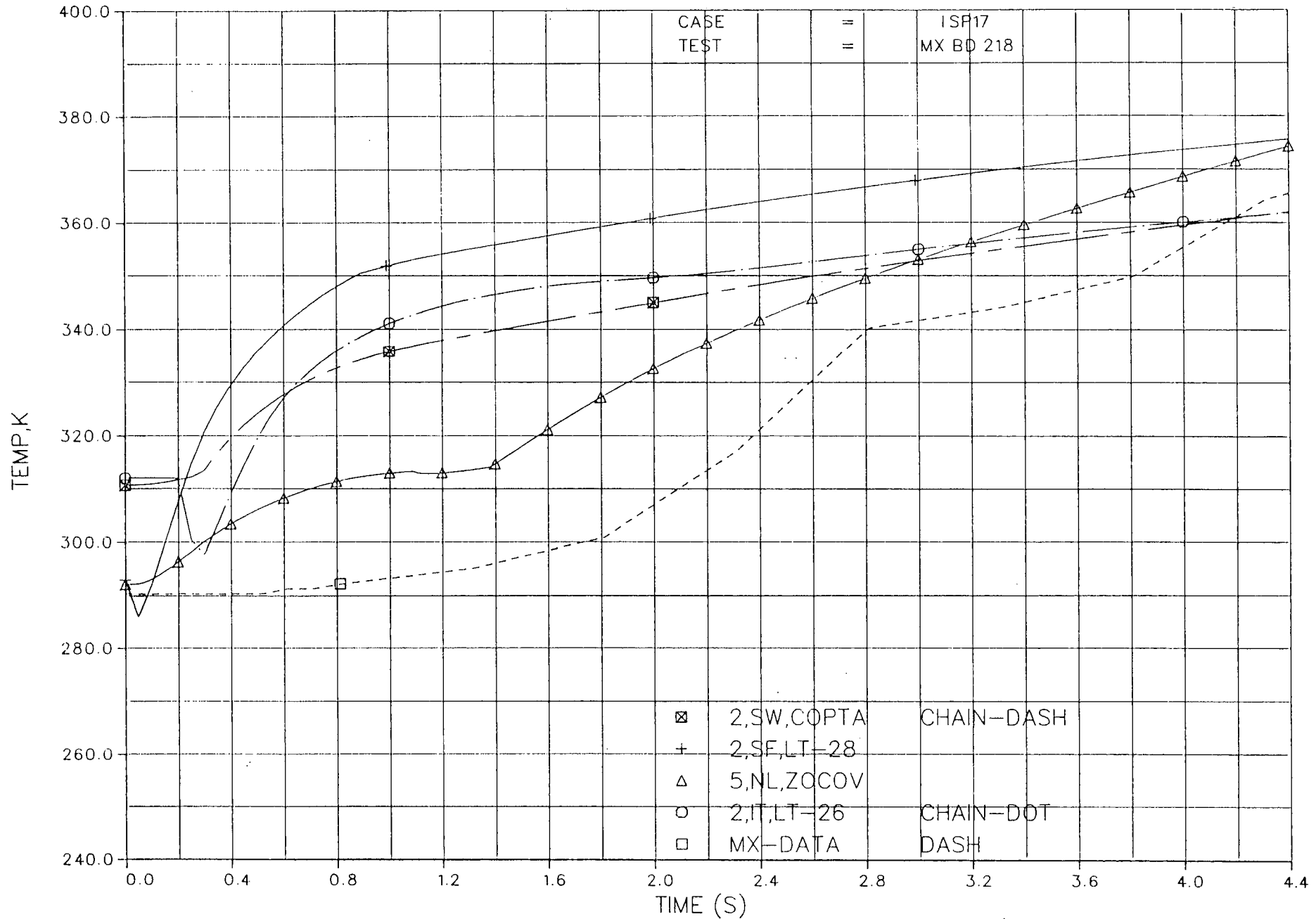


Diagram 14B. Short-time temperature transient in room 106

ISP17,TEMPERATURE IN ROOM 105,VAPOR,AVERAGE,DIAG E.16,TABLE E.6 (MX-DATA SLOW?)

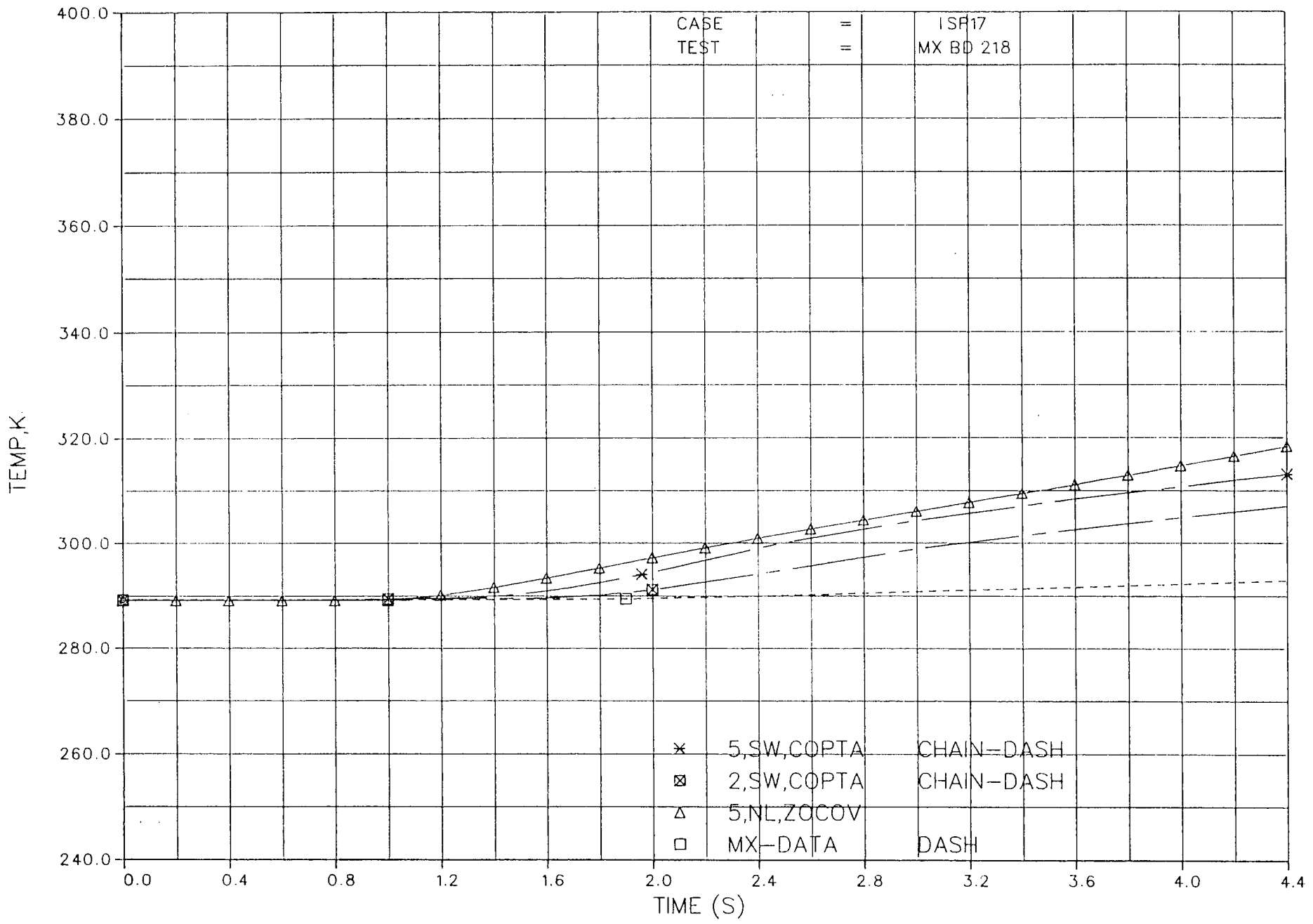


Diagram 15A. Short-time temperature transient in wetwell vapor

ISP17,TEMPERATURE IN ROOM 105,VAPOR,AVERAGE,DIAG E.16,TABLE E.6 (MX-DATA SLOW?)

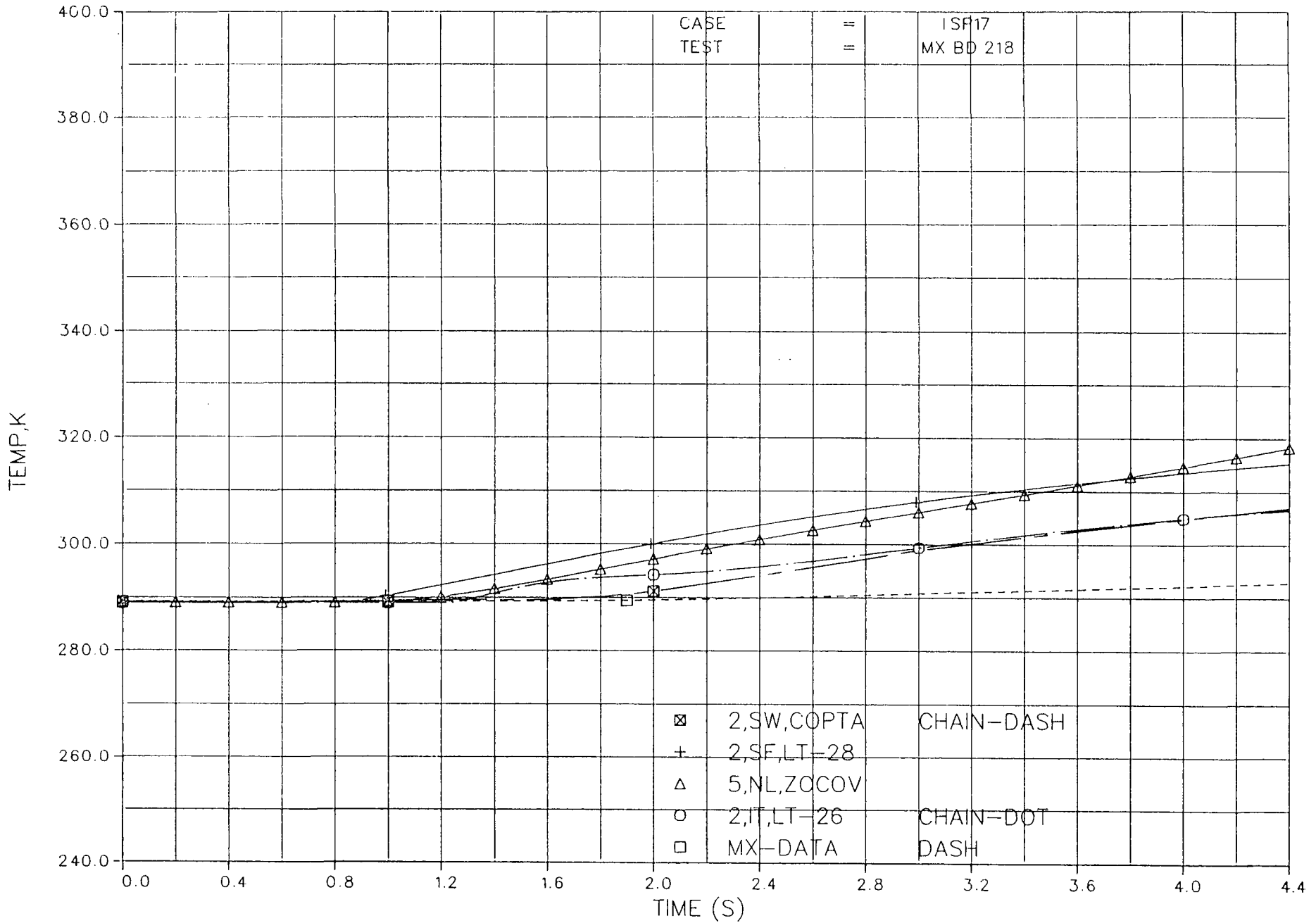


Diagram 15B. Short-time temperature transient in wetwell vapor



ISP17, WATER PLUG SIZE IN VENT PIPES, DIAG E.29

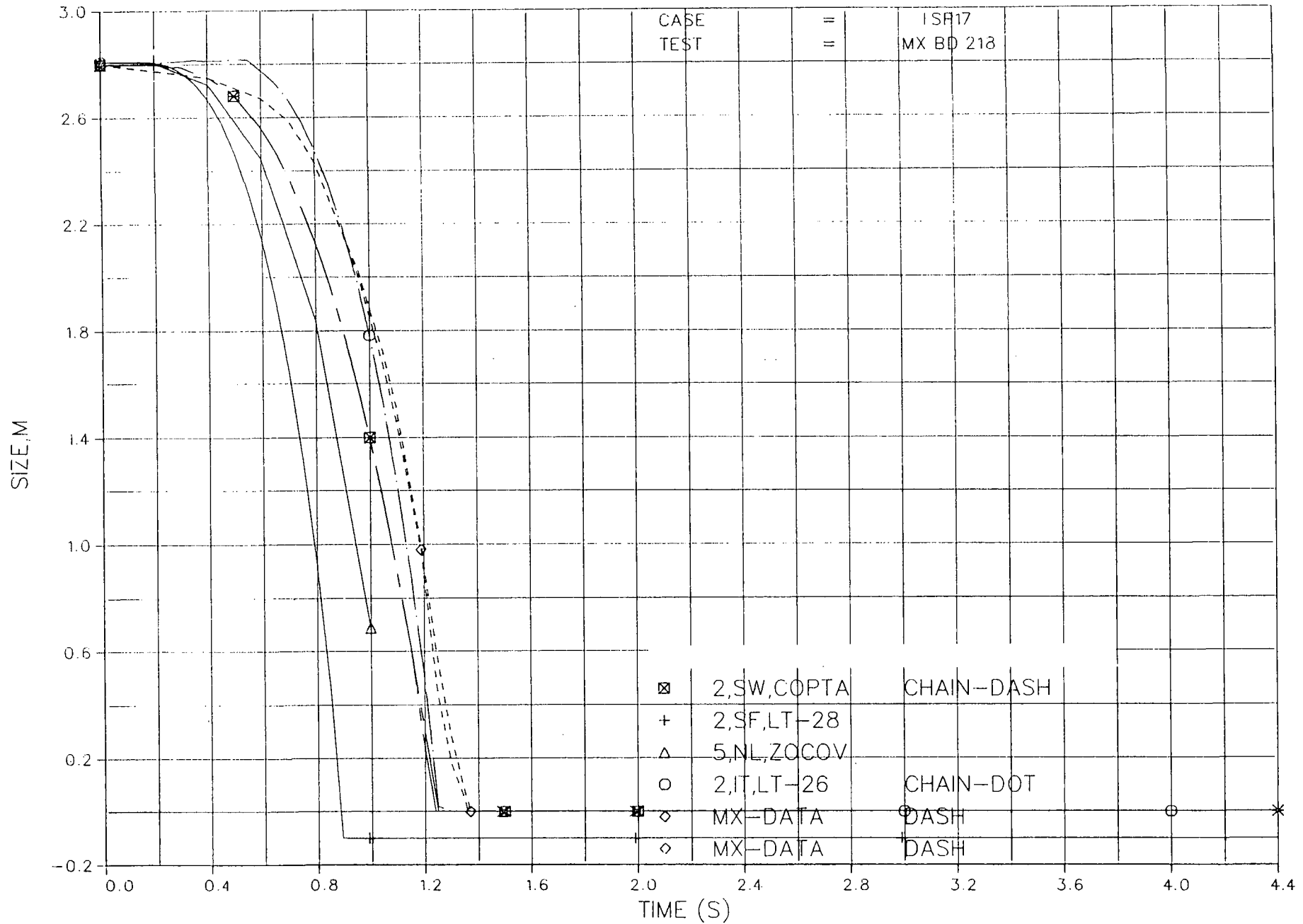


Diagram 16B. Water plug size



ISP17, POOL LEVEL, DIAG E.27

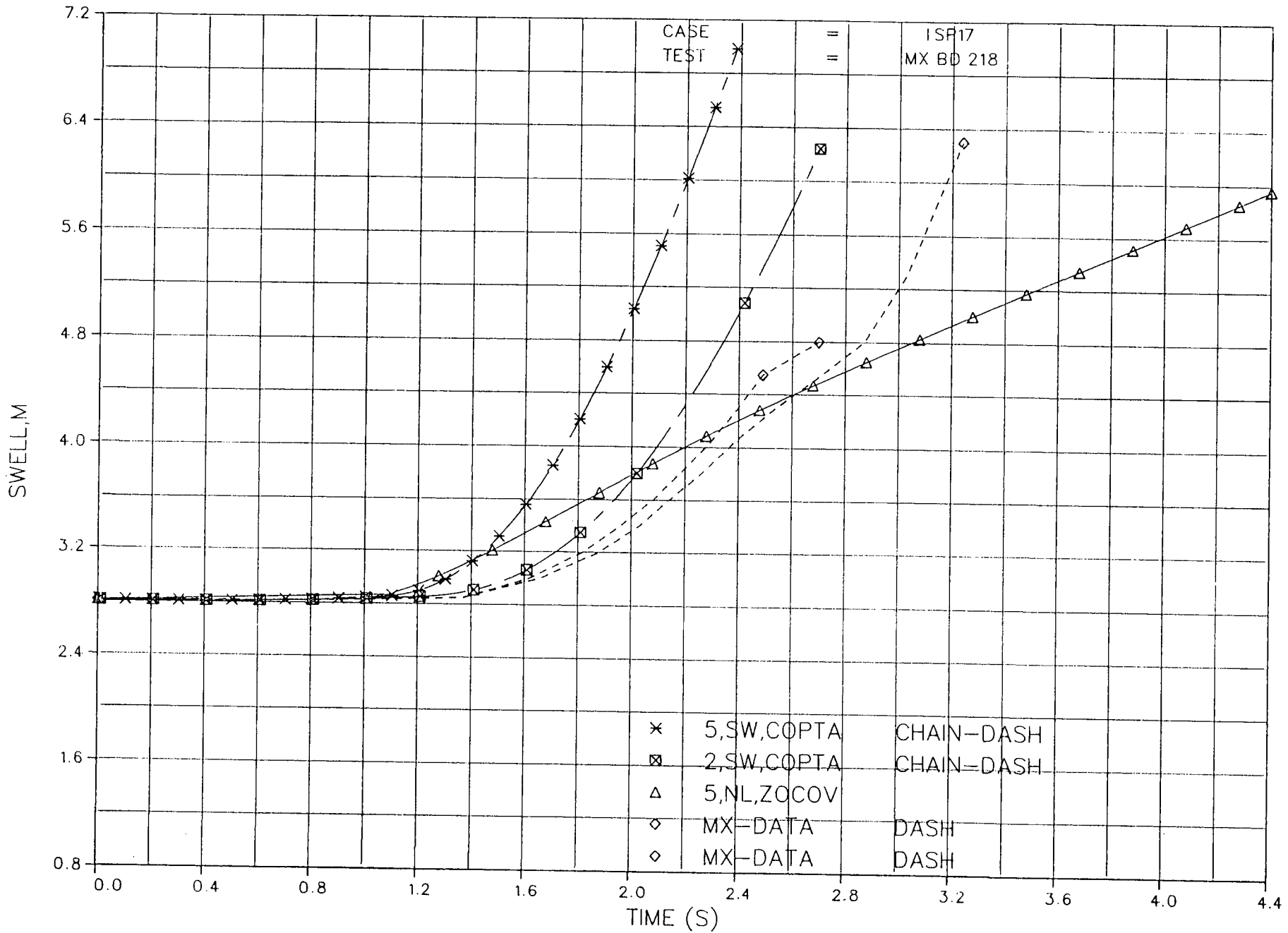


Diagram 17A. Pool level

Diagram 17B. Intentionally omitted

ISP17,PRESSURE DIFF DRYWELL-WETWELL,110M213,DIAG M.22,TABLE M.4

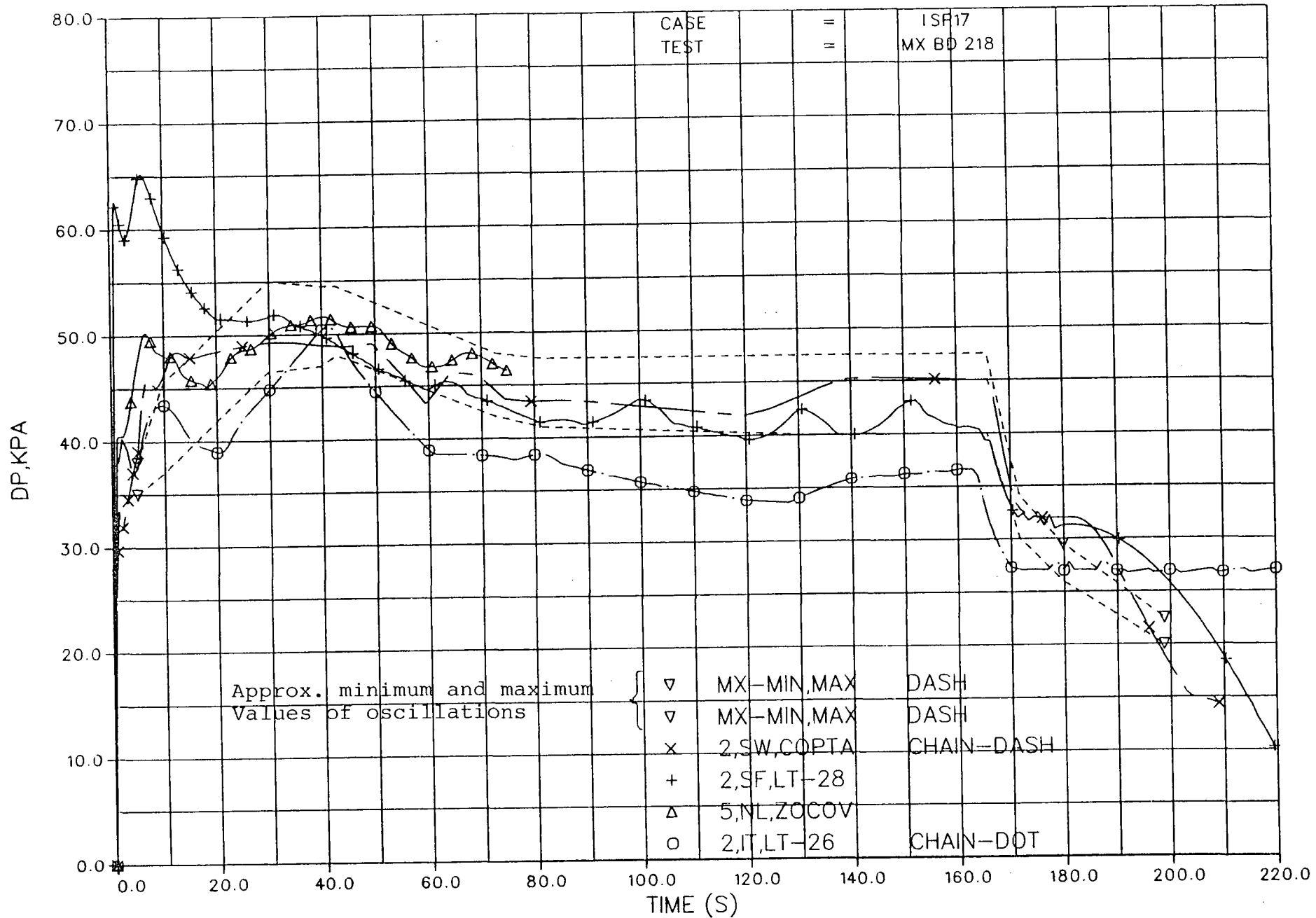


Diagram 18. Long-time pressure difference drywell-wetwell

ISP17,PRESSURE DIFF HEADER-WETWELL,106M215,DIAG M.23,TABLE M.4

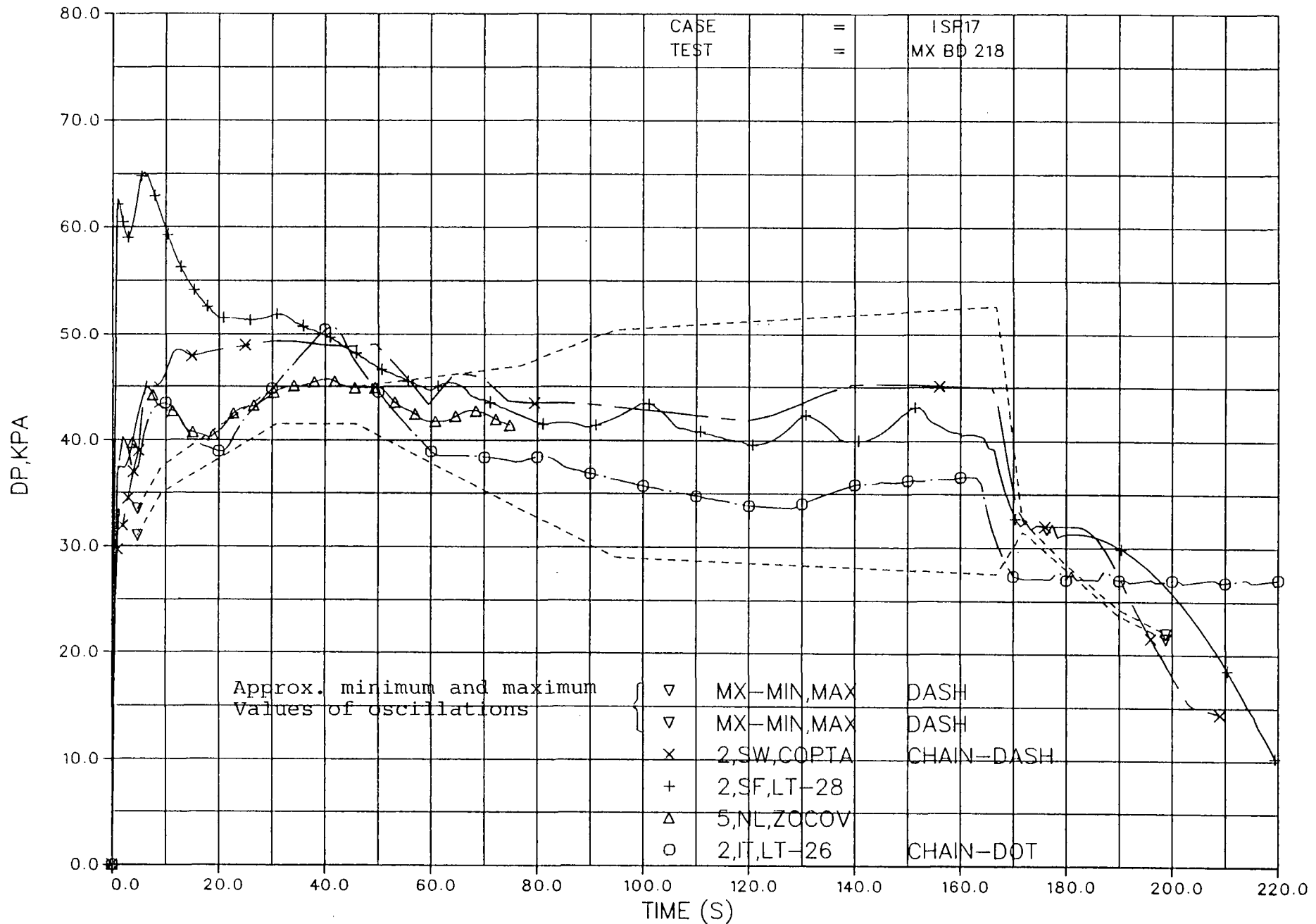


Diagram 19. Long-time pressure difference header-wetwell

ISP17, DRYWELL PRESURE, 110M147, DIAG M.9, TABLE M.2

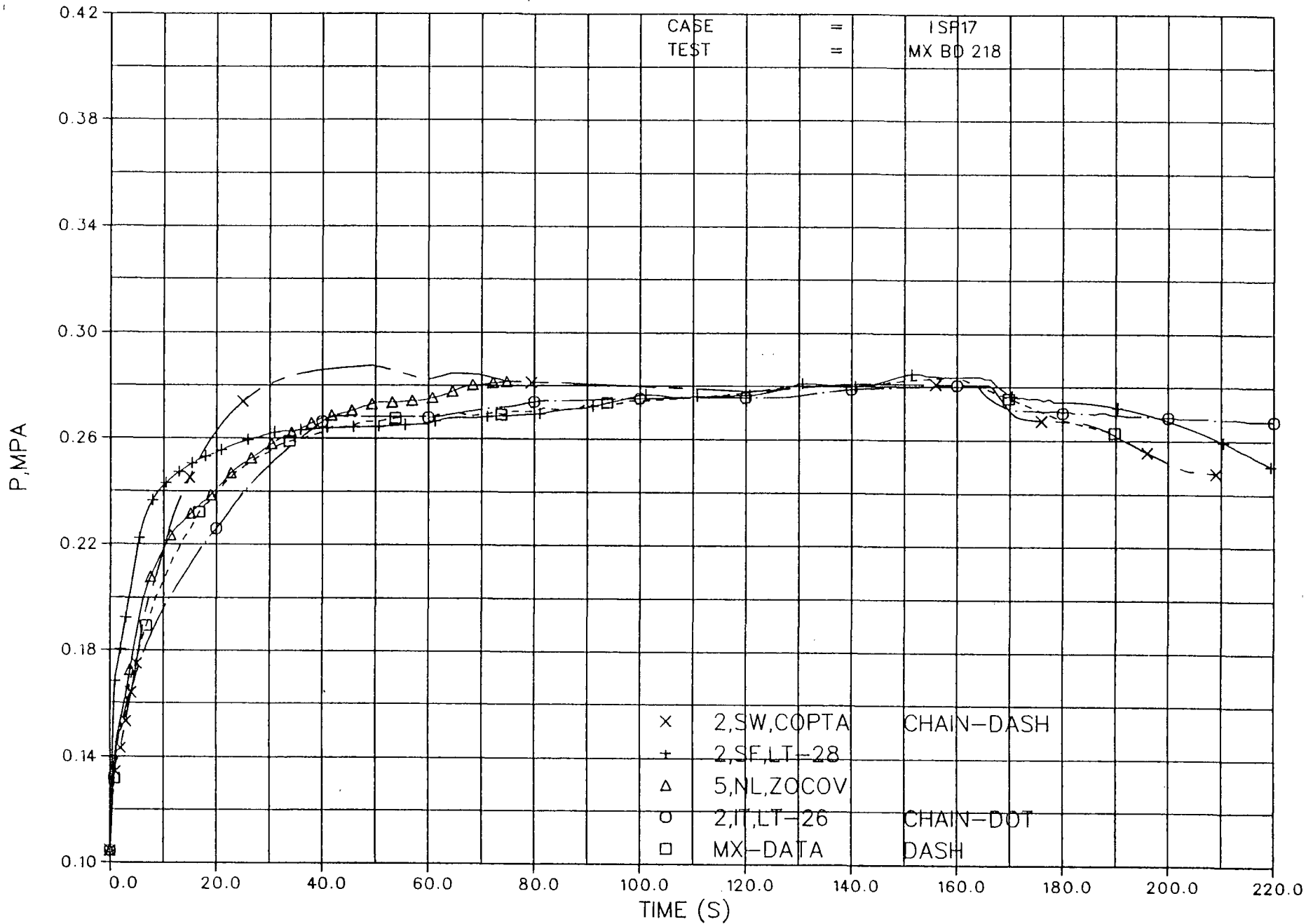


Diagram 20. Drywell pressure

ISP17,HEADER PRESSURE,106M163,DIAG M.14,TABLE M.5

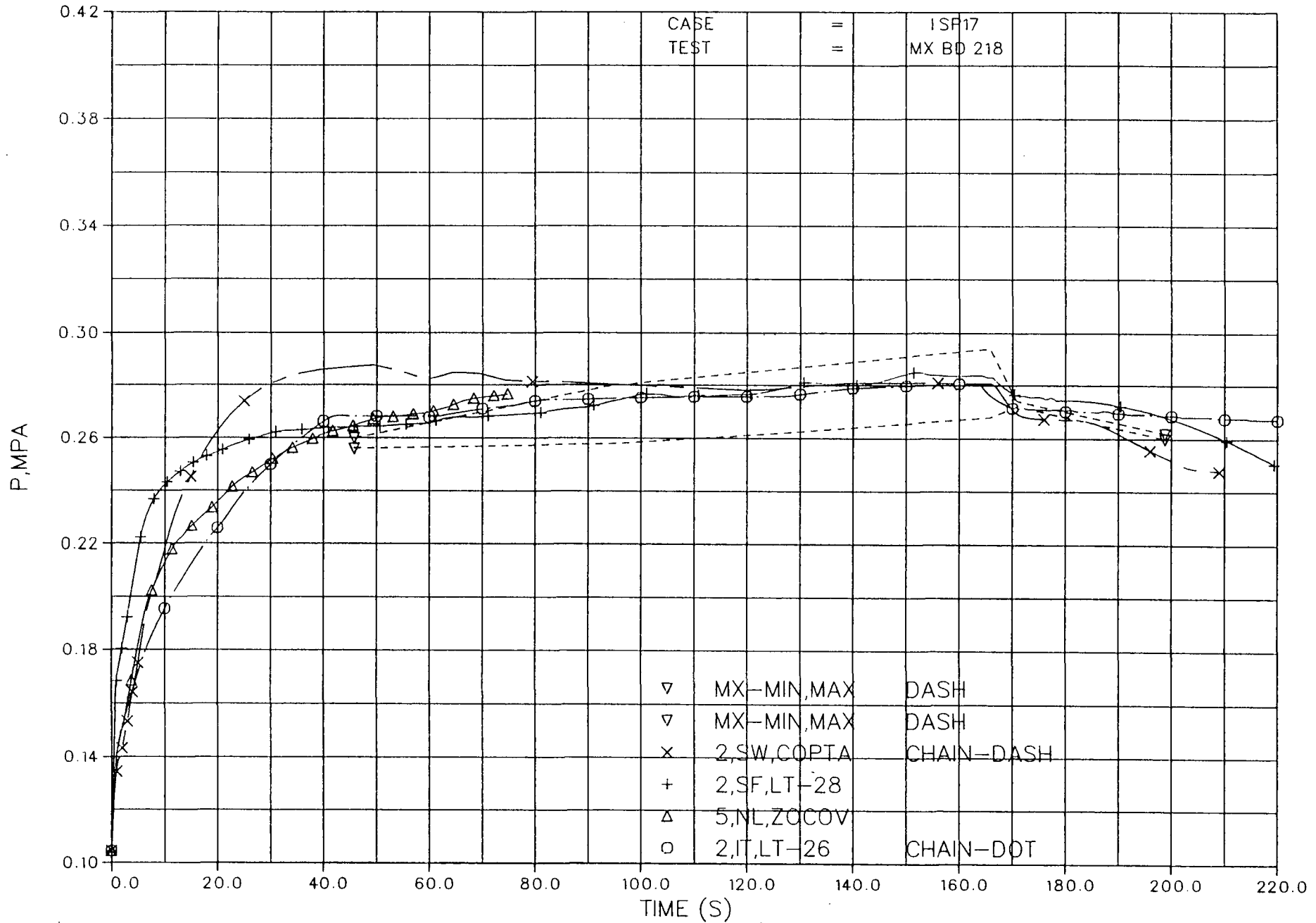


Diagram 21. Header pressure

ISP17, WETWELL PRESSURE, 105M122, DIAG M.18, TABLE M.4

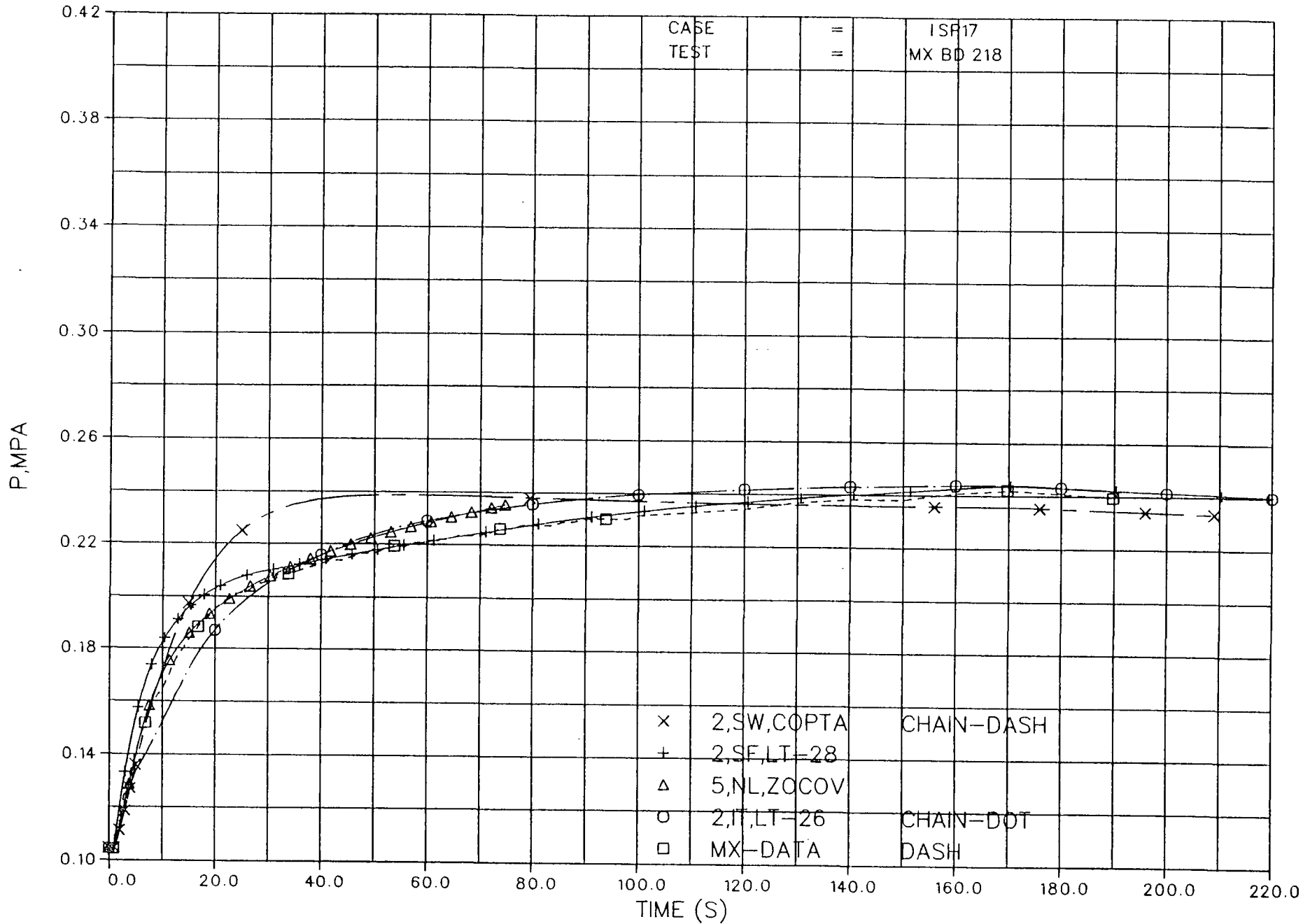


Diagram 22. Wetwell pressure

ISP17, DRYWELL TEMPERATURE, 111M576, DIAG M.25, TABLE M.6

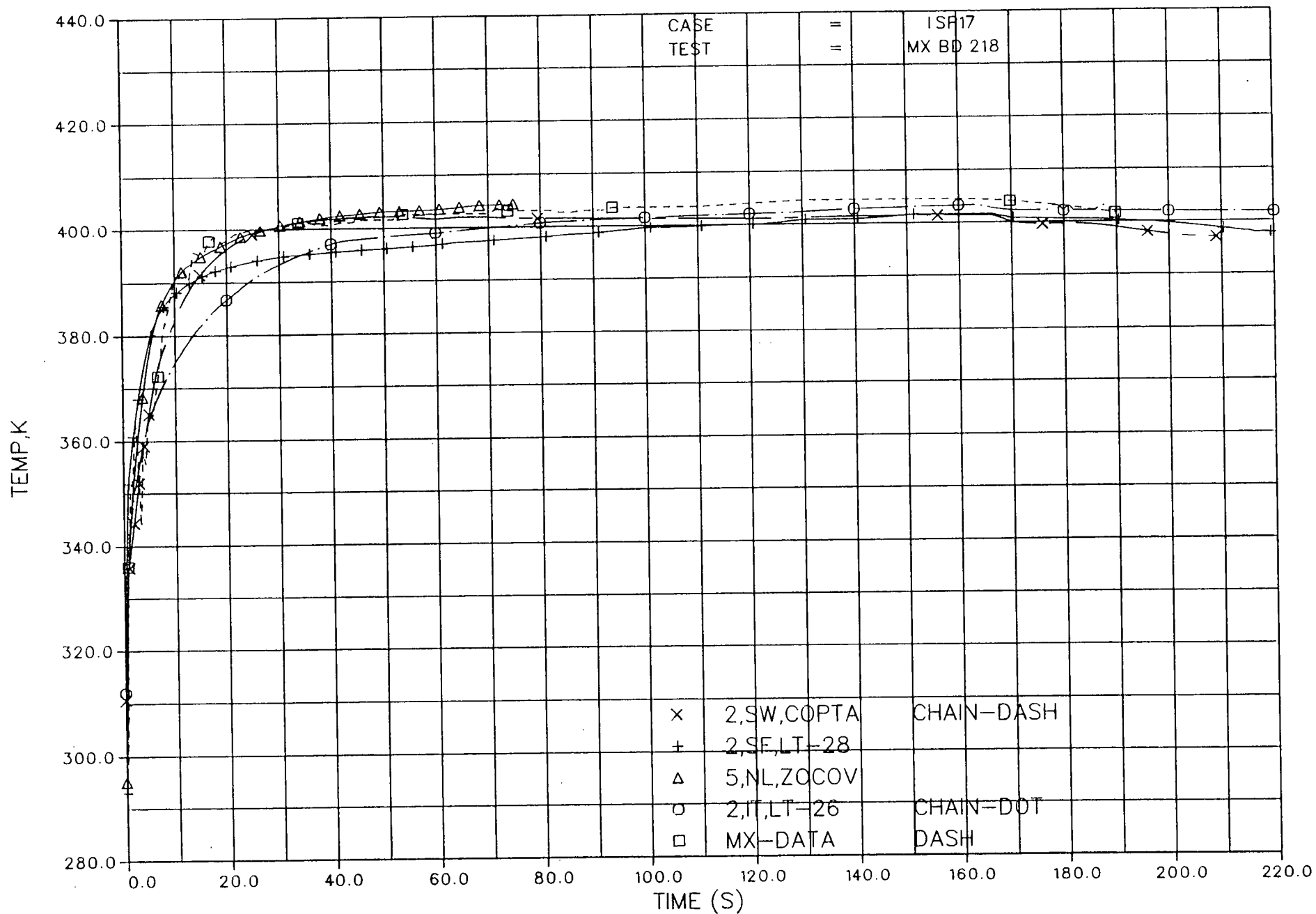


Diagram 23. Drywell temperature

SD-84/43  
 NR-84/428  
 1984-06-04



ISP17,HEADER TEMPERATURE,106M586,DIAG M.28,TABLE M.7

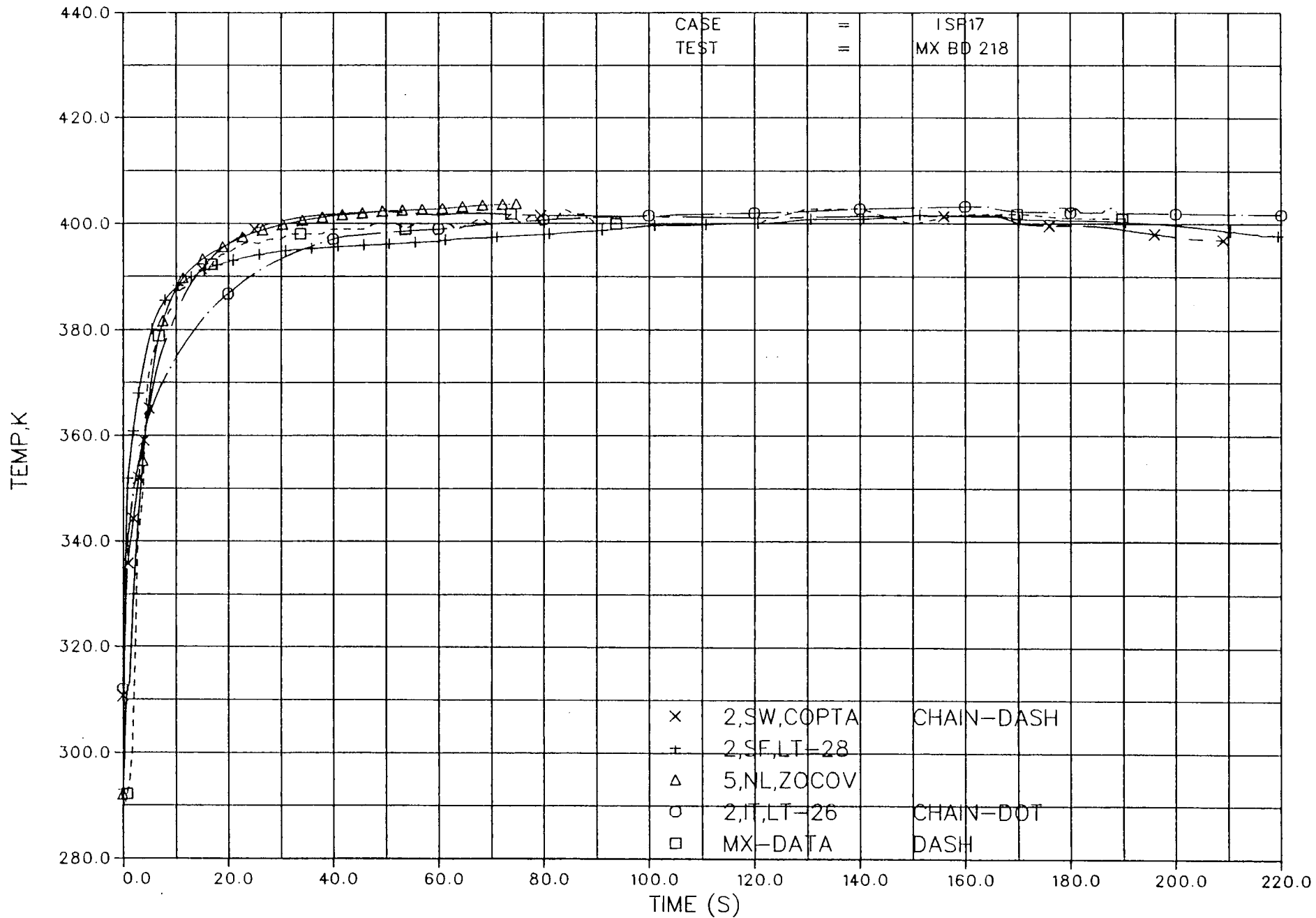


Diagram 24. Header temperature

ISP17,WETWELL GAS TEMPERATURE,AVERAGE,DIAG E.16,TABLE E.6

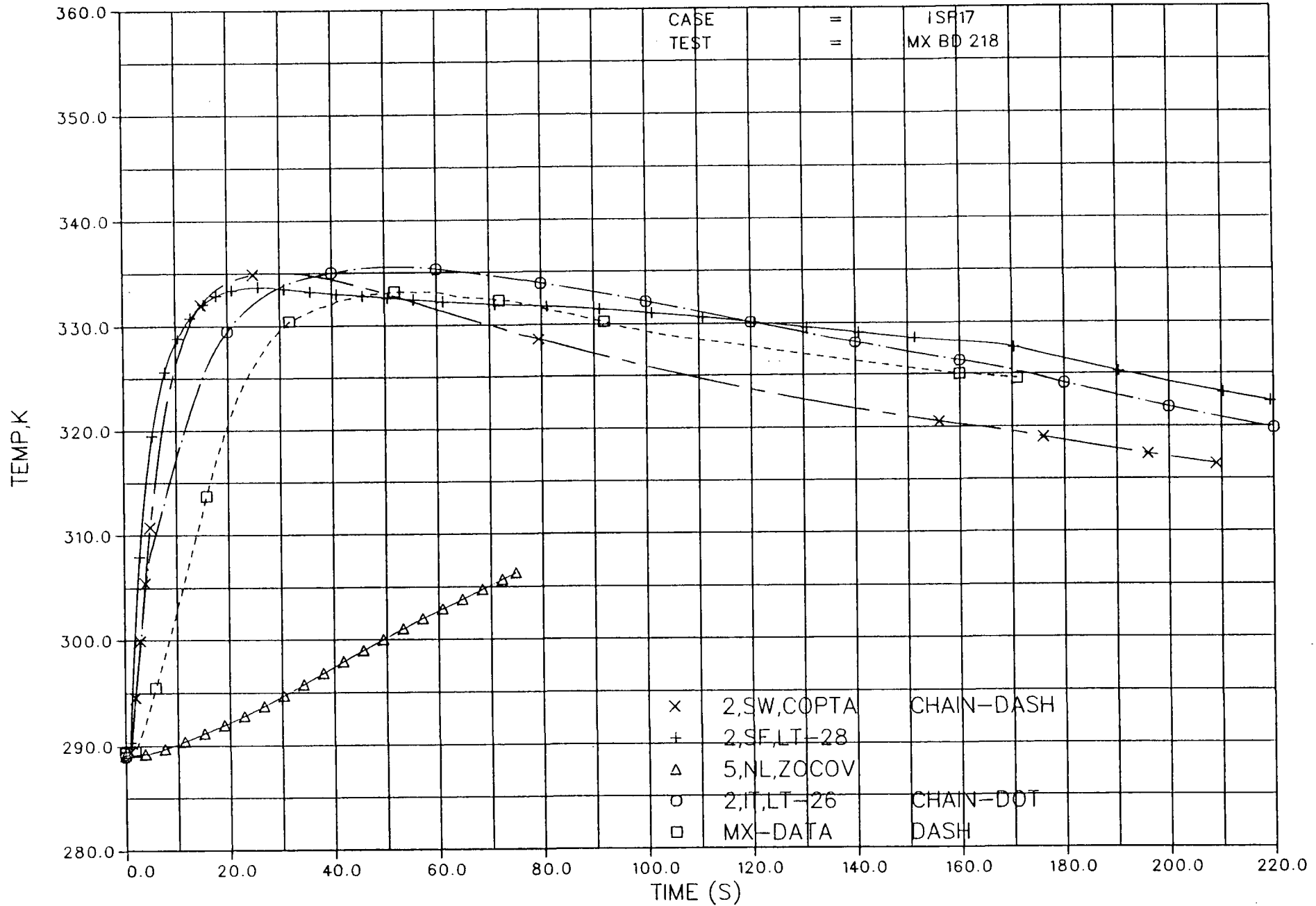


Diagram 25. Average wetwell gas temperature

ISP17, AVERAGE POOL TEMPERATURE, DIAG E.16, TABLE E.6

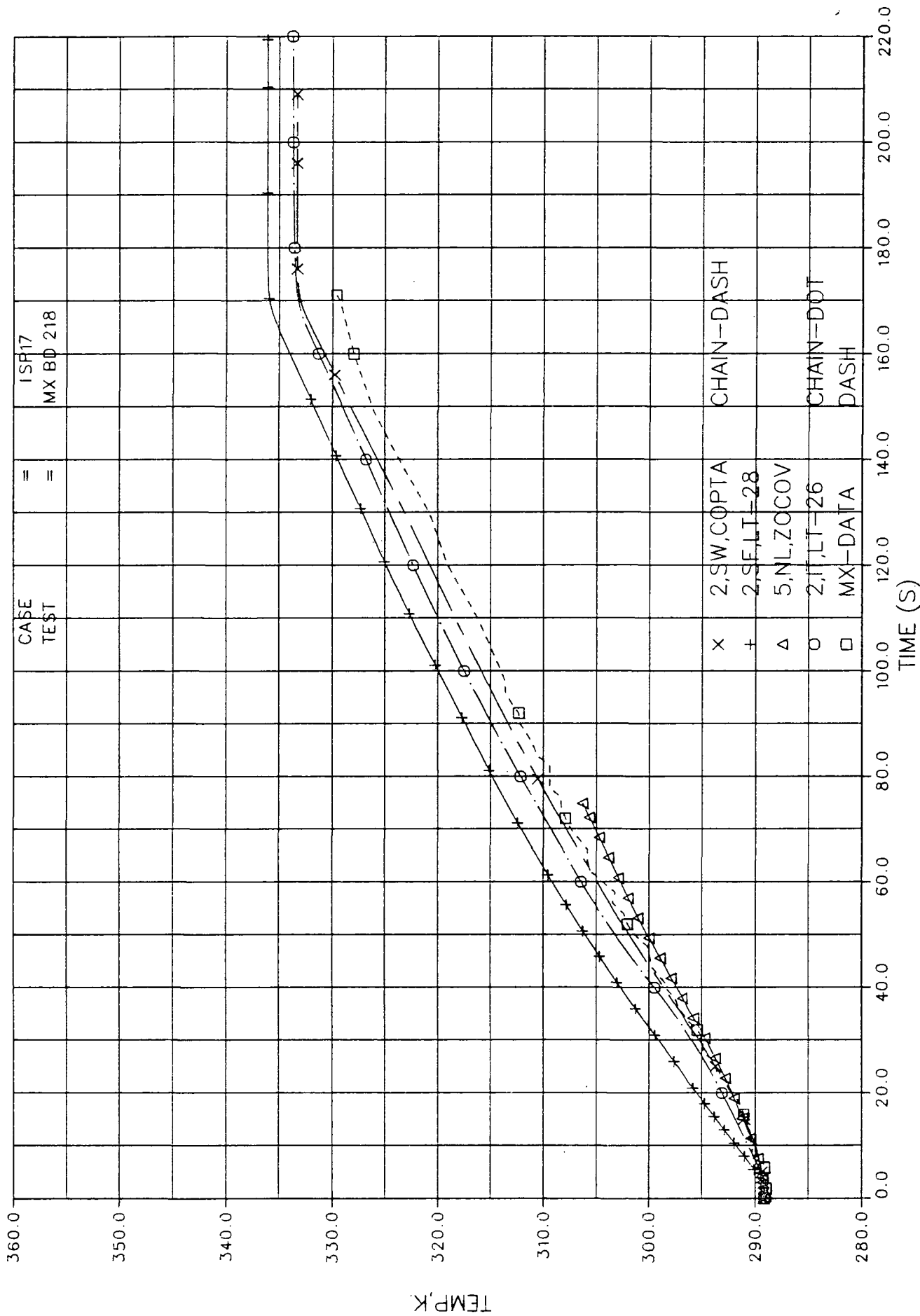


Diagram 26. Average pool temperature

ISP17, VENT PIPE AIR FLOW, DIAG E.12,25, TABLE E.5 AND IRE (ENLARGED)

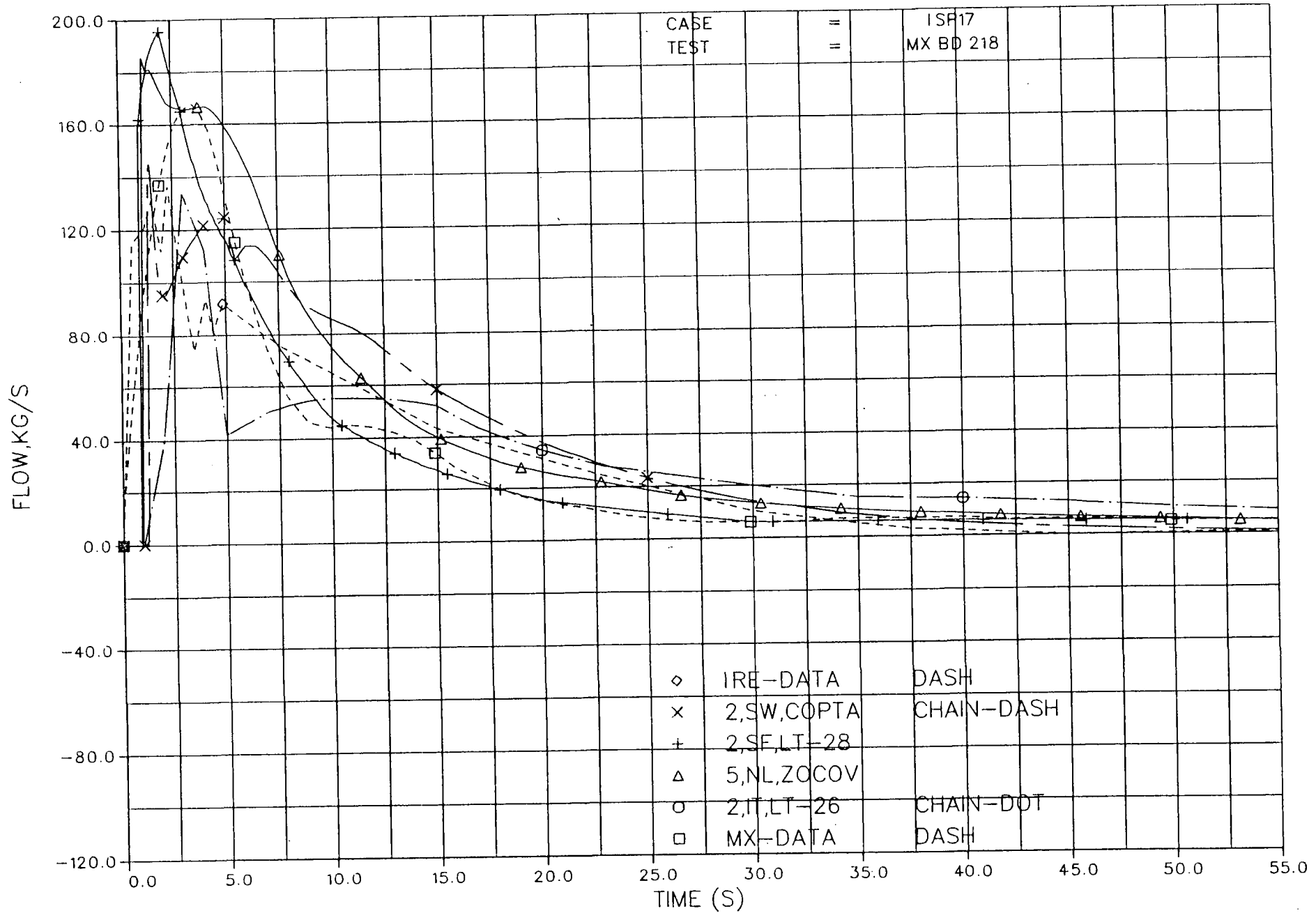


Diagram 27. Vent pipe air flow

ISP17, VENT PIPE STEAM FLOW, DIAG E.10, 41, TABLE E.5 AND IRE

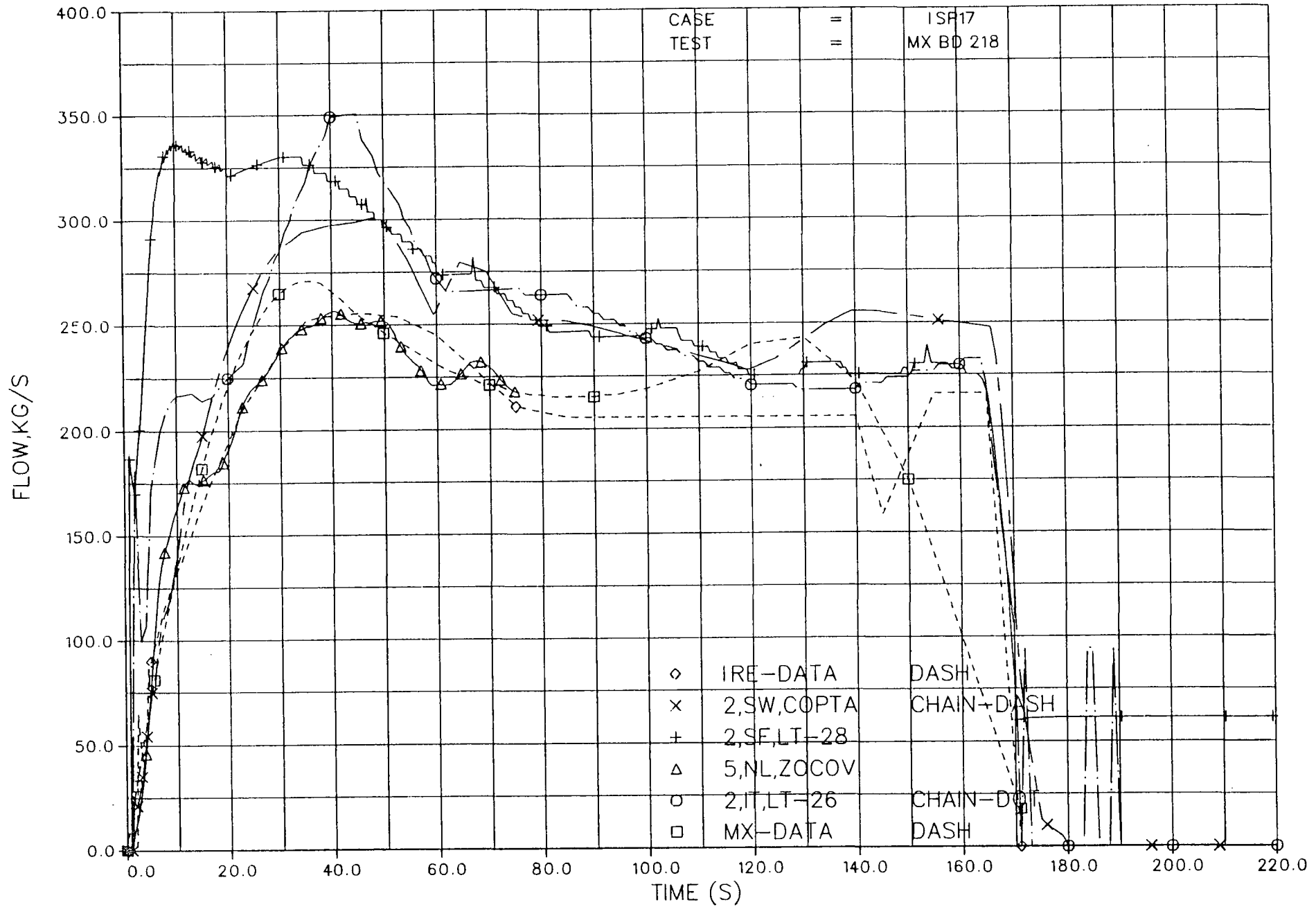


Diagram 28. Vent pipe steam flow

ISP17, VENT PIPE FLOW OF WATER, DIAG E.11,39, TABLE E.5 AND IRE

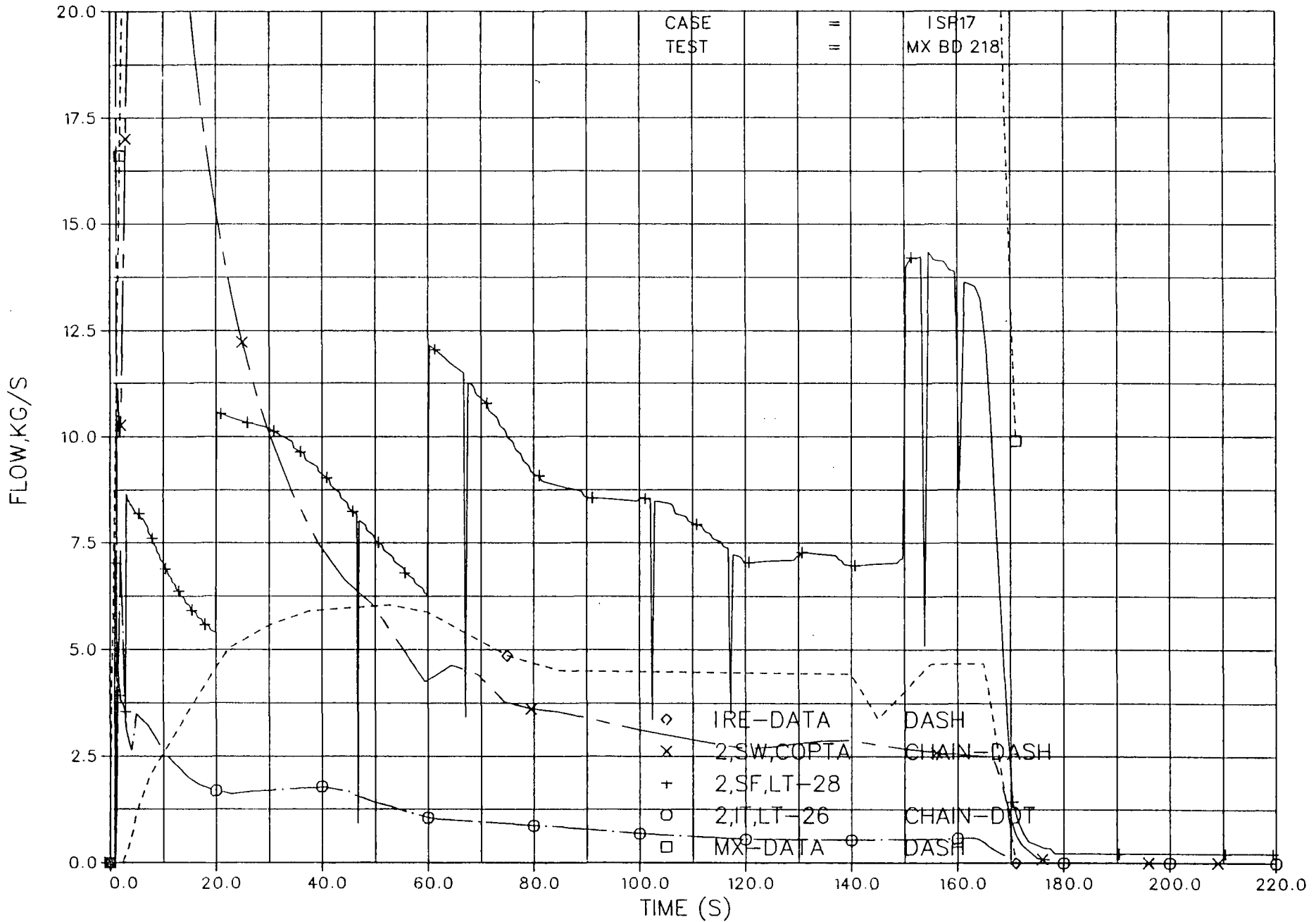


Diagram 29. Vent pipe flow of liquid water

ISP17, TOTAL AIR THROUGH VENTS, DIAG E.15,25, TABLE E.5 AND IRE

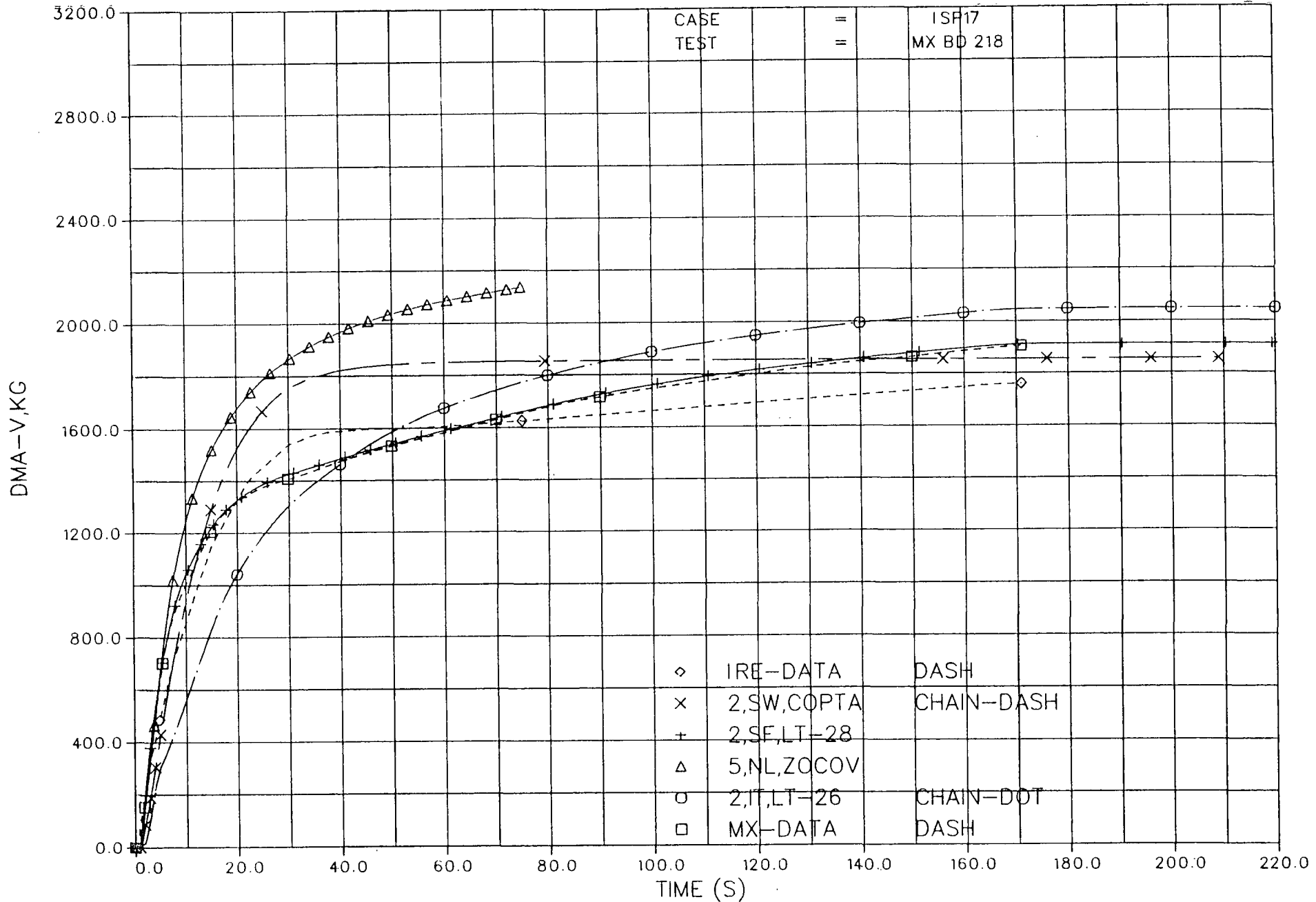


Diagram 30. Total air through vents

ISP17, TOTAL STEAM THROUGH VENTS, DIAG E.13, TABLE E.5 AND IRE

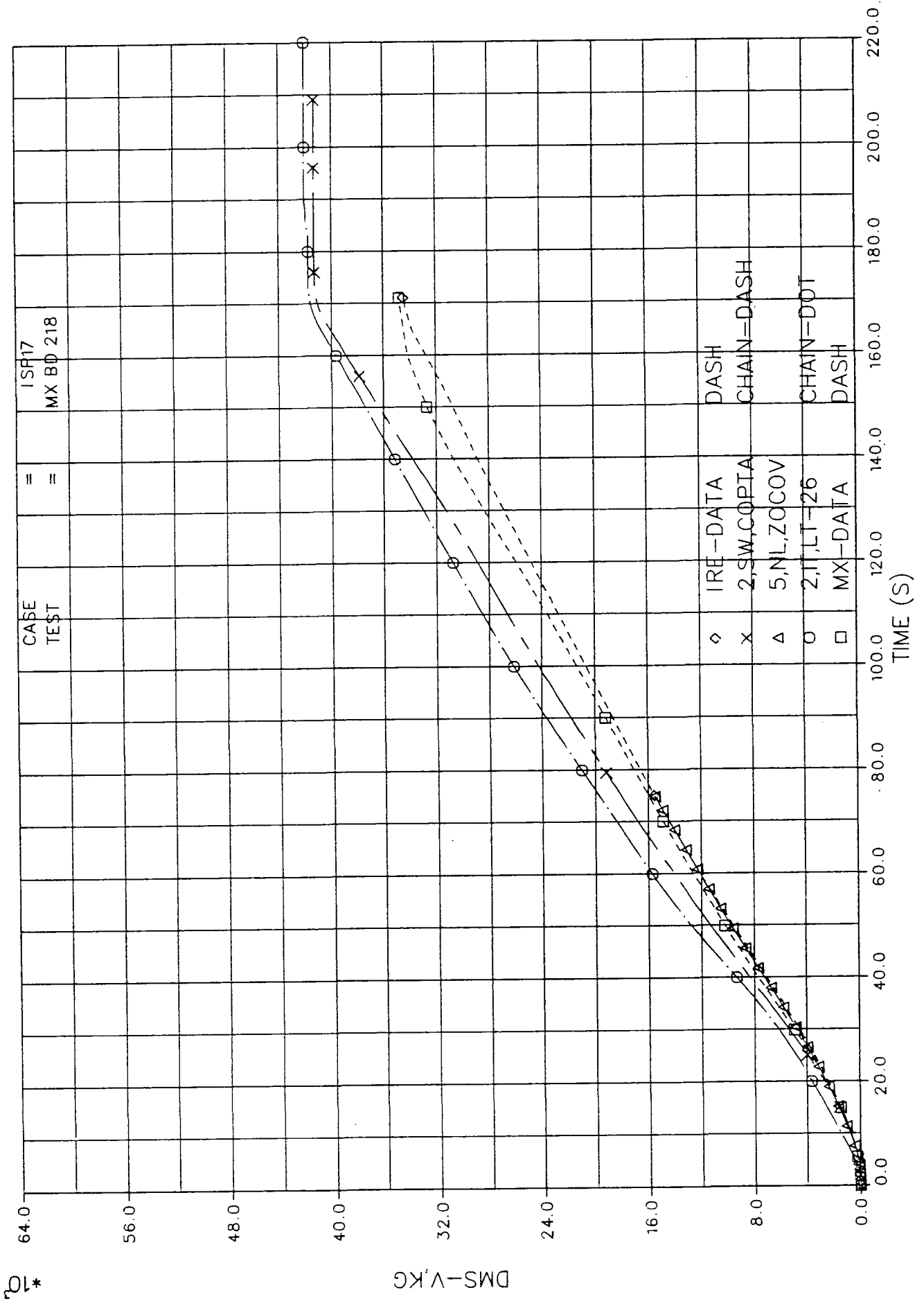


Diagram 31. Total steam through vents



ISP17, TOTAL LIQUID WATER THROUGH VENTS, DIAG E.14, TABLE E.5 AND IRE

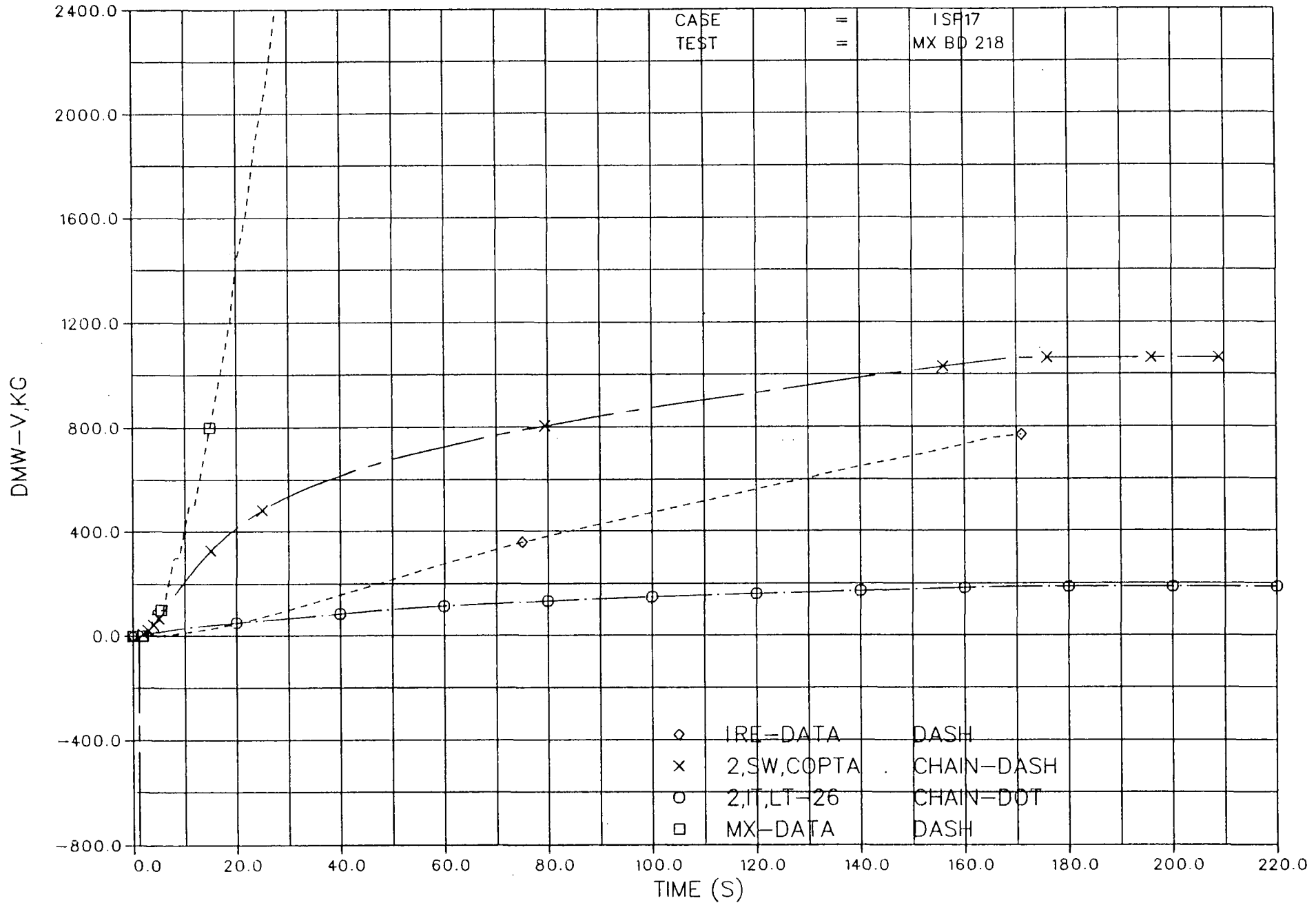


Diagram 32. Total liquid water through vents

ISP17, MASS OF SUMP WATER, TABLE E.7 (MX-DATA TOO HIGH)

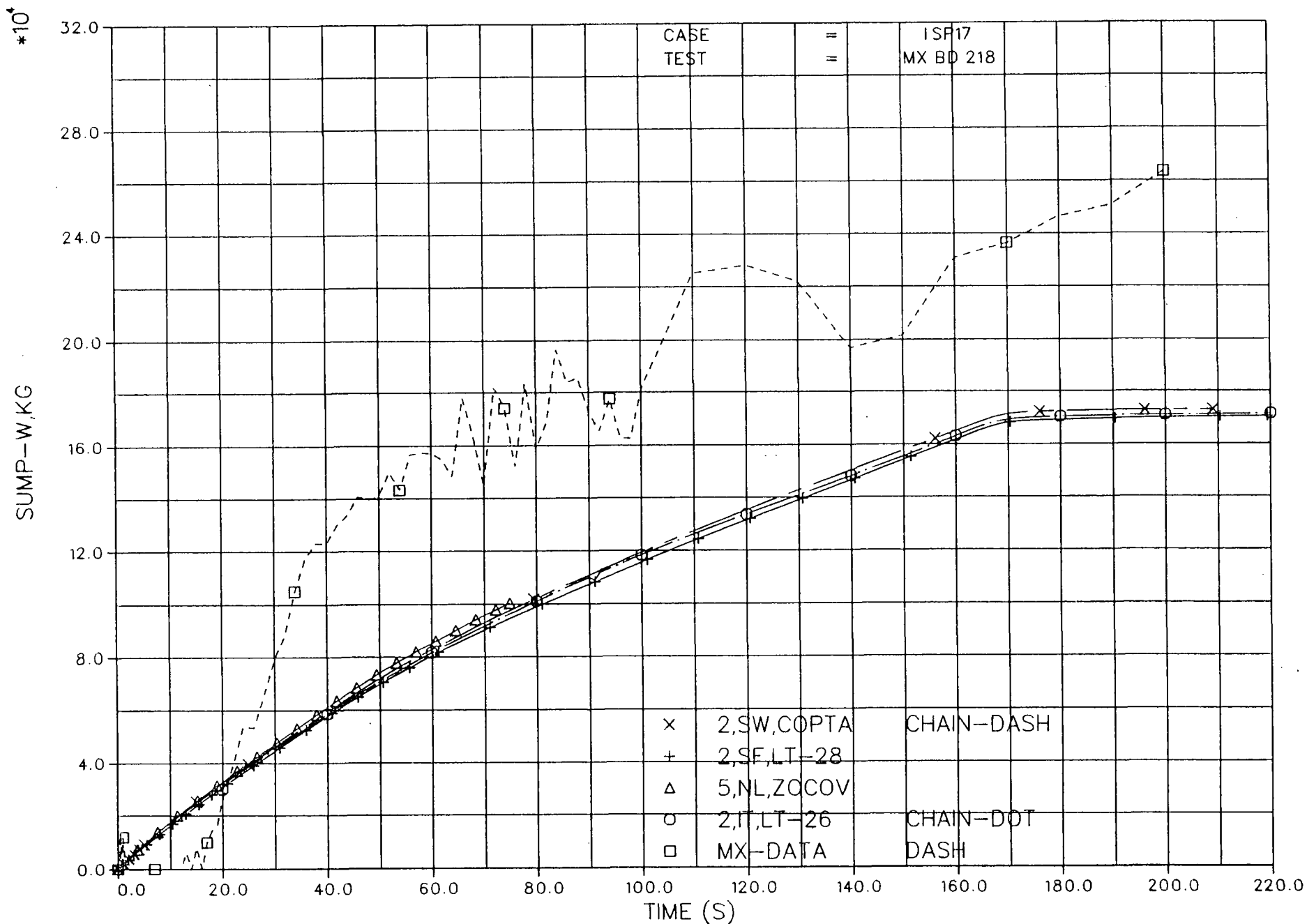


Diagram 33. Mass of sump water

ISP17, MASS OF STEAM IN WETWELL GAS, DIAG E.26, TABLE E.6

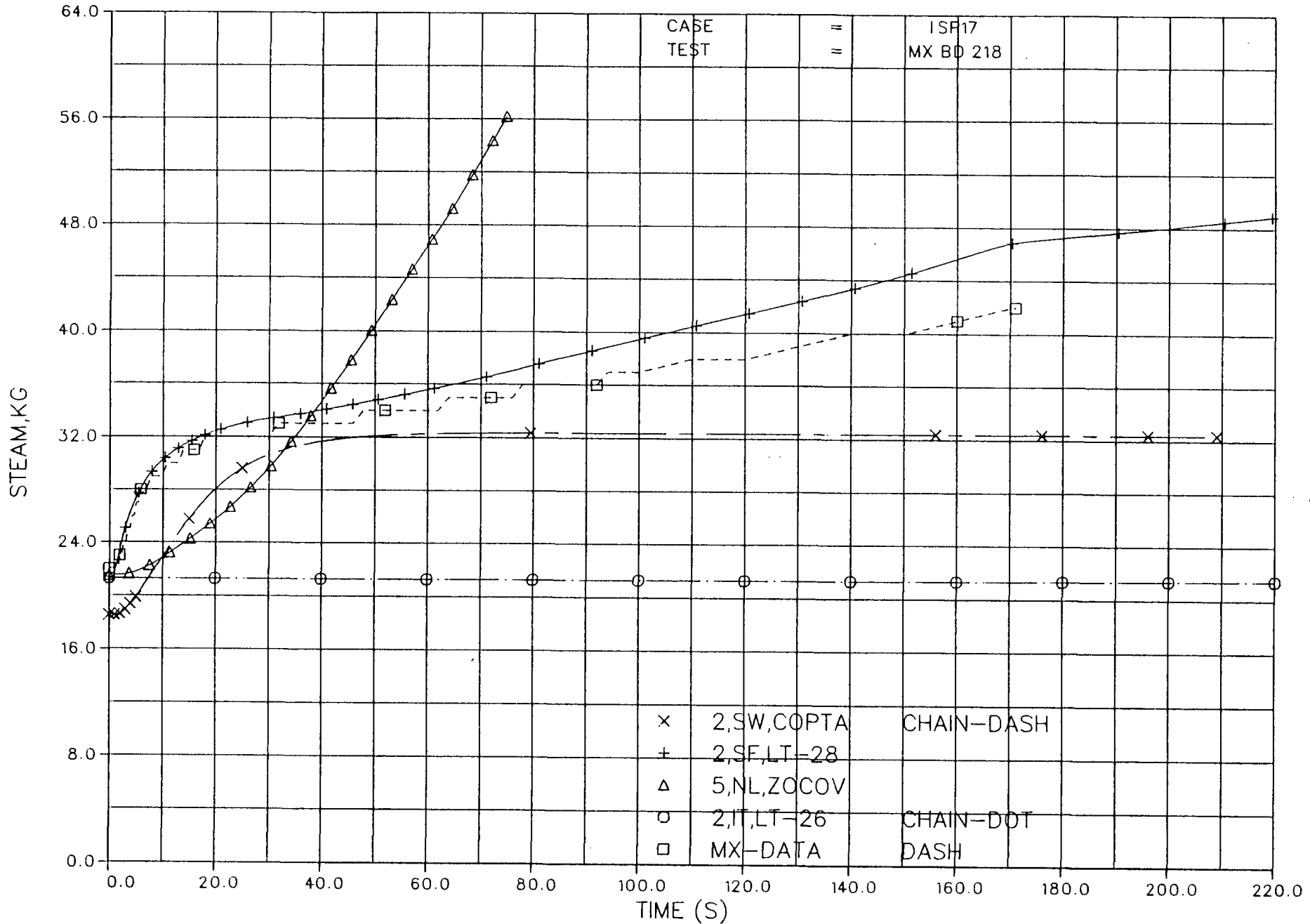


Diagram 34. Mass of steam in wetwell gas

ISP17, TOTAL MASS OF STEAM + WATER THROUGH VENTS, DIAG E.21, TABLE E.5 AND IRE

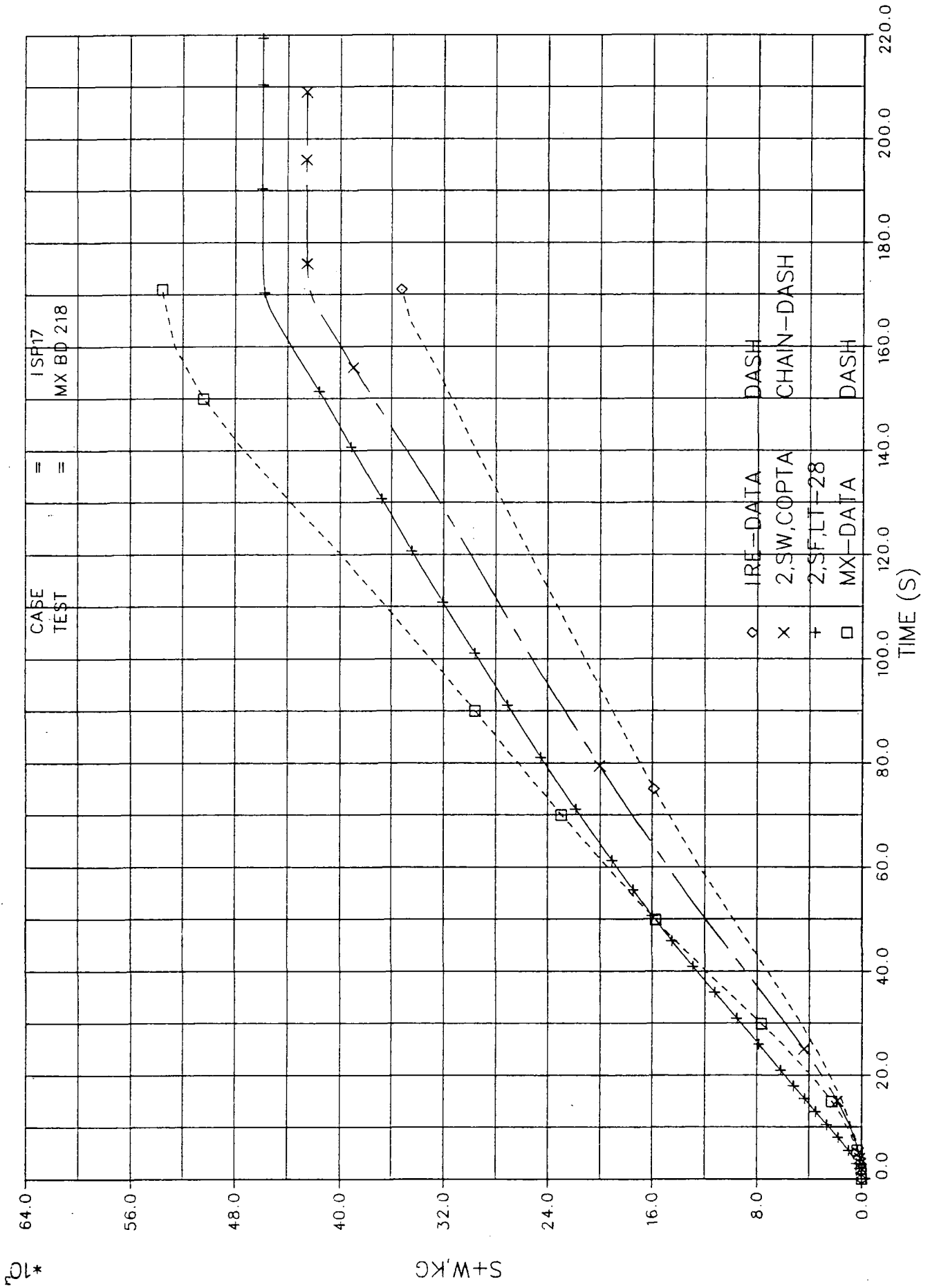


Diagram 35. Total mass of steam + water through vents